MARTIN MARIETTA ENERGY SYSTEMS LIBRARIES
3 4456 0280310 7

ornl

NUREG/CR-4880
VOL. 1
(ORNL-6484/V1)

OAK RIDGE
NATIONAL
LABORATORY

MARTIN MARIETTA

Characterization of Irradiated Current-Practice Welds and A533 Grade B Class 1 Plate for Nuclear Pressure Vessel Service

J. J. McGowan
R. K. Nanstad
K. R. Thoms

OAK RIDGE NATIONAL LABORATORY
CENTRAL RESEARCH LIBRARY
CIRCULATION SECTION
4500N ROOM 175
LIBRARY LOAN COPY
DO NOT TRANSFER TO ANOTHER PERSON
If you wish someone else to see this report, send in name with report and the library will arrange a loan.
UCN-7969 3 9 77

Prepared for the
U.S. Nuclear Regulatory Commission
Office of Nuclear Regulatory Research
Under Interagency Agreement DOE 40-551-75

OPERATED BY
MARTIN MARIETTA ENERGY SYSTEMS, INC.
FOR THE UNITED STATES
DEPARTMENT OF ENERGY

NOTICE

This report was prepared as an account of work sponsored by an agency of the United States Government. Neither the United States Government nor any agency thereof, or any of their employees, makes any warranty, expressed or implied, or assumes any legal liability or responsibility for any third party's use, or the results of such use, of any information, apparatus product or process disclosed in this report, or represents that its use by such third party would not infringe privately owned rights.

Available from

Superintendent of Documents
U.S. Government Printing Office
Post Office Box 37082
Washington, D.C. 20013-7982

and

National Technical Information Service
Springfield, VA 22161

NUREG/CR-4880
Vol. 1
ORNL-6484/V1
Distribution
Category RF

Metals and Ceramics Division

CHARACTERIZATION OF IRRADIATED CURRENT-PRACTICE WELDS AND A533 GRADE B CLASS 1 PLATE FOR NUCLEAR PRESSURE VESSEL SERVICE

J. J. McGowan, R. K. Nanstad, and K. R. Thoms

Date Published - July 1988

Prepared for the
U.S. Nuclear Regulatory Commission
Office of Nuclear Regulatory Research
Washington, DC 20555
Under Interagency Agreement DOE 40-551-75

NRC FIN. No. B0119

Prepared by the
OAK RIDGE NATIONAL LABORATORY
Oak Ridge, Tennessee 37831
operated by
MARTIN MARIETTA ENERGY SYSTEMS, INC.
for the
U.S. DEPARTMENT OF ENERGY
under contract DE-AC05-84OR21400

MARTIN MARIETTA ENERGY SYSTEMS LIBRARIES
3 4456 0280310 7

FOREWORD

The work reported here was performed at Oak Ridge National Laboratory (ORNL) under the Heavy-Section Steel Technology Program, C. E. Pugh, Program Manager. The program is sponsored by the Office of Nuclear Regulatory Research, U.S. Nuclear Regulatory Commission (NRC). The technical monitor for the NRC is Michael E. Mayfield.

This report is designated HSST Program Technical Report 88. It is published in two volumes. Volume 1 contains the main body with Appendices A and B. Volume 2 contains only Appendices C through F which provide detailed load-displacement traces, fracture surfaces, etc. In recognition of its very large size, Volume 2 will be distributed only to those in the RF distribution requesting a copy from the HSST Program Office. Other reports in this series include:

1. S. Yukawa, *Evaluation of Periodic Proof Testing and Warm Prestressing Procedures for Nuclear Reactor Vessels*, HSSTP-TR-1, General Electric Company, Schenectady, N.Y., July 1, 1969.

2. L. W. Loechel, *The Effect of Testing Variables on the Transition Temperature in Steel*, MCR-69-189, Martin Marietta Corporation, Denver, Nov. 20, 1969.

3. P. N. Randall, *Gross Strain Measure of Fracture Toughness of Steels*, HSSTP-TR-3, TRW Systems Group, Redondo Beach, Calif., Nov. 1, 1969.

4. C. Visser, S. E. Gabrielse, and W. VanBuren, *A Two-Dimensional Elastic-Plastic Analysis of Fracture Test Specimens*, WCAP-7368, Westinghouse Electric Corp., PWR Systems Div., Pittsburgh, October 1969.

5. T. R. Mager and F. O. Thomas, *Evaluation by Linear Elastic Fracture Mechanics of Radiation Damage to Pressure Vessel Steels*, WCAP-7328 (Rev.), Westinghouse Electric Corp., PWR Systems Div., Pittsburgh, October 1969.

6. W. O. Shabbits, W. H. Pryle, and E. T. Wessel, *Heavy-Section Fracture Toughness Properties of A533 Grade B Class 1 Steel Plate and Submerged Arc Weldment*, WCAP-7414, Westinghouse Electric Corp., PWR Systems Div., Pittsburgh, December 1969.

7. F. J. Loss, *Dynamic Tear Test Investigations of the Fracture Toughness of Thick-Section Steel*, NRL-7056, Naval Research Laboratory, Washington, D.C., May 14, 1970.

8. P. B. Crosley and E. J. Ripling, *Crack Arrest Fracture Toughness of A533 Grade B Class 1 Pressure Vessel Steel*, HSSTP-TR-8, Materials Research Laboratory, Inc., Glenwood, Ill., March 1970.

9. T. R. Mager, *Post-Irradiation Testing of 2T Compact Tension Specimens*, WCAP-7561, Westinghouse Electric Corp., PWR Systems Div., Pittsburgh, August 1970.

10. T. R. Mager, *Fracture Toughness Characterization Study of A533, Grade B, Class 1 Steel*, WCAP-7578, Westinghouse Electric Corp., PWR Systems Div., Pittsburgh, October 1970.

11. T. R. Mager, *Notch Preparation in Compact Tension Specimens*, WCAP-7579, Westinghouse Electric Corp., PWR Systems Div., Pittsburgh, November 1970.

12. N. Levy and P. V. Marcal, *Three-Dimensional Elastic-Plastic Stress and Strain Analysis for Fracture Mechanics, Phase I: Simple Flawed Specimens*, HSSTP-TR-12, Brown University, Providence, R.I., December 1970.

13. W. O. Shabbits, *Dynamic Fracture Toughness Properties of Heavy Section A533 Grade B Class 1 Steel Plate*, WCAP-7623, Westinghouse Electric Corp., PWR Systems Div., Pittsburgh, December 1970.

14. P. N. Randall, *Gross Strain Crack Tolerance of A533-B Steel*, HSSTP-TR-14, TRW Systems Group, Redondo Beach, Calif., May 1, 1971.

15. H. T. Corten and R. H. Sailors, *Relationship Between Material Fracture Toughness Using Fracture Mechanics and Transition Temperature Tests*, T&AM Report 346, University of Illinois, Urbana, August 1, 1971.

16. T. R. Mager and V. J. McLoughlin, *The Effect of an Environment of High Temperature Primary Grade Nuclear Reactor Water on the Fatigue Crack Growth Characteristics of A533 Grade B Class 1 Plate and Weldment Material*, WCAP-7776, Westinghouse Electric Corp., PWR Systems Div., Pittsburgh, October 1971.

17. N. Levy and P. V. Marcal, *Three-Dimensional Elastic-Plastic Stress and Strain Analysis for Fracture Mechanics, Phase II: Improved Modelling*, HSSTP-TR-17, Brown University, Providence, R.I., November 1971.

18. S. C. Grigory, *Tests of 6-Inch-Thick Flawed Tensile Specimens, First Technical Summary Report, Longitudinal Specimens Numbers 1 Through 7*, HSSTP-TR-18, Southwest Research Institute, San Antonio, Texas, June 1972.

19. P. N. Randall, *Effects of Strain Gradients on the Gross Strain Crack Tolerance of A533-B Steel*, HSSTP-TR-19, TRW Systems Group, Redondo Beach, Calif., June 15, 1972.

20. S. C. Grigory, *Tests of 6-Inch-Thick Flawed Tensile Specimens, Second Technical Summary Report, Transverse Specimens Numbers 8 Through 10, Welded Specimens Numbers 11 Through 13*, HSSTP-TR-20, Southwest Research Institute, San Antonio, Texas, June 1972.

21. L. A. James and J. A. Williams, *Heavy Section Steel Technology Program Technical Report No. 21, The Effect of Temperature and Neutron Irradiation Upon the Fatigue-Crack Propagation Behavior of ASTM A533 Grade B, Class 1 Steel*, HEDL-TME 72-132, Hanford Engineering Development Laboratory, Richland, Wash., September 1972.

22. S. C. Grigory, *Tests of 6-Inch Thick Flawed Tensile Specimens, Third Technical Summary Report, Longitudinal Specimens Numbers 14 Through 16, Unflawed Specimen Number 17*, HSSTP-TR-22, Southwest Research Institute, San Antonio, Texas, October 1972.

23. S. C. Grigory, *Tests of 6-Inch Thick Flawed Tensile Specimens, Fourth Technical Summary Report, Tests of 1-Inch-Thick Flawed Tensile Specimens for Size Effect Evaluation*, HSSTP-TR-23, Southwest Research Institute, San Antonio, Texas, June 1973.

24. S. P. Ying and S. C. Grigory, *Tests of 6-Inch-Thick Tensile Specimens, Fifth Technical Summary Report, Acoustic Emission Monitoring of 1-Inch and 6-Inch Thick Tensile Specimens*, HSSTP-TR-24, Southwest Research Institute, San Antonio, Texas, November 1972.

25. R. W. Derby, J. G. Merkle, G. C. Robinson, G. D. Whitman, and F. J. Witt, *Tests of 6-Inch-Thick Pressure Vessels. Series 1: Intermediate Test Vessels V-1 and V-2*, ORNL-4895, February 1974.

26. W. J. Stelzman and R. G. Berggren, *Radiation Strengthening and Embrittlement in Heavy-Section Steel Plates and Welds*, ORNL-4871, June 1973.

27. P. B. Crosley and E. J. Ripling, *Crack Arrest in an Increasing K-Field*, HSSTP-TR-27, Materials Research Laboratory, Inc., Glenwood, Ill., January 1973.

28. P. V. Marcal, P. M. Stuart, and R. S. Bettes, *Elastic-Plastic Behavior of a Longitudinal Semi-Elliptic Crack in a Thick Pressure Vessel*, HSSTP-TR-28, Brown University, Providence, R.I., June 1973.

29. W. J. Stelzman, R. G. Berggren, and T. N. Jones, *ORNL Characterization of Heavy-Section Steel Technology Program Plates 01, 02, and 03*, NUREG/CR-4092 (ORNL/TM-9491), April 1985.

30. Canceled.

31. J. A. Williams, *The Irradiation and Temperature Dependence of Tensile and Fracture Properties of ASTM A533, Grade B, Class 1 Steel Plate and Weldment*, HEDL-TME 73-75, Hanford Engineering Development Laboratory, Richland, Wash., August 1973.

32. J. M. Steichen and J. A. Williams, *High Strain Rate Tensile Properties of Irradiated ASTM A533 Grade B Class 1 Pressure Vessel Steel*, Hanford Engineering Development Laboratory, Richland, Wash., July 1973.

33. P. C. Riccardella and J. L. Swedlow, *A Combined Analytical-Experimental Fracture Study of the Two Leading Theories of Elastic-Plastic Fracture (J-Integral and Equivalent Energy)*, WCAP-8224, Westinghouse Electric Corp., Pittsburgh, October 1973.

34. R. J. Podlasek and R. J. Eiber, *Final Report on Investigation of Mode III Crack Extension in Reactor Piping*, Battelle Columbus Laboratories, Columbus, Ohio, Dec. 14, 1973.

35. T. R. Mager, J. D. Landes, D. M. Moon, and V. J. McLaughlin, *Interim Report on the Effect of Low Frequencies on the Fatigue Crack Growth Characteristics of A533 Grade B Class 1 Plate in an Environment of High-Temperature Primary Grade Nuclear Reactor Water*, WCAP-8256, Westinghouse Electric Corp., Pittsburgh, December 1973.

36. J. A. Williams, *The Irradiated Fracture Toughness of ASTM A533, Grade B, Class 1 Steel Measured with a Four-Inch-Thick Compact Tension Specimen*, HEDL-TME 75-10, Hanford Engineering Development Laboratory, Richland, Wash., January 1975.

37. R. H. Bryan, J. G. Merkle, M. N. Raftenberg, G. C. Robinson, and J. E. Smith, *Test of 6-Inch-Thick Pressure Vessels. Series 2: Intermediate Test Vessels V-3, V-4, and V-6*, ORNL-5059, November 1975.

38. T. R. Mager, S. E. Yanichko, and L. R. Singer, *Fracture Toughness Characterization of HSST Intermediate Pressure Vessel Material*, WCAP-8456, Westinghouse Electric Corp., Pittsburgh, December 1974.

39. J. G. Merkle, G. D. Whitman, and R. H. Bryan, *An Evaluation of the HSST Program Intermediate Pressure Vessel Tests in Terms of Light-Water-Reactor Pressure Vessel Safety*, ORNL/TM-5090, November 1975.

40. J. G. Merkle, G. C. Robinson, P. P. Holz, J. E. Smith, and R. H. Bryan, *Test of 6-In.-Thick Pressure Vessels. Series 3: Intermediate Test Vessel V-7*, ORNL/NUREG-1, August 1976.

41. J. A. Davidson, L. J. Ceschini, R. P. Shogan, and G. V. Rao, *The Irradiated Dynamic Fracture Toughness of ASTM A533, Grade B, Class 1 Steel Plate and Submerged Arc Weldment*, WCAP-8775, Westinghouse Electric Corp., Pittsburgh, October 1976.

42. R. D. Cheverton, *Pressure Vessel Fracture Studies Pertaining to PWR LOCA-ECC Thermal Shock: Experiments TSE-1 and TSE-2*, ORNL/NUREG/TM-31, September 1976.

43. J. G. Merkle, G. C. Robinson, P. P. Holz, and J. E. Smith, *Test of 6-In.-Thick Pressure Vessels. Series 4: Intermediate Test Vessels V-5 and V-9 with Inside Nozzle Corner Cracks*, ORNL/NUREG-7, August 1977.

44. J. A. Williams, *The Ductile Fracture Toughness of Heavy Section Steel Plate*, NUREG/CR-0859, Hanford Engineering Development Laboratory, Richland, Wash., September 1979.

45. R. H. Bryan, T. M. Cate, P. P. Holz, T. A. King, J. G. Merkle, G. C. Robinson, G. C. Smith, J. E. Smith, and G. D. Whitman, *Test of 6-in.-Thick Pressure Vessels. Series 3: Intermediate Test Vessel V-7A Under Sustained Loading*, ORNL/NUREG-9, February 1978.

46. R. D. Cheverton and S. E. Bolt, *Pressure Vessel Fracture Studies Pertaining to a PWR LOCA-ECC Thermal Shock: Experiments TSE-3 and TSE-4 and Update of TSE-1 and TSE-2 Analysis*, ORNL/NUREG-22, December 1977.

47. D. A. Canonico, *Significance of Reheat Cracks to the Integrity of Pressure Vessels for Light-Water Reactors*, ORNL/NUREG-15, July 1977.

48. G. C. Smith and P. P. Holz, *Repair Weld Induced Residual Stresses in Thick-Walled Steel Pressure Vessels*, NUREG/CR-0093 (ORNL/NUREG/TM-153), June 1978.

49. P. P. Holz and S. W. Wismer, *Half-Bead (Temper) Repair Welding for HSST Vessels*, NUREG/CR-0113 (ORNL/NUREG/TM-177), June 1978.

50. G. C. Smith, P. P. Holz, and W. J. Stelzman, *Crack Extension and Arrest Tests of Axially Flawed Steel Model Pressure Vessels*, NUREG/CR-0126 (ORNL/NUREG/TM-196), October 1978.

51. R. H. Bryan, P. P. Holz, J. G. Merkle, G. C. Smith, J. E. Smith, and W. J. Stelzman, *Test of 6-in.-Thick Pressure Vessels. Series 3: Intermediate Test Vessel V-7B*, NUREG/CR-0309 (ORNL/NUREG-38), October 1978.

52. R. D. Cheverton, S. K. Iskander, and S. E. Bolt, *Applicability of LEFM to the Analysis of PWR Vessels Under LOCA-ECC Thermal Shock Conditions*, NUREG/CR-0107 (ORNL/NUREG-40), October 1978.

53. R. H. Bryan, D. A. Canonico, P. P. Holz, S. K. Iskander, J. G. Merkle, J. E. Smith, and W. J. Stelzman, *Test of 6-in.-Thick Pressure Vessels. Series 3: Intermediate Test Vessel V-8*, NUREG/CR-0675 (ORNL/NUREG-58), December 1979.

54. R. D. Cheverton and S. K. Iskander, *Application of Static and Dynamic Crack Arrest Theory to TSE-4*, NUREG/CR-0767 (ORNL/NUREG-57), June 1979.

55. J. A. Williams, *Tensile Properties of Irradiated and Unirradiated Welds of A533 Steel Plate and A508 Forgings*, NUREG/CR-1158 (ORNL/SUB-79/50917/2), Hanford Engineering Development Laboratory, Richland, Wash., July 1979.

56. K. W. Carlson and J. A. Williams, *The Effect of Crack Length and Side Grooves on the Ductile Fracture Toughness Properties of ASTM A533 Steel*, NUREG/CR-1171 (ORNL/SUB-79/50917/3), Hanford Engineering Development Laboratory, Richland, Wash., October 1979.

57. P. P. Holz, *Flaw Preparations for HSST Program Vessel Fracture Mechanics Testing; Mechanical-Cyclic Pumping and Electron-Beam Weld-Hydrogen Charge Cracking Schemes*, NUREG/CR-1274 (ORNL/NUREG/TM-369), May 1980.

58. S. K. Iskander, *Two Finite Element Techniques for Computing Mode I Stress Intensity Factors in Two- or Three-Dimensional Problems*, NUREG/CR-1499 (ORNL/NUREG/CSD/TM-14), February 1981.

59. P. B. Crosley and E. J. Ripling, *Development of a Standard Test for Measuring K_{Ia} with a Modified Compact Specimen*, NUREG/CR-2294, August 1981.

60. S. N. Atluri, B. R. Bass, J. W. Bryson, and K. Kathiresan, *NOZ-FLAW: A Finite Element Program for Direct Evaluation of Stress Intensity Factors for Pressure Vessel Nozzle-Corner Flaws*, NUREG/CR-1843 (ORNL/NUREG/CSD/TM-18), March 1981.

61. A. Shukla, W. L. Fourney, and G. R. Irwin, *Study of Energy Loss and Its Mechanisms in Homalite 100 During Crack Propagation and Arrest*, NUREG/CR-2150 (ORNL/SUB-7778/1), University of Maryland, College Park, August 1981.

62. S. K. Iskander, R. D. Cheverton, and D. G. Ball, *OCA-1, A Code for Calculating the Behavior of Flaws on the Inner Surface of a Pressure Vessel Subjected to Temperature and Pressure Transients*, NUREG/CR-2113 (ORNL/NUREG-84), August 1981.

63. R. J. Sanford, R. Chona, W. L. Fourney, and G. R. Irwin, *A Photoelastic Study of the Influence of Non-Singular Stresses in Fracture Test Specimens*, NUREG/CR-2179 (ORNL/SUB-7778/2), University of Maryland, College Park, August 1981.

64. B. R. Bass, S. N. Atluri, J. W. Bryson, and K. Kathiresan, *OR-FLAW: A Finite Element Program for Direct Evaluation of K-Factors for User-Defined Flaws in Plate, Cylinders, and Pressure-Vessel Nozzle Corners*, NUREG/CR-2494 (ORNL/CSD/TM-165), April 1982.

65. B. R. Bass and J. W. Bryson, *ORMGEN-3D: A Finite Element Mesh Generator for 3-Dimensional Crack Geometries*, NUREG/CR-2997, vol. 1 (ORNL/TM-8527/V1), December 1982.

66. B. R. Bass and J. W. Bryson, *ORVIRT: A Finite Element Program for Energy Release Rate Calculations for 2-Dimensional and 3-Dimensional Crack Models*, NUREG/CR-2997, vol. 2 (ORNL/TM-8527/V2), February 1983.

67. R. D. Cheverton, S. K. Iskander, and D. G. Ball, *PWR Pressure Vessel Integrity During Overcooling Accidents: A Parametric Analysis*, NUREG/CR-2895 (ORNL/TM-7931), February 1983.

68. D. G. Ball, R. D. Cheverton, J. B. Drake, and S. K. Iskander, *OCA-II, A Code for Calculating Behavior of 2-D and 3-D Surface Flaws in a Pressure Vessel Subjected to Temperature and Pressure Transients*, NUREG/CR-3491 (ORNL-5934), February 1984.

69. A. Sauter, R. D. Cheverton, and S. K. Iskander, *Modification of OCA-1 for Application to a Reactor Pressure Vessel with Cladding on the Inner Surface*, NUREG/CR-3155 (ORNL/TM-8649), May 1983.

70. R. D. Cheverton and D. G. Ball, *OCA-P, A Deterministic and Probabilistic Fracture-Mechanics Code for Application to Pressure Vessels*, NUREG/CR-3618 (ORNL-5991), May 1984.

71. J. G. Merkle, *An Examination of the Size Effects and Data Scatter Observed in Small Specimen Cleavage Fracture Toughness Testing*, NUREG/CR-3672 (ORNL/TM-9088), April 1984.

72. C. E. Pugh et al., *Heavy-Section Steel Technology Program — Five-Year Plan, FY 1983–1987*, NUREG/CR-3595 (ORNL/TM-9008), April 1984.

73. D. G. Ball, B. R. Bass, J. W. Bryson, R. D. Cheverton, and J. B. Drake, *Stress Intensity Factor Influence Coefficients for Surface Flaws in Pressure Vessels*, NUREG/CR-3723 (ORNL/CSD/TM-216), February 1985.

74. W. R. Corwin, R. G. Berggren, and R. K. Nanstad, *Charpy Toughness and Tensile Properties of a Neutron Irradiated Stainless Steel Submerged-Arc Weld Cladding Overlay*, NUREG/CR-3927 (ORNL/TM-9709), September 1984.

75. C. W. Schwartz, R. Chona, W. L. Fourney, and G. R. Irwin, *SAMCR: A Two-Dimensional Dynamic Finite Element Code for the Stress Analysis of Moving Cracks*, NUREG/CR-3891 (ORNL/SUB/79-7778/3), University of Maryland, College Park, November 1984.

76. W. R. Corwin, G. C. Robinson, R. K. Nanstad, J. G. Merkle, R. G. Berggren, G. M. Goodwin, R. L. Swain, and T. D. Owings, *Effects of Stainless Steel Weld Overlay Cladding on the Structural Integrity of Flawed Steel Plates in Bending, Series 1*, NUREG/CR-4015 (ORNL/TM-9390), April 1985.

77. R. H. Bryan, B. R. Bass, S. E. Bolt, J. W. Bryson, D. P. Edmonds, R. W. McCulloch, J. G. Merkle, G. C. Robinson, K. R. Thoms, and G. D. Whitman, *Pressurized-Thermal Shock Test of 6-in.-Thick Pressure Vessels. PTSE-1: Investigation of Warm Prestressing and Upper-Shelf Arrest*, NUREG/CR-4106 (ORNL-6135), April 1985.

78. R. D. Cheverton, D. G. Ball, S. K. Iskander, and R. K. Nanstad, *Pressure Vessel Fracture Studies Pertaining to the PWR Thermal-Shock Issue: Experiments TSE-5, TSE-5A, and TSE-6*, NUREG/CR-4249 (ORNL-6163), June 1985.

79. R. D. Cheverton, D. G. Ball, S. E. Bolt, S. K. Iskander, and R. K. Nanstad, *Pressure Vessel Fracture Studies Pertaining to the PWR Thermal-Shock Issue: Experiment TSE-7*, NUREG/CR-4304 (ORNL-6177), August 1985.

80. R. H. Bryan, B. R. Bass, S. E. Bolt, J. W. Bryson, J. G. Merkle, R. K. Nanstad, and G. C. Robinson, *Test of 6-in.-Thick Pressure Vessels. Series 3: Intermediate Test Vessel V-8A — Tearing Behavior of Low Upper-Shelf Material*, NUREG/CR-4760 (ORNL-6187), to be published.

81. R. D. Cheverton and D. G. Ball, *A Parametric Study of PWR Pressure Vessel Integrity During Overcooling Accidents, Considering Both 2-D and 3-D Flaws*, NUREG/CR-4325 (ORNL/TM-9682), August 1985.

82. E. C. Rodabaugh, *Comments on the Leak-Before-Break Concept for Nuclear Power Plant Piping Systems*, NUREG/CR-4305 (ORNL/Sub/82-22252/3), August 1985.

83. J. W. Bryson, *ORVIRT.PC: A 2-D Finite Element Fracture Analysis Program for a Microcomputer*, NUREG/CR-4367 (ORNL-6208), October 1985.

84. D. G. Ball and R. D. Cheverton, *Adaptation of OCA-P, A Probabilistic Fracture-Mechanics Code, to a Personal Computer*, NUREG/CR-4468 (ORNL/CSD/TM-233), January 1986.

85. J. W. Bryson and B. R. Bass, *ORMGEN.PC: A Microcomputer Program for Automatic Mesh Generation of 2-D Crack Geometries*, NUREG/CR-4475 (ORNL-6250), March 1986.

86. G. D. Whitman, *Historical Summary of the Heavy-Section Steel Technology Program and Some Related Activities in Light-Water Reactor Pressure Vessel Safety Research*, NUREG/CR-4489 (ORNL-6259), March 1986.

87. C. Inversini and J. W. Bryson, *ORPLOT.PC: A Graphic Utility for ORMGEN.PC and ORVIRT.PC*, NUREG/CR-4633 (ORNL-6291), June 1986.

88. This report.

89. K. V. Cook and R. W. McClung, *Flaw Density Examinations of a Clad Boiling Water Reactor Pressure Vessel Segment*, NUREG/CR-4860, Revision 1 (ORNL/TM-10364/R1), February 1988.

90. D. J. Naus et al., *Crack-Arrest Behavior in SEN Wide Plates of Quenched and Tempered A 533 Grade B Steel Tested Under Nonisothermal Conditions*, NUREG/CR-4930 (ORNL-6388), August 1987.

91. D. B. Barker et al., *A Report on the Round Robin Program Conducted to Evaluate the Proposed ASTM Standard Test Method for Determining the Plane Strain Crack Arrest Fracture Toughness K_{Ia}, of Ferritic Materials,* NUREG/CR-4966 (ORNL/Sub/79-7778/4), to be published.

92. W. H. Bamford, *A Summary of Environmentally Assisted Crack-Growth Studies Performed at Westinghouse Electric Corporation Under Funding from the Heavy-Section Steel Technology Program,* NUREG/CR-5020 (ORNL/Sub/82/21598/1), to be published.

93. R. H. Bryan et al., *Pressurized-Thermal-Shock Test of 6-in.-Thick Pressure Vessels. PTSE-2: Investigation of Low Tearing Resistance and Warm Prestressing,* NUREG/CR-4888 (ORNL-6377), to be published.

94. J. H. Giovanola and R. W. Klopp, *Viscoplastic Stress-Strain Characterization of A533B Class 1 Steel,* NUREG/CR-5066 (ORNL/Sub/87-SA193/1), to be published.

95. L. F. Miller et al., *Neutron Exposure Parameters for the Metallurgical Test Specimens in the Fifth Heavy-Section Steel Technology Irradiation Series Capsules,* NUREG/CR-5019 (ORNL/TM-10582), to be published.

96. B. R. Bass et al., *Viscoplastic Dynamic Fracture Analyses of the WP-1 Series of Wide-Plate Crack-Arrest Tests*, NUREG/CR report (ORNL report), to be published.

CONTENTS

FOREWORD iii
LIST OF TABLES xv
LIST OF FIGURES xix
ABSTRACT 1
INTRODUCTION 1
MATERIALS AND SPECIMENS 2
CAPSULE DESIGN AND IRRADIATION 3
MATERIAL CHARACTERIZATION 16
    TENSILE TESTING 16
    CHARPY IMPACT TESTING 17
    FRACTURE TOUGHNESS TESTING 35
    COMPARISON OF RESULTS AND STATISTICAL ANALYSES 72
DISCUSSION 82
CONCLUSIONS 85
ACKNOWLEDGMENTS 86
REFERENCES 86
APPENDIX A. SPECIMEN LOADINGS AND IRRADIATION FACILITIES 91
APPENDIX B. TENSILE AND CHARPY V-NOTCH IMPACT DATA 115

LIST OF TABLES

Table 1. Chemical composition of Plate 02 and submerged-arc welds 4

Table 2. Submerged-arc weld parameter summary 4

Table 3. Average tensile strength changes with irradiation . . 23

Table 4. Comparison of Charpy impact energy for unirradiated pressure vessel plate and submerged-arc welds 29

Table 5. Comparison of Charpy impact energy for irradiated pressure vessel plate and submerged-arc welds 30

Table 6. Effect of irradiation on Charpy impact properties of plate and submerged-arc welds 33

Table 7. Comparison among several predictive expressions of Charpy impact transition temperature increase for pressure vessel plate and submerged-arc welds 34

Table 8. Transition region 1TCS test data for unirradiated pressure vessel plate and submerged-arc welds 38

Table 9. Ductile-shelf region 1TCS test data for unirradiated pressure vessel plate and submerged-arc welds 41

Table 10. Statistical comparison of 1TCS K_{Jc} results for unirradiated pressure vessel plate and submerged-arc welds 49

Table 11. Statistical comparison of 1TCS mean tearing modulus and mean J = 8.8T value with temperature for unirradiated plate and submerged-arc welds 60

Table 12. Transition-region 1TCS test data for irradiated pressure vessel plate and submerged-arc welds 62

Table 13. Ductile-shelf region 1TCS test data for irradiated pressure vessel plate and submerged-arc welds 65

Table 14. Statistical comparison of 1TCS KJc results for irradiated pressure vessel plate and submerged-arc welds 68

Table 15. Transition-region 1TCS test data for irradiated Plate 02; test temperature adjusted for mean fluence = 1.95×10^{23} neutrons/m^2 (>1 MeV) 69

Table 16. Statistical comparison of 1TCS mean tearing modulus and mean J = 8.8T value with temperature for irradiated plate and submerged-arc welds 73

LIST OF TABLES (CONTINUED)

Table 17. Comparison of Charpy V-notch and 1TCS transition temperature shifts due to irradiation 74

Table 18. Comparison of Charpy V-notch and 1TCS ductile shelf changes due to irradiation 76

Table 19. Comparison of PVRC-MPC predicted fracture toughness behavior and experimentally determined behavior 79

Table 20. Coefficients of variation for unirradiated Charpy impact and fracture toughness tests 82

Table 21. Statistical variations in fracture toughness results for HSST Plate 02 83

Table 22. Comparison of 95% confidence intervals for transition temperature shifts of Charpy impact and fracture toughness tests . . 84

Table A1. Location of 1T specimens in capsule A 93

Table A2. Location of Charpy specimens in capsule A 94

Table A3. Location of 1T specimens in capsule B 96

Table A4. Location of Charpy specimens in capsule B 97

Table A5. Location of 1T specimens in capsule C 99

Table A6. Location of Charpy specimens in capsule C 100

Table A7. Chronological history of the irradiation of the three capsules of the Fourth Irradiation Series 105

Table A8. Operating conditions of capsule A thermocouples through entire irradiation period 107

Table A9. Operating conditions of capsule B thermocouples through entire irradiation period 108

Table A10. Operating conditions of capsule C thermocouples through entire irradiation period 109

Table A11. History of operation of thermocouples in capsule A . 110

Table A12. History of operation of thermocouples in capsule B . 111

Table A13. History of operation of thermocouples in capsule C . 112

Table B1. Unirradiated tensile properties for Plate 02 and submerged-arc welds 115

LIST OF TABLES (CONTINUED)

Table B2. Irradiated tensile properties for Plate 02 and submerged-arc welds 117

Table B3. Curve fit coefficients for yield and ultimate strengths 118

Table B4. Unirradiated Charpy impact properties for Plate 02 . 119

Table B5. Unirradiated Charpy impact properties for weld 68W . 121

Table B6. Unirradiated Charpy impact properties for weld 69W . 122

Table B7. Unirradiated Charpy impact properties for weld 70W . 124

Table B8. Unirradiated Charpy impact properties for weld 71W . 125

Table B9. Irradiated Charpy impact properties for Plate 02 . . 126

Table B10. Irradiated Charpy impact properties for weld 68W . . 128

Table B11. Irradiated Charpy impact properties for weld 69W . . 129

Table B12. Irradiated Charpy impact properties for weld 70W . . 130

Table B13. Irradiated Charpy impact properties for weld 71W . . 131

Table B14. Irradiated Charpy impact properties for Plate 02 . . 132

LIST OF FIGURES

Fig. 1. HSST Plate 02 microstructure 5

Fig. 2. HSST weld 68W microstructure 6

Fig. 3. HSST weld 69W microstructure 7

Fig. 4. HSST weld 70W microstructure 8

Fig. 5. HSST weld 71W microstructure 9

Fig. 6. Tensile specimen configuration 10

Fig. 7. Charpy V-notch specimen configuration 11

Fig. 8. Fracture toughness specimen (1TCS) configuration . . . 12

Fig. 9. Irradiation capsule design 13

Fig. 10. Specimen holder frame and loading configuration . . . 14

Fig. 11. Rear view of partially assembled capsule 15

Fig. 12. Effects of irradiation on variation of tensile strengths with temperature for Plate 02 18

Fig. 13. Effects of irradiation on variation of tensile strengths with temperature for weld 68W 19

Fig. 14. Effects of irradiation on variation of tensile strengths with temperature for weld 69W 20

Fig. 15. Effects of irradiation on variation of tensile strengths with temperature for weld 70W 21

Fig. 16. Effects of irradiation on variation of tensile strengths with temperature for weld 71W 22

Fig. 17. Effects of irradiation on variation of Charpy V-notch energy with temperature for Plate 02 24

Fig. 18. Effects of irradiation on variation of Charpy V-notch energy with temperature for weld 68W 25

Fig. 19. Effects of irradiation on variation of Charpy V-notch energy with temperature for weld 69W 26

Fig. 20. Effects of irradiation on variation of Charpy V-notch energy with temperature for weld 70W 27

LIST OF FIGURES (CONTINUED)

Fig. 21. Effects of irradiation on variation of Charpy V-notch energy with temperature for weld 71W 28

Fig. 22. Effects of irradiation on variation of Charpy V-notch energy with temperature for Plate 02; test temperatures adjusted to mean fluence of 1.77×10^{23} neutrons/m^2 (>1 MeV) 32

Fig. 23. Typical J-integral R-curve (weld 69W, 121°C, unirradiated), produced with the single-specimen unloading compliance technique 36

Fig. 24. Effects of irradiation on variation of fracture toughness with temperature for Plate 02 44

Fig. 25. Effects of irradiation on variation of fracture toughness with temperature for weld 68W 45

Fig. 26. Effects of irradiation on variation of fracture toughness with temperature for weld 69W 46

Fig. 27. Effects of irradiation on variation of fracture toughness with temperature for weld 70W 47

Fig. 28. Effects of irradiation on variation of fracture toughness with temperature for weld 71W 48

Fig. 29. Effects of irradiation on variation of β-corrected fracture toughness with temperature for Plate 02 50

Fig. 30. Effects of irradiation on variation of β-corrected fracture toughness with temperature for weld 68W 51

Fig. 31. Effects of irradiation on variation of β-corrected fracture toughness with temperature for weld 69W 52

Fig. 32. Effects of irradiation on variation of β-corrected fracture toughness with temperature for weld 70W 53

Fig. 33. Effects of irradiation on variation of β-corrected fracture toughness with temperature for weld 71W 54

Fig. 34. Effects of irradiation on variation of tearing modulus with temperature for Plate 02 55

Fig. 35. Effects of irradiation on variation of tearing modulus with temperature for weld 68W 56

Fig. 36. Effects of irradiation on variation of tearing modulus with temperature for weld 69W 57

LIST OF FIGURES (CONTINUED)

Fig. 37. Effects of irradiation on variation of tearing modulus with temperature for weld 70W 58

Fig. 38. Effects of irradiation on variation of tearing modulus with temperature for weld 71W 59

Fig. 39. Effects of irradiation on variation of fracture toughness with temperature for Plate 02, test temperatures adjusted to mean fluence of 1.95×10^{23} neutrons/m^2 (>1 MeV) 70

Fig. 40. Effects of irradiation on variation of β-corrected fracture toughness with temperature for Plate 02, test temperatures adjusted to mean fluence of 1.95×10^{23} neutrons/m^2 (>1 MeV) 71

Fig. 41. Correlation of radiation-induced Charpy V-notch 41-J transition temperature shift with radiation-induced fracture toughness (K_{Jc} at 125 MPa$\sqrt{m}$) shift and with radiation-induced β-corrected fracture toughness ($K_{\beta c}$ at 90 MPa$\sqrt{m}$) shift 75

Fig. 42. Correlation of radiation-induced Charpy V-notch upper-shelf energy change with radiation-induced 1TCS-J_{Ic} change (at 204°C) 77

Fig. 43. Correlation of radiation-induced flow stress change (at 204°C) with radiation-induced 1TCS-tearing-modulus change (at 204°C) and with radiation-induced 1TCS-J = 8.8*T change (at 204°C) 78

Fig. 44. Comparison of radiation-induced fracture toughness transition temperature shift (K_{Jc} at 125 MPa$\sqrt{m}$) with PVRC-MPC predictions 80

Fig. 45. Comparison of radiation-induced upper-shelf fracture toughness changes (K_{Jc} at 204°C) with PVRC-MPC predictions 81

Fig. A1. Location of thermocouples and specimen positions for the Fourth Series 92

Fig. A2. Capsule irradiation positions at the BSR utilized for the Fourth Series 102

Fig. A3. Flow diagram of irradiation facility 103

Fig. A4. Record of daily temperature range of 39 thermocouples during the first 6 months of operation of capsule A 106

CHARACTERIZATION OF IRRADIATED CURRENT-PRACTICE WELDS AND A533 GRADE B CLASS 1 PLATE FOR NUCLEAR PRESSURE VESSEL SERVICE*

J. J. McGowan,† R. K. Nanstad, and K. R. Thoms‡

ABSTRACT

Studies of the effects of neutron irradiation on fracture toughness properties of steels have generally included a minimum number of tests for each material condition. The present study attempts to apply statistical analyses, with multiple testing at selected temperatures, to assess the accuracy and reliability of the results. Fracture toughness test specimens were irradiated in the Bulk Shielding Reactor at Oak Ridge National Laboratory at 288°C to target neutron fluences of 2×10^{23} neutrons/m^2 (>1 MeV). The materials were ASTM A533 grade B class 1 plate (HSST Plate 02) and four submerged-arc welds representing the current fabrication practice for nuclear pressure vessels. Both unirradiated and irradiated specimens were tested by two separate laboratories, and multiple tests were conducted at selected temperatures. Statistical analyses permitted the determination of material and test variability and an interlaboratory comparison. Behavior in both the transition and ductile-shelf regions was studied. The results demonstrated the relatively low radiation sensitivity of low copper/nickel welds and the qualitative agreement between Charpy impact and fracture toughness observations of toughness degradation.

INTRODUCTION

Exposure of materials in light-water reactors to neutron irradiation may result in serious embrittlement, which may take the form of a decrease in Charpy V-notch (CVN) upper-shelf energy and/or an increase in CVN brittle-to-ductile transition temperature. For materials in light-water reactor pressure vessels that have CVN upper-shelf energy less than 68 J, Federal Regulations (10 CFR Part 50) require the performance of fracture mechanics analyses that demonstrate a safe margin for continued vessel operation. One acceptable analysis is presented in Generic Safety

---

*Research sponsored by the Office of Nuclear Regulatory Research, Division of Engineering Safety, U.S. Nuclear Regulatory Commission under Interagency Agreement DOE 40-551-75 with the U.S. Department of Energy under contract DE-AC05-84OR21400 with Martin Marietta Energy Systems, Inc.

†Formerly with Oak Ridge National Laboratory, now with Virginia Military Institute, Lexington, VA 24450.

‡Engineering Technology Division.

Issue A-11 on Reactor Vessel Materials Toughness.[1] In this particular method, the concept of tearing instability is used under elastic-plastic conditions. The primary material properties needed to perform this analysis are the J-integral resistance (J-R) curves.

Previous irradiation programs[2] [Second and Third Heavy-Section Steel Technology (HSST) Irradiation Series] have considered materials with low CVN upper-shelf energy. These previous programs utilized a large range of specimen sizes (12.5 to 101.6 mm thick), because the aim of the program was to produce data applicable to actual reactor vessels and to study size effects on irradiated J-R behavior. The low upper-shelf materials showed a considerable decrease in J-R curve performance as a consequence of irradiation. The results of the program indicated that 25-mm-thick specimens would be adequate to describe the ductile tearing behavior of the thicker reactor vessel.

The Second and Third Series dealt with materials that were representative of welds from "early" vessels. Because the results showed a pronounced effect of irradiation on J-R curves, there was also considerable interest in the effects of irradiation on other materials. Therefore, another irradiation program, the Fourth Heavy-Section Steel Technology Irradiation Series, was initiated to study the effect of neutron irradiation on weld metals fabricated with "current" welding practice. This new practice minimized residual elements (notably phosphorus, nickel, and copper) that heightened irradiation sensitivity. The program includes four "current-practice" welds and one ASTM A533 grade B class 1 plate. Tensile, Charpy V-notch, and 25-mm fracture toughness specimens were characterized before and after irradiation at 288°C to 2×10^{23} neutrons/m^2 (>1 MeV). A sufficient number of specimens were tested in a cooperative program with Materials Engineering Associates (MEA) to determine the statistical variation in the Charpy V-notch and fracture toughness properties. Multiple tests were conducted at each of several temperatures for each material. Standard deviations and coefficients of variation were determined, and results from the two laboratories were compared. This report describes the materials, irradiation, testing, and analyses of specimens in the Fourth HSST Irradiation Series.

MATERIALS AND SPECIMENS

The plate material was fabricated from 305-mm-thick ASTM A533 grade B class 1 Mn-Mo-Ni steel produced by Lukens Steel Company for the HSST Program.[3] This plate material was designated HSST Plate 02, and portions of it have been used in many investigations around the world. All test specimens were prepared in the transverse (TL) orientation. The chemical composition of the plate material is listed in Table 1.

All four submerged-arc weldments were made in A533 grade B class 1 plate. Two of the weldments fabricated by Combustion Engineering, Inc., were supplied by the Electric Power Research Institute (EPRI). HSST weld 68W was produced as a 178-mm-thick, submerged-arc weldment, using Linde 0091 flux and 4.8-mm-diam MIL-B-4 (low copper and phosphorus) wire, and was designated "CGS" in EPRI studies.[4] HSST weld 69W was produced as a 300-mm-thick, submerged-arc weldment, using Linde 0091 flux and 4.8-mm-diam MIL-B-4 wire, and was designated "CHS" in EPRI studies.[4] The other two welds were supplied by Babcock and Wilcox Company.[5] Both welds

were produced as 174-mm-thick, submerged-arc weldments using Mn-Mo-Ni (SFA-5.23EF2N) filler wire. HSST weld 70W was fabricated with Linde 0124 flux, whereas HSST weld 71W was fabricated with Linde 0080 flux. A summary of the weld parameters is listed in Table 2. All test specimens from welds were prepared with longitudinal axes perpendicular to the weld centerline and crack propagation direction parallel to the surface. The four weldments are considered "current-practice" and are of low copper content. Two of the welds, 68W and 69W, also had low nickel contents. The chemical compositions of the four weld materials are also presented in Table 1.

Micrographs of all five materials are shown in Figs. 1 through 5. For comparison purposes, micrographs at 400 and 800× are shown for each material. Plate 02 has a microstructure typical of an A533 grade B class 1 alloy that has been quenched and tempered in thick sections. In the quarter- to mid-thickness of the plate, as shown in Fig. 1, the alloy is composed primarily of upper bainite and granular bainite. The grain size is about ASTM 8–9 and the hardness is about HRB 90. The four welds are also primarily bainite, but the microstructures are finer than that of Plate 02. Figures 2 through 5 are micrographs of the four welds that are typical of Mn-Mo-Ni submerged-arc welds. The grain size of welds 68W, 69W, and 70W are all about ASTM 12–13, whereas that of weld 71W is about ASTM 9–10. The inclusion content in these welds is relatively small. Some inclusions can be seen in the 800× micrographs for all the materials. Hardnesses are about HRB 95, 100, 93, and 92 for welds 68W through 71W, respectively. The differences in the hardness of the welds are reflective of the strength differences; that is, higher hardness corresponds to higher strength.

Miniature tensile specimens were used in this study, as shown in Fig. 6. The specimen size and design were dictated primarily by the physical space available for irradiation. The impact specimen used was the full-size Charpy V-notch specimen shown in Fig. 7. The fracture toughness specimen used here was the 25.4-mm compact specimen modified for load-line displacement (Fig. 8), as recommended in ASTM Standard Test Method E813.[6]

CAPSULE DESIGN AND IRRADIATION

The specimens for this program were irradiated in three capsules at the Bulk Shielding Reactor (BSR). All three capsules were of identical design, with each holding a complement of sixty 25-mm-thick (1-in.) compact specimens (1TCS) and 100 smaller specimens (Charpy V-notch, tensile, or precracked Charpy). The general construction features of the capsules are shown in Fig. 9. The specimens were held in a carbon steel frame (shown in Fig. 10), with spring assemblies placed behind them so that they would press against an aluminum heater plate. The heater plate is divided into 12 individually controlled zones. A gas gap of 2.4 mm was maintained between the heater plate and the capsule front face. A much larger gap (12.7 mm) was maintained between the other faces and the capsule containment walls (12.7-mm-thick 6061-T6 aluminum). To remove heat from the capsule, a water jacket was installed over the capsule front face. A partially assembled capsule (Fig. 11, viewed from the back of the capsule) shows how the specimens were stacked in compartments. There were 15 compartments for 1TCS specimens (4 in each) and 5 compartments for

Table 1. Chemical composition of Plate 02 and submerged-arc welds

Material	Average composition (wt %)									
	C	Mn	P	S	Si	Cr	Ni	Mo	Cu	V
Plate 02	0.23	1.55	0.009	0.014	0.20	0.04	0.67	0.53	0.140	0.003
Weld 68W	0.15	1.38	0.008	0.009	0.16	0.04	0.13	0.60	0.040	0.007
Weld 69W	0.14	1.19	0.010	0.009	0.19	0.09	0.10	0.54	0.120	0.005
Weld 70W	0.10	1.48	0.011	0.011	0.44	0.13	0.63	0.47	0.056	0.004
Weld 71W	0.12	1.58	0.011	0.011	0.54	0.12	0.63	0.45	0.046	0.005

Table 2. Submerged-arc weld parameter summary

Weld	Manufacturer	Manufacturer's code	Thickness (m)	Linde flux	Postweld heat treatment		Comments
					Temperature (°C)	Time (h)	
68W	CE for EPRI	CGS	0.178	0091	621	25	Straight-wall groove
69W	CE for EPRI	CHS	0.300	0091	621	25	Double-U groove, cylindrical constraint
70W	B&W	MK-W-124	0.175	0124	607	48	Double-V groove
71W	B&W	MK-W-80	0.175	0080	607	48	Double-V groove

Y205726

Y206140

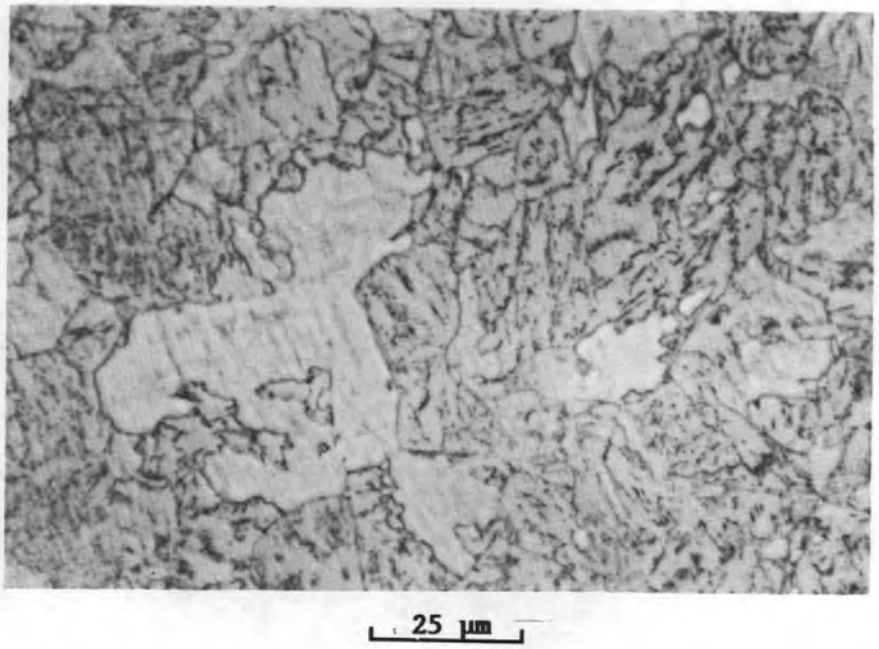

Fig. 1. HSST plate 02 microstructure.

Y205729

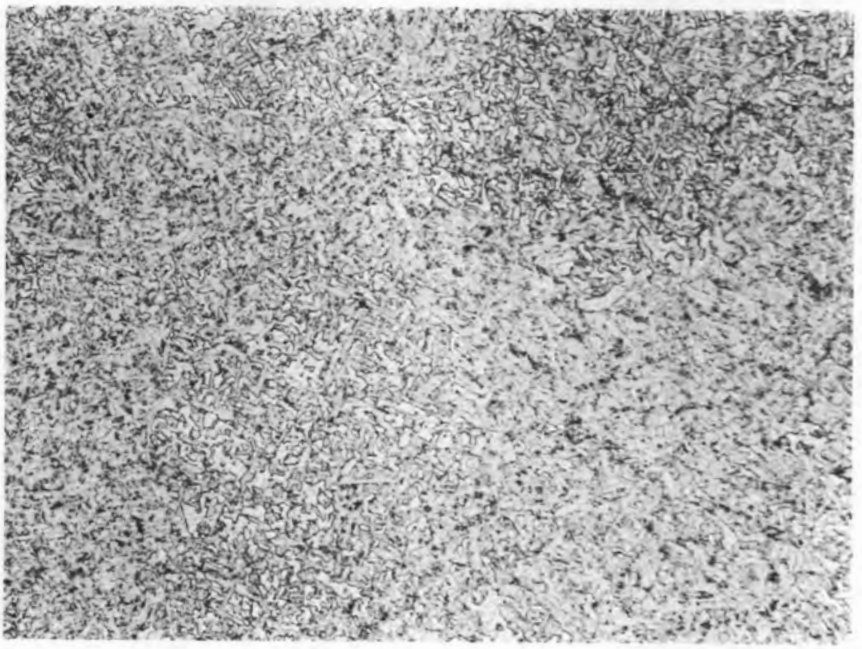

50 μm

Y206141

25 μm

Fig. 2. HSST weld 68W microstructure.

Y205733

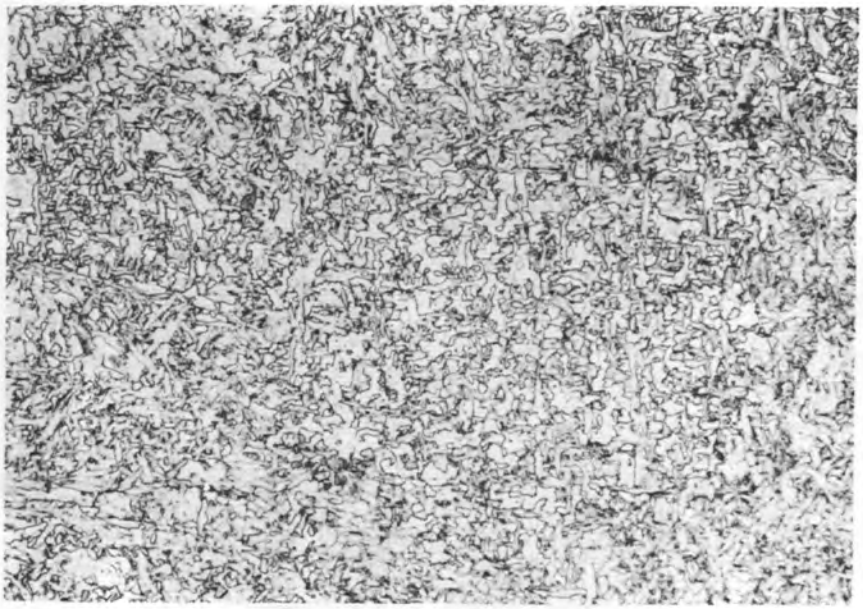

50 μm

Y206142

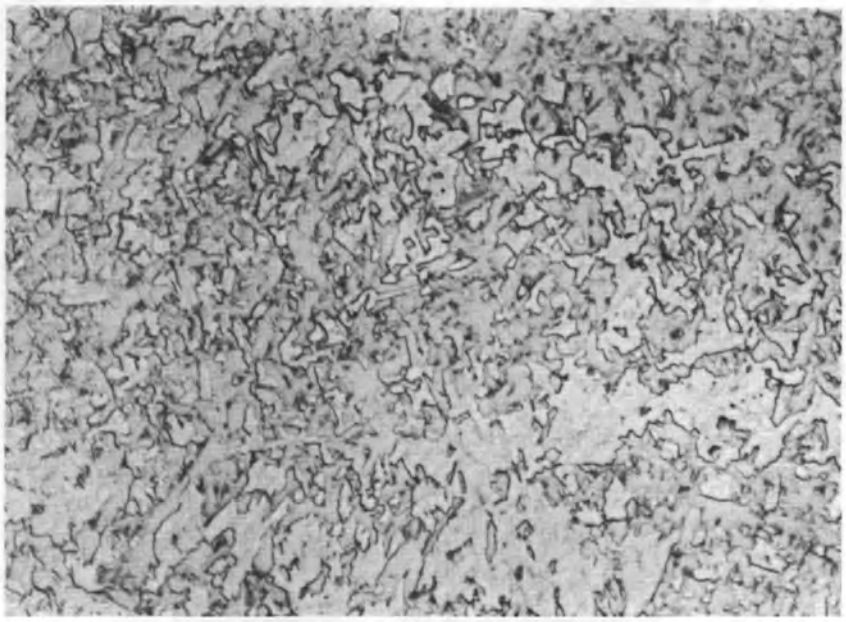

25 μm

Fig. 3. HSST weld 69W microstructure.

Y205738

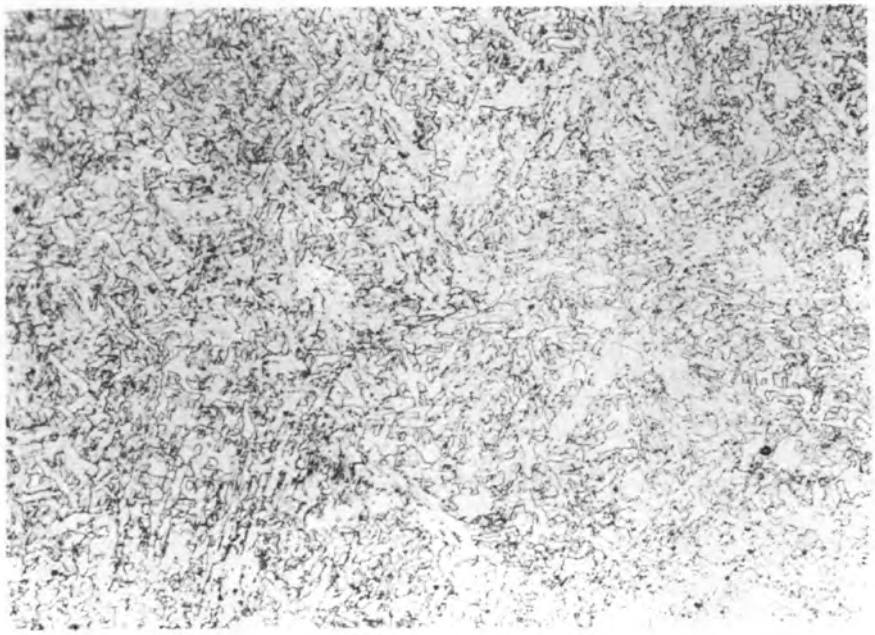

50 μm

Y206143

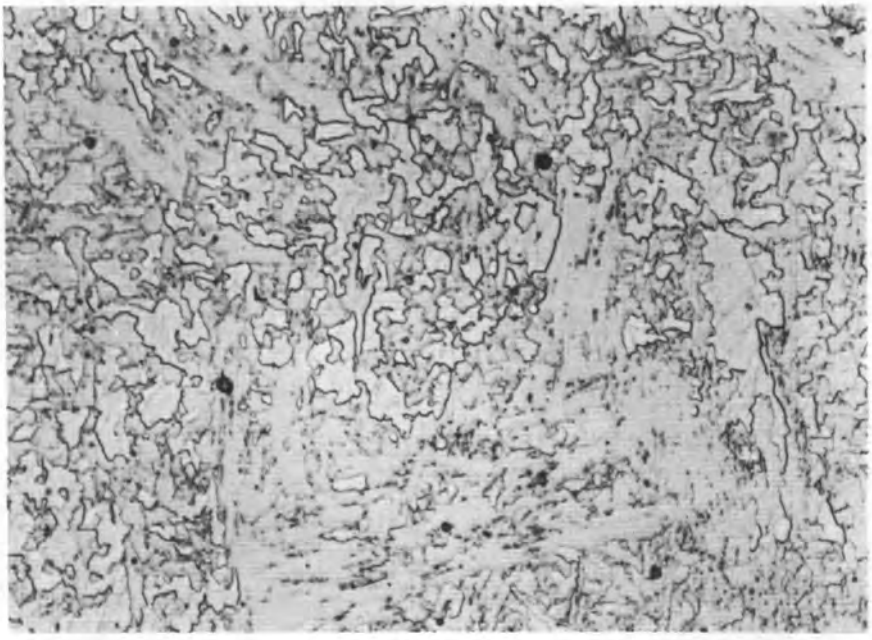

25 μm

Fig. 4. HSST weld 70W microstructure.

Y205741

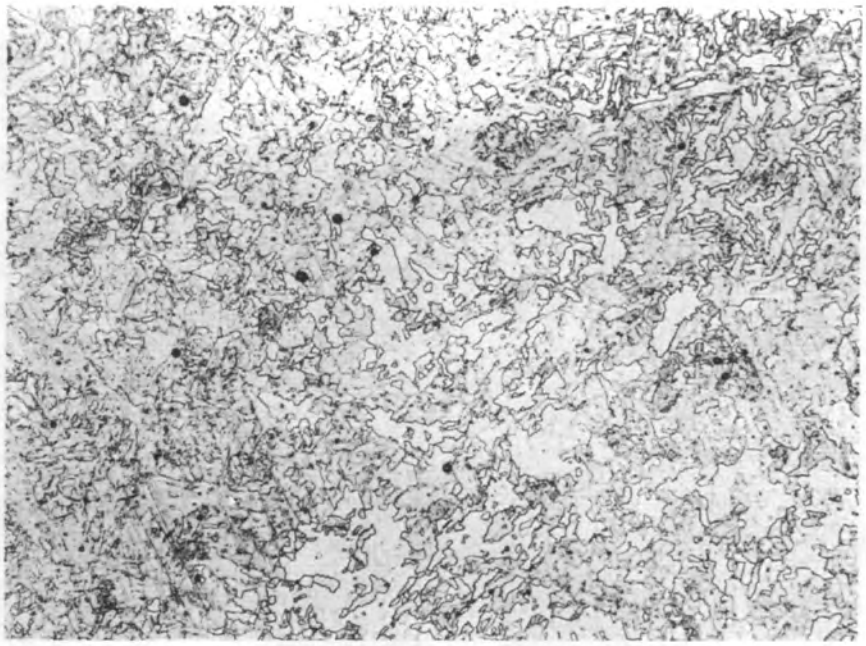

50 μm

Y206144

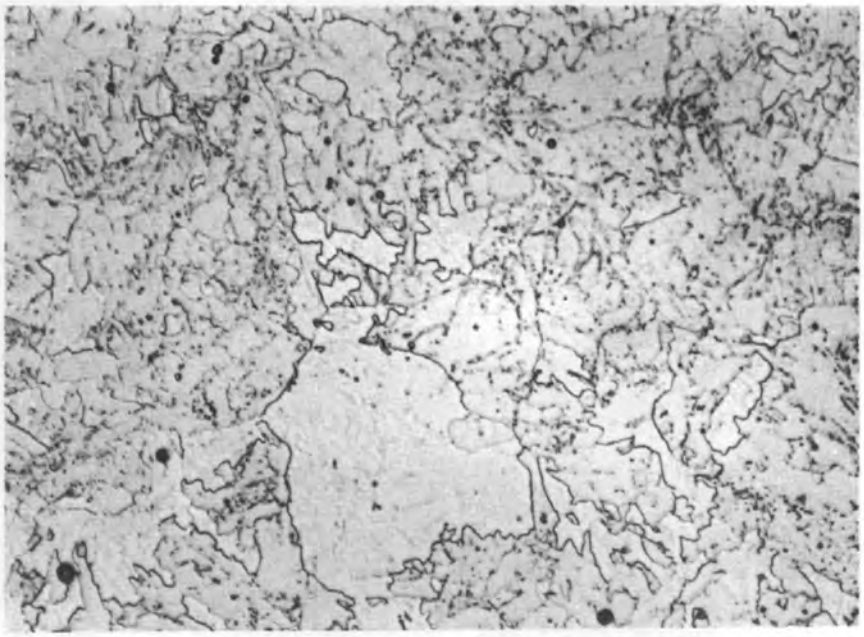

25 μm

Fig. 5. HSST weld 71W microstructure.

ORNL-DWG 84C-17315

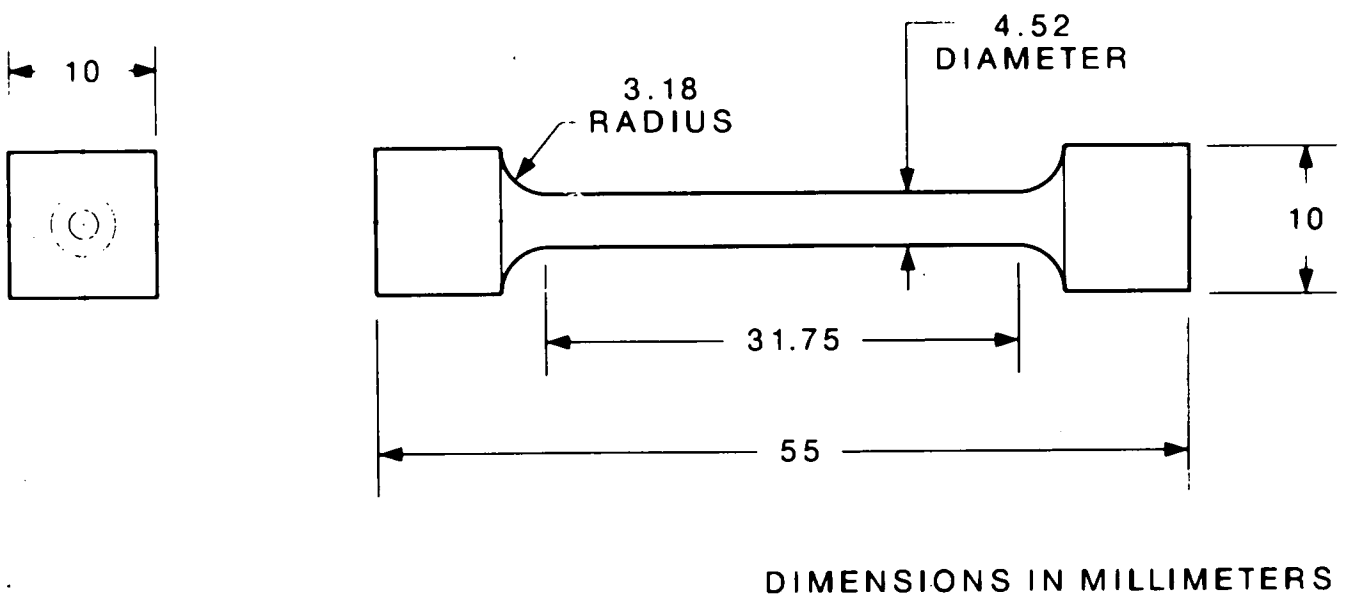

Fig. 6. Tensile specimen configuration.

ORNL-DWG 80-10832

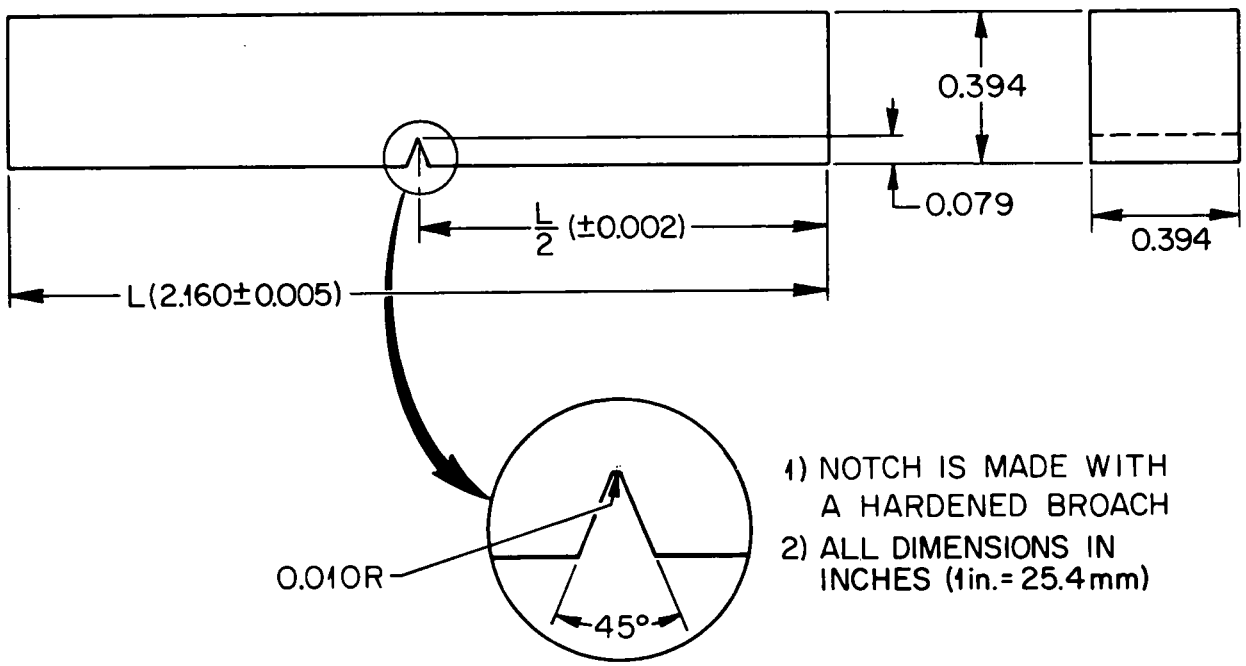

Fig. 7. Charpy V-notch specimen configuration.

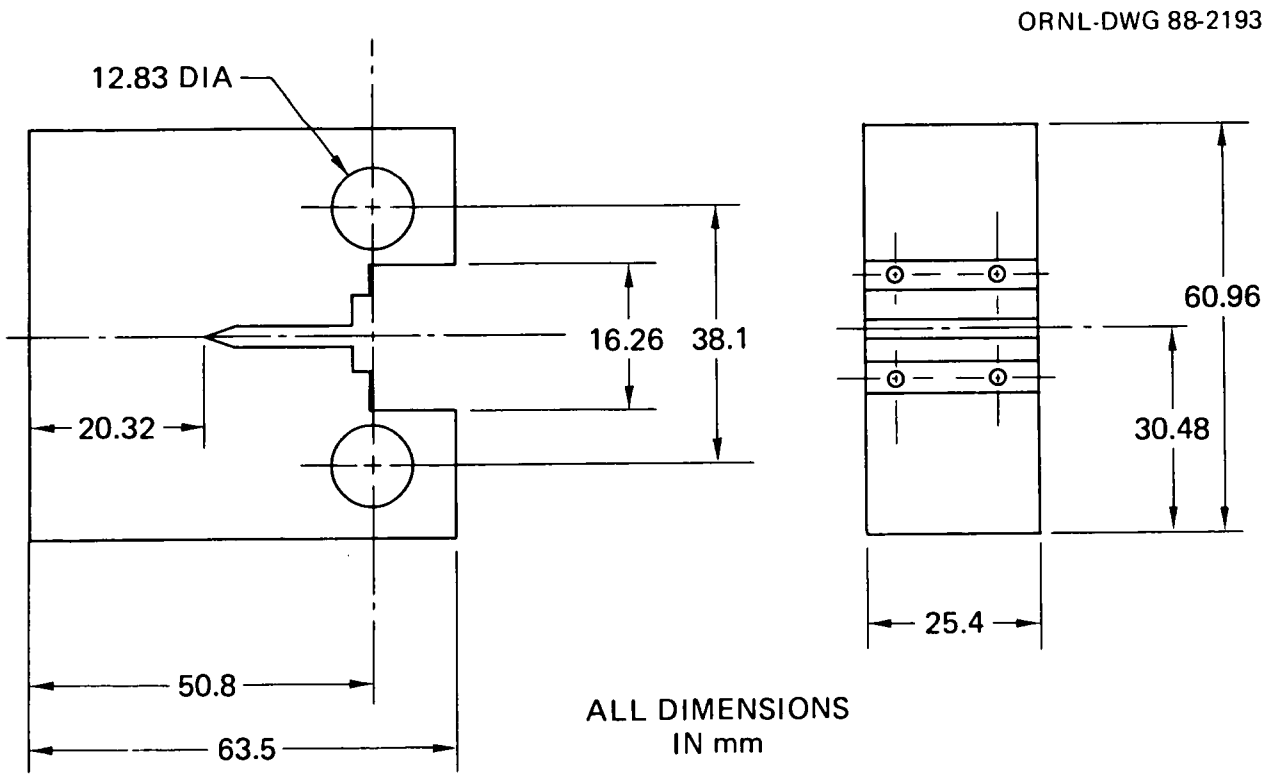

Fig. 8. Fracture toughness specimen (1TCS) configuration.

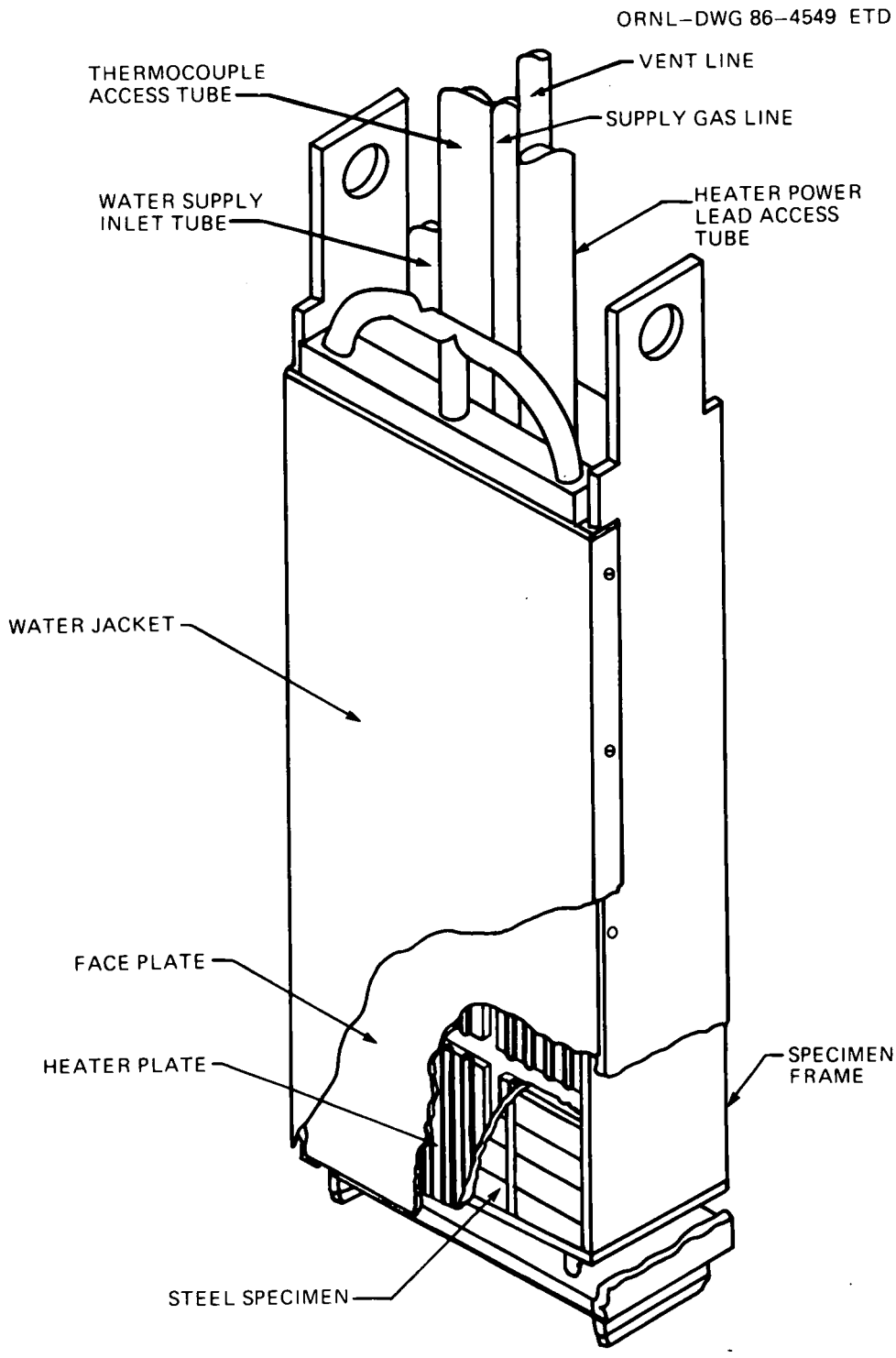

Fig. 9. Irradiation capsule design.

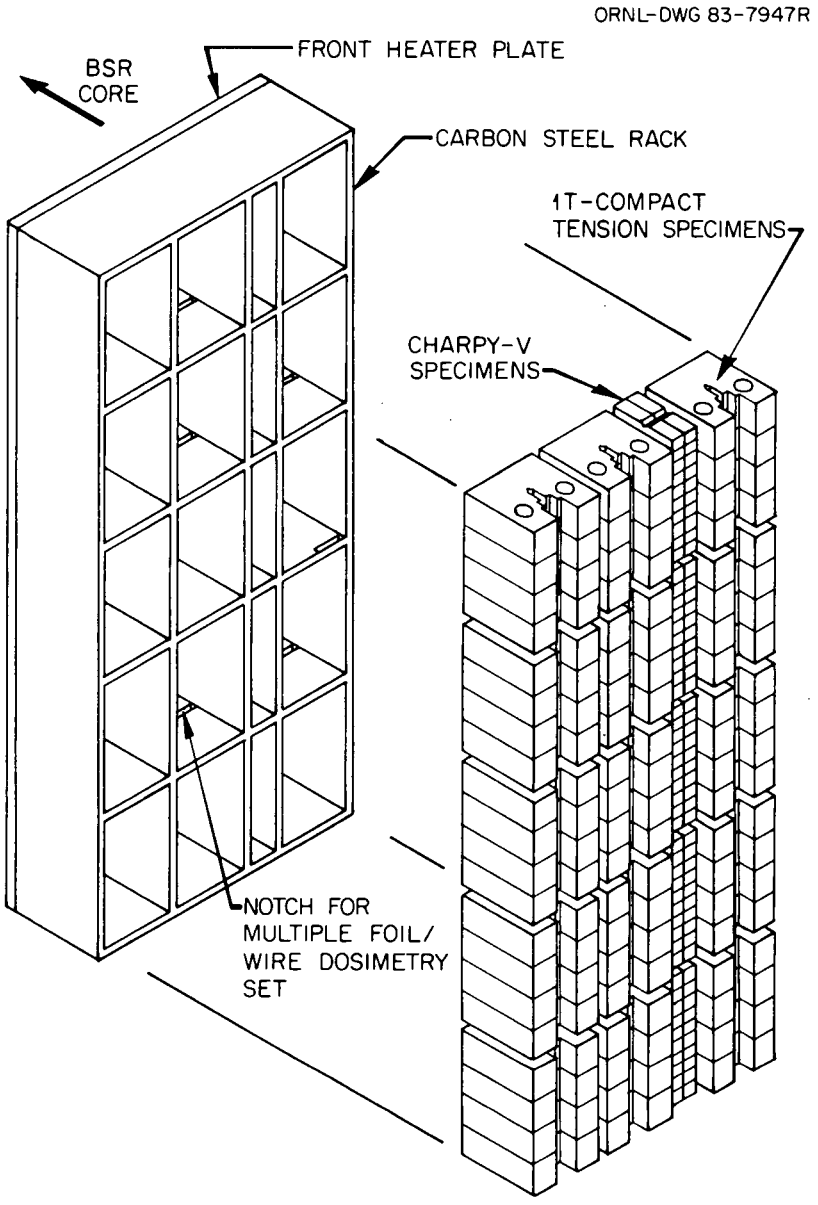

Fig. 10. Specimen holder frame and loading configuration.

Y-165053A

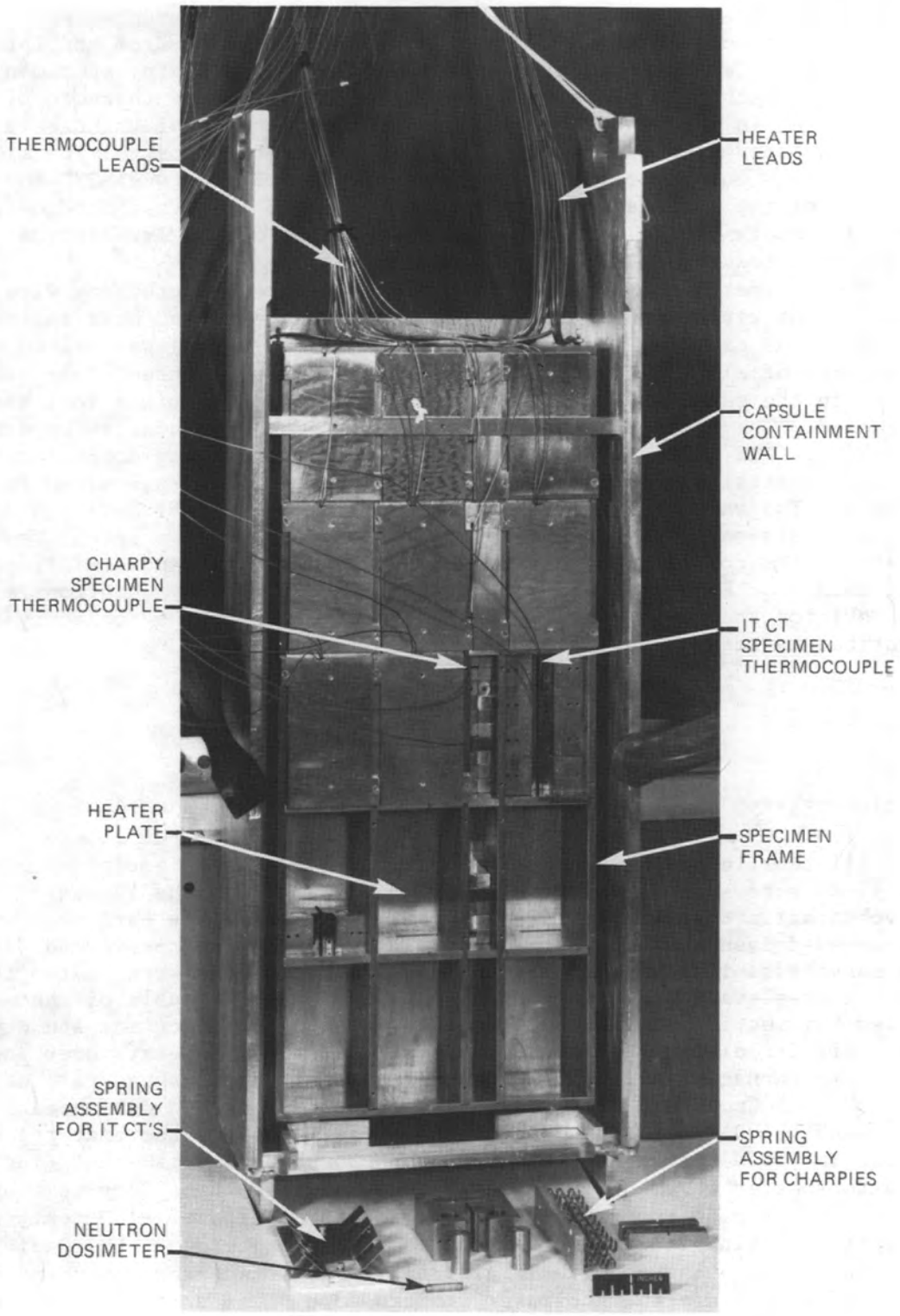

Fig. 11. Rear view of partially assembled capsule.

Charpy or tensile specimens (20 in each). A total of 40 thermocouples were used to monitor temperatures throughout each capsule. One-half of the 1TCS specimens (two in each compartment) were instrumented with thermocouples located at specimen mid-thickness, 1.6 mm from the fatigue crack plane. Two thermocouples were located in each Charpy specimen compartment by machining slots in the specimen frame; these thermocouples were located in the V-notch of the specimens. Because of the careful design and operation of the capsules, the temperature control for all specimens was quite good, with the temperature being between 283 and 293°C for most of the irradiation period. Each capsule was irradiated over about a 9-month period. (A detailed description of the irradiation history and results is provided in Appendix A.)

The dosimetry consisted of multiple foil sets and gradient wires. The gradient wires were sheathed iron wires that extended over the entire length of the capsule. One group of wires (short wires) was placed at the crack tips of all 1TCS specimens. Also included were three "long" wire groups in the capsule. Both fission and nonfission multiple foil sets were used. The fission sets used ^{238}U and ^{237}Np. The nonfission sets used ^{63}Cu, ^{46}Ti, ^{54}Fe, ^{58}Ni, ^{58}Fe, and ^{59}Co. Using these dosimeters, a complete spatial map of damage exposure parameters was determined for each capsule. The values of neutron fluences (>0.1 MeV and >1 MeV) and displacements per atom (dpa) were determined for each specimen. The uncertainties for the damage exposure parameters (standard deviation) were less than 8%. Fluences varied from about 1 to 2.5 × 10^{23} neutrons/m^2 (>1 MeV) for the experiment. Detailed information on the dosimetry is described in refs. 7 and 8.

MATERIAL CHARACTERIZATION

TENSILE TESTING

All tensile tests were performed at ORNL on three testing machines: two 45-kN screw-driven universal testing machines and one 490-kN servohydraulic test frame. All unirradiated testing was performed with the screw-driven system, whereas irradiated testing was performed with the servohydraulic system. The unirradiated specimens were heated for testing at elevated temperatures by a bath of water-soluble oil and were cooled for testing at low temperature by a bath of isopentane and dry ice. All irradiated specimens were tested at room temperature or above in an air furnace. All testing was performed at a crosshead rate of 0.5 mm/min. Crosshead displacement vs load was recorded during each test, and the 0.2% offset yield strength was measured from that trace. Errors in yield strength determined from crosshead displacement (instead of extensometer movement) were established at less than 3% by testing with an extensometer at room temperature. Upon completion of each test, neck diameter and final length were measured on each specimen. Unirradiated specimens were measured with Vernier calipers; irradiated specimens were measured with a digital toolmaker's microscope. The uniform strain was determined from the plastic displacement to maximum load on the trace of load vs crosshead motion.

Detailed tensile results for unirradiated and irradiated materials are given in Appendix B, Tables B1 and B2, respectively. Preirradiation

strength and ductility values are similar for four of the materials, with weld 69W having 20 to 30% higher strength than the other welds. Irradiation to fluences of 7 to 20 × 10^{22} neutrons/m^2 (>1 MeV) at 288°C had a pronounced effect on the strength of all the materials. The strengths before and after irradiation are shown in Figs. 12 through 16 for Plate 02 and welds 68W through 71W, respectively. Second degree polynomials for the unirradiated and irradiated strengths were determined by a least-squares procedure, and the coefficients for each material are listed in Appendix B, Table B3. Curve fits were used to average the yield and ultimate strengths over the temperature range from 22 to 288°C. The averages, listed in Table 3, show that irradiation affected the yield strength more than it did the ultimate strength. Table 3 also shows that the strength of Plate 02 was more sensitive to irradiation than were the strengths of the welds. The percentage increases in flow strengths, important in the analysis of tearing moduli, were about the same for all four welds. The plate, however, experienced a percentage increase in flow strength about double that of the welds. That behavior was expected because Plate 02 contained more copper and nickel than did the welds. Further information on tensile testing is available in ref. 9.

CHARPY IMPACT TESTING

The Charpy V-notch impact testing was divided between MEA and ORNL so that both laboratories would test specimens with equivalent irradiation fluences insofar as possible. The impact machines at both laboratories were calibrated in conformance with ASTM Standard Method E23,[10] including proof tests using "standardized specimens." The test procedures used at MEA were an alcohol bath at test temperatures below 0°C, a water bath between 0 and 100°C, and a recirculating air oven for temperatures above 100°C. All tests were conducted at MEA in less than 6 s after removal from the bath or oven. The test procedure at ORNL used electrical heating or cold gas (nitrogen) to adjust specimen temperature and a calibrated contact thermocouple to determine the specimen temperature. All tests were conducted at ORNL in less than 3 s after removal from the temperature conditioning chamber. This automated procedure has been verified by tests with instrumented specimens.

Preliminary tests of both unirradiated and irradiated specimens were conducted to approximate the Charpy transition curve, and specific temperatures were selected for the balance of the testing. Specimens were selected so that tests at each temperature would be conducted by both laboratories using specimens with similar neutron exposure and similar location in the weld or plate. The exception to this plan was weld 68W; ORNL tested all of the unirradiated specimens because of the small number of available specimens. Upon completion of testing, lateral expansion was measured and fracture appearance was estimated for each specimen. The test temperature, fracture energy, lateral expansion, and fracture appearance for each irradiated and unirradiated specimen are listed in Appendix B in Tables B4 through B13. The fracture energy results for both irradiated and unirradiated specimens of Plate 02 and welds 68W through 71W are shown graphically in Figs. 17 through 21, respectively.

Mean energies and standard deviations were determined for each selected temperature for each laboratory and for the combined data set, as listed in Tables 4 and 5 for unirradiated and irradiated specimens, respectively. For unirradiated specimens (Table 4), the means for the

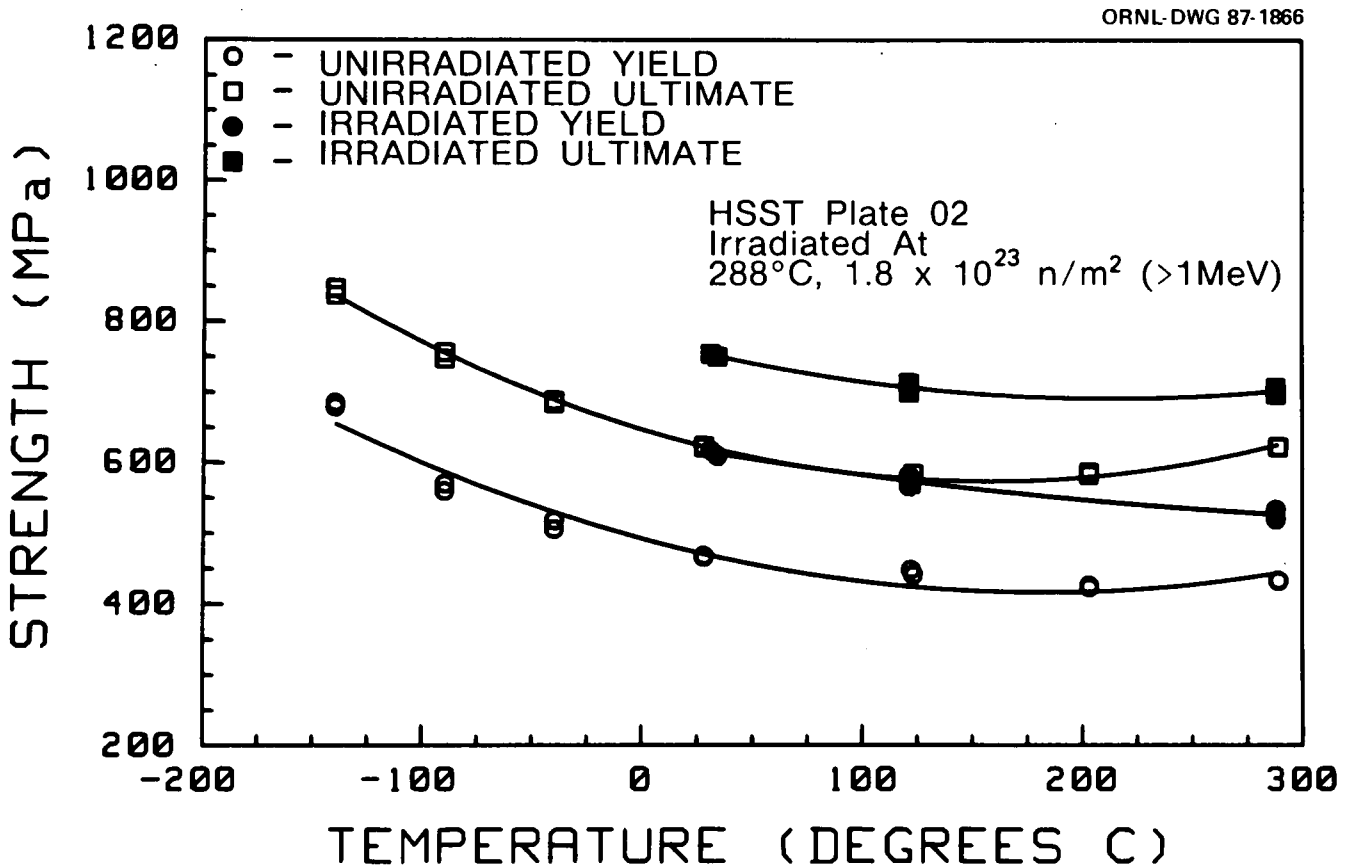

Fig. 12. Effects of irradiation on variation of tensile strengths with temperature for Plate 02.

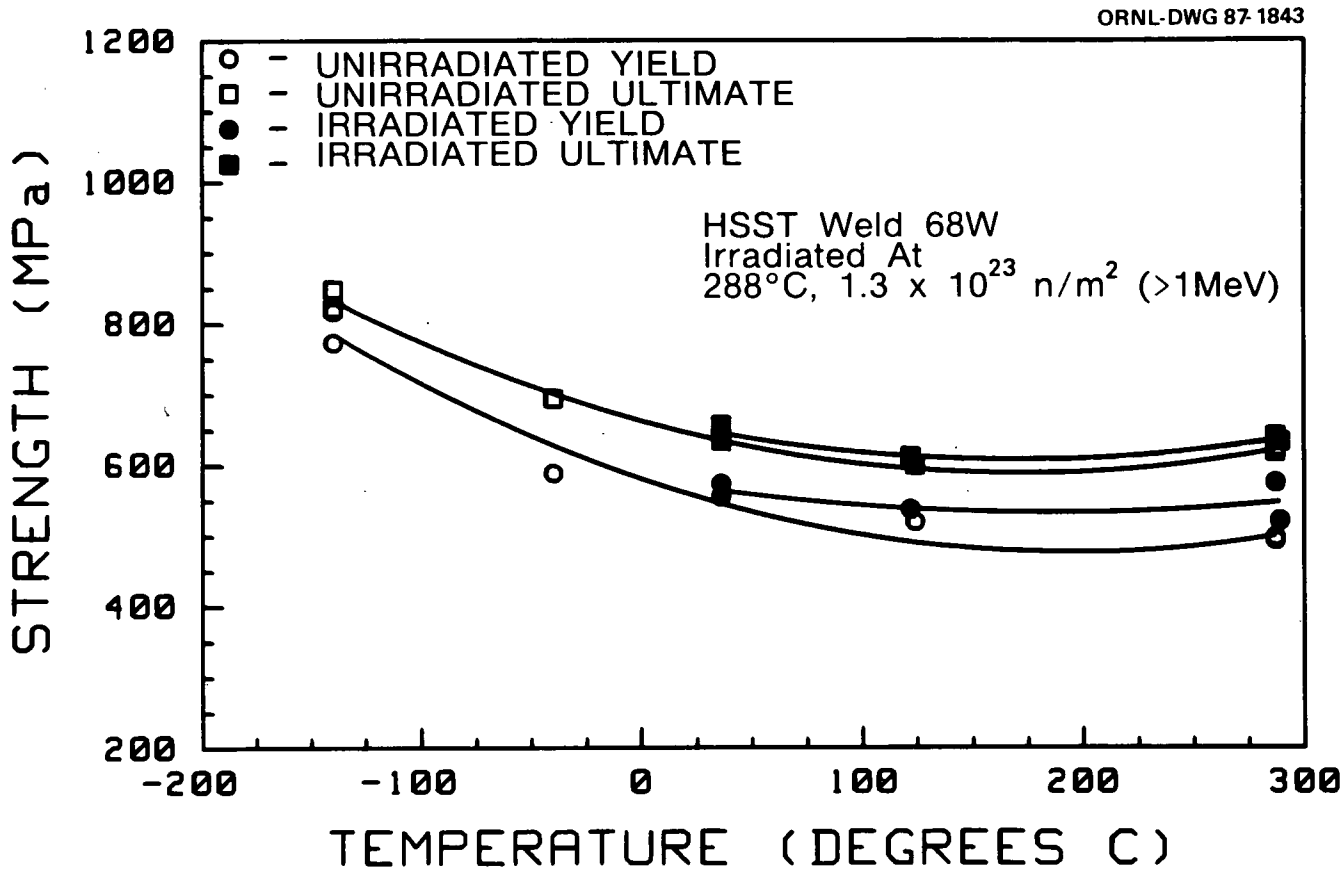

Fig. 13. Effects of irradiation on variation of tensile strengths with temperature for weld 68W.

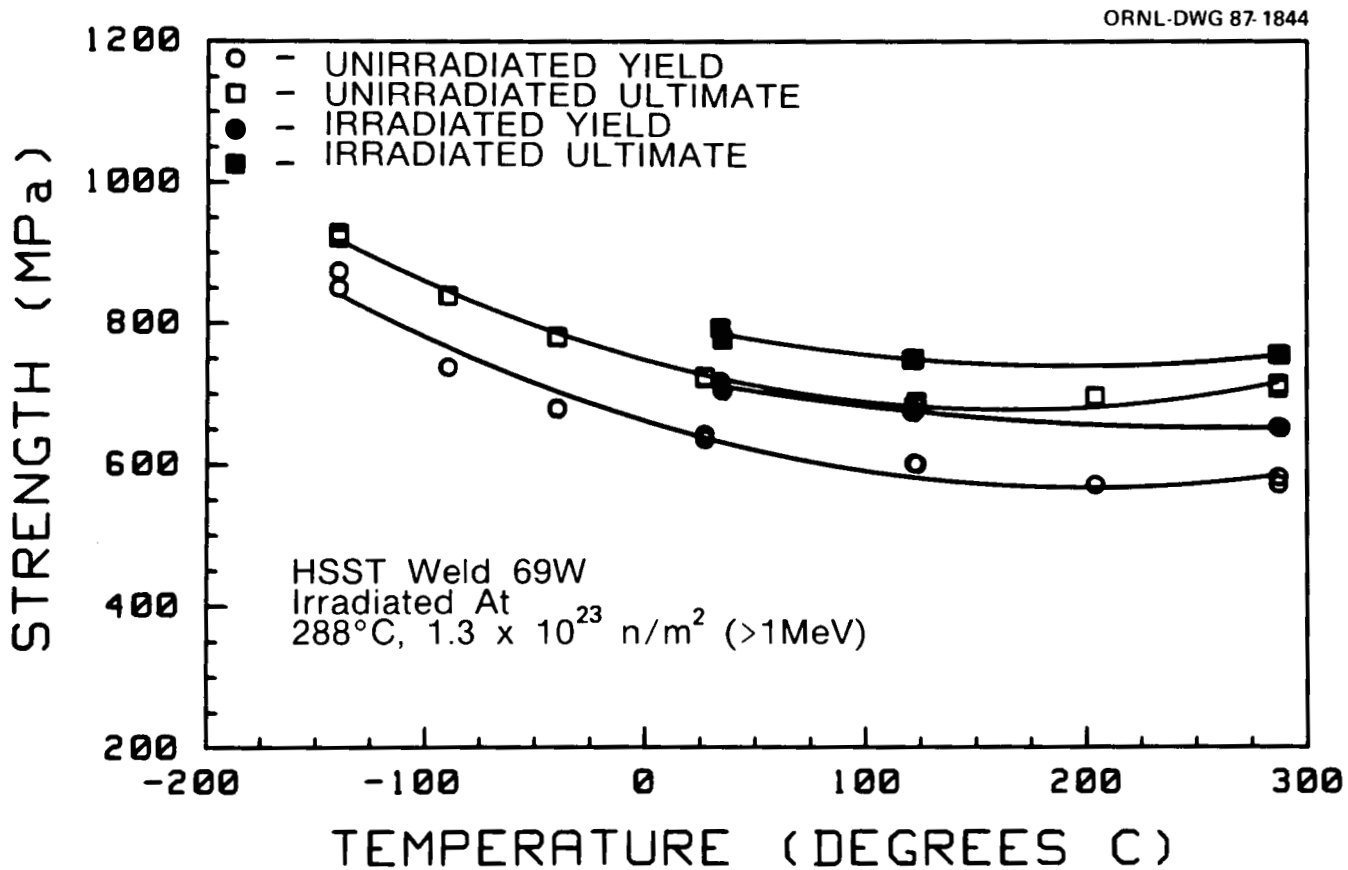

Fig. 14. Effects of irradiation on variation of tensile strengths with temperature for weld 69W.

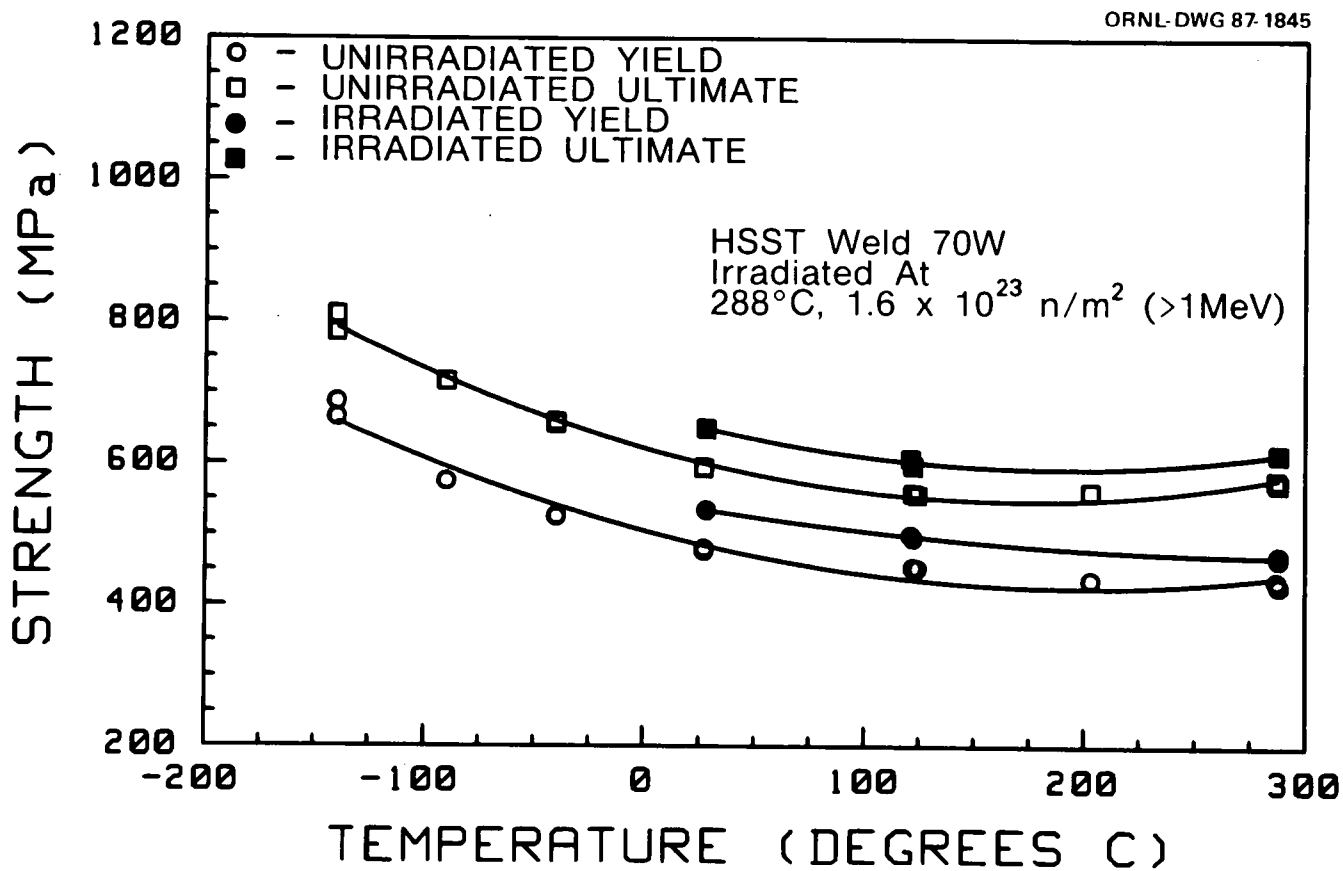

Fig. 15. Effects of irradiation on variation of tensile strengths with temperature for weld 70W.

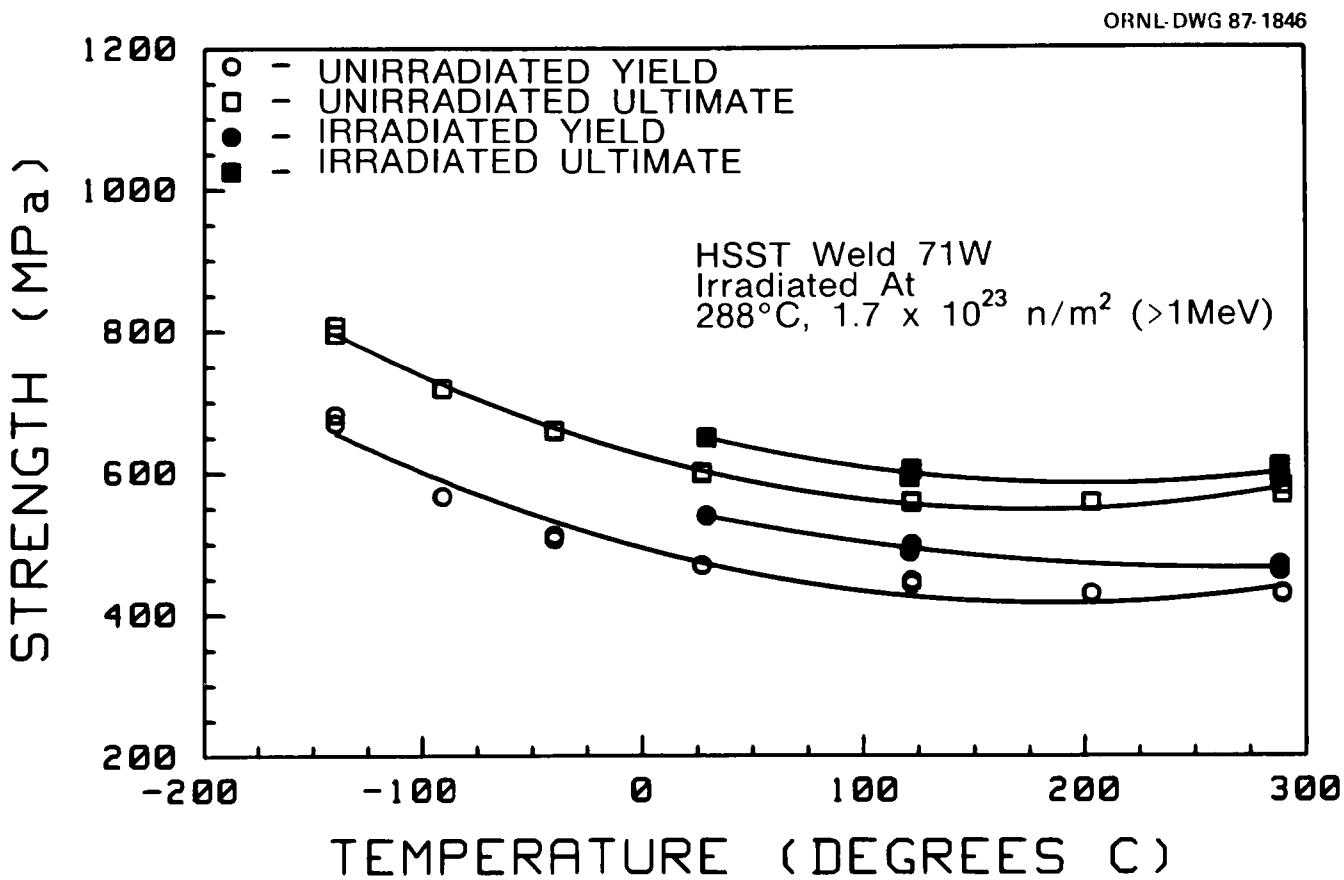

Fig. 16. Effects of irradiation on variation of tensile strengths with temperature for weld 71W.

Table 3. Average tensile strength changes with irradiation

Average fluence, 10^{23} n/m^2 (>1 MeV)	Average yield strength[a]			Average ultimate strength[a]			Average flow strength[a,b]		
	Unirradiated (MPa)	Irradiated (MPa)	Increase (%)	Unirradiated (MPa)	Irradiated (MPa)	Increase (%)	Unirradiated (MPa)	Irradiated (MPa)	Increase (%)
A533 grade B class 1 (HSST-02)									
1.85	432	564	31	590	707	20	511	635	24
Submerged-arc weld (HSST-68W)									
1.30	496	590	19	604	620	3	550	605	10
Submerged-arc weld (HSST-69W)									
1.31	584	672	15	692	752	9	638	712	12
Submerged-arc weld (HSST-70W)									
1.64	440	493	12	562	608	8	501	550	10
Submerged-arc weld (HSST-71W)									
1.66	430	489	14	563	602	7	496	545	10

[a]Note that the average is determined over the temperature range from 22 to 288°C.

[b]Flow strength is defined as the average of yield and ultimate strengths.

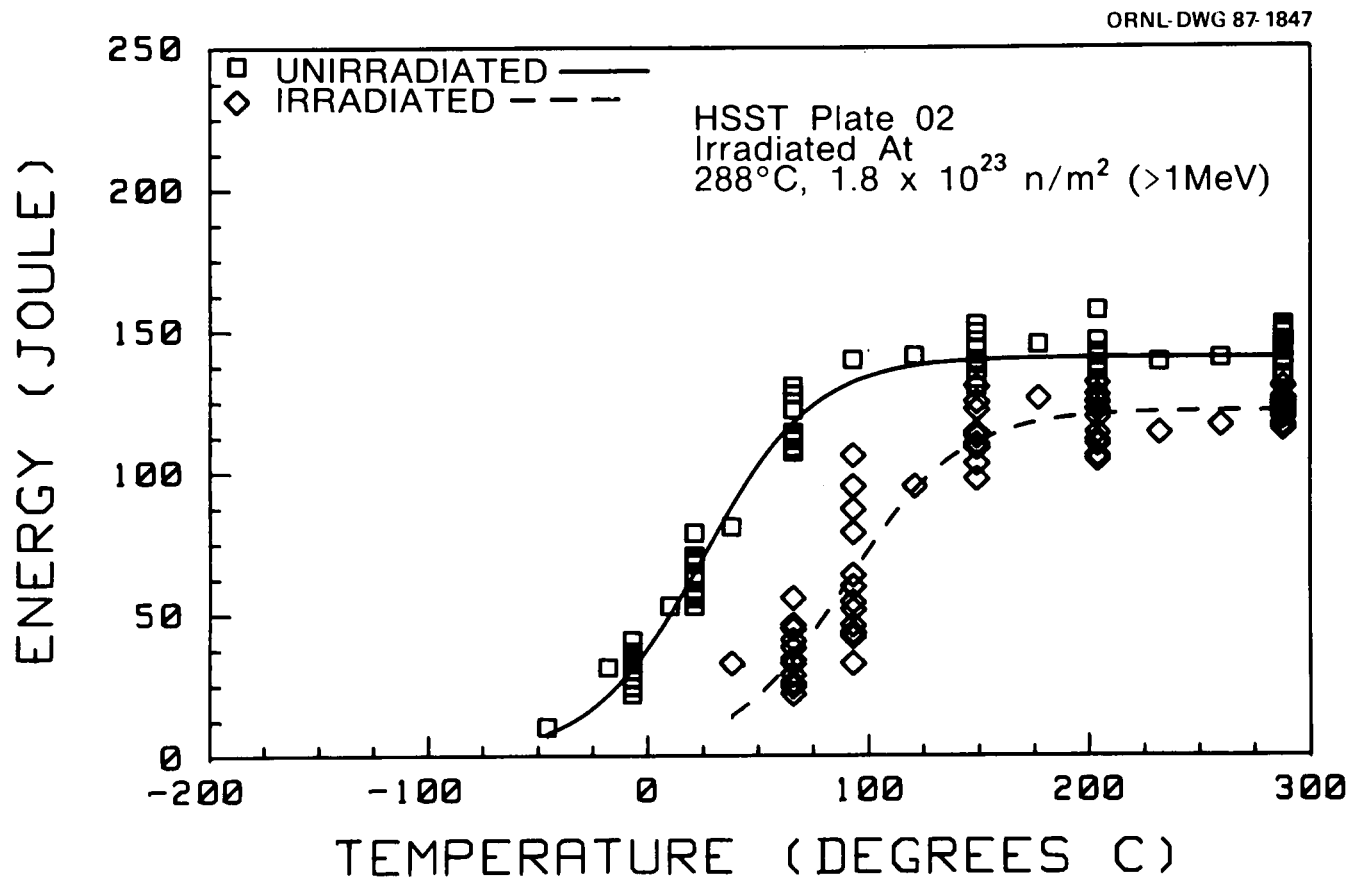

Fig. 17. Effects of irradiation on variation of Charpy V-notch energy with temperature for Plate 02.

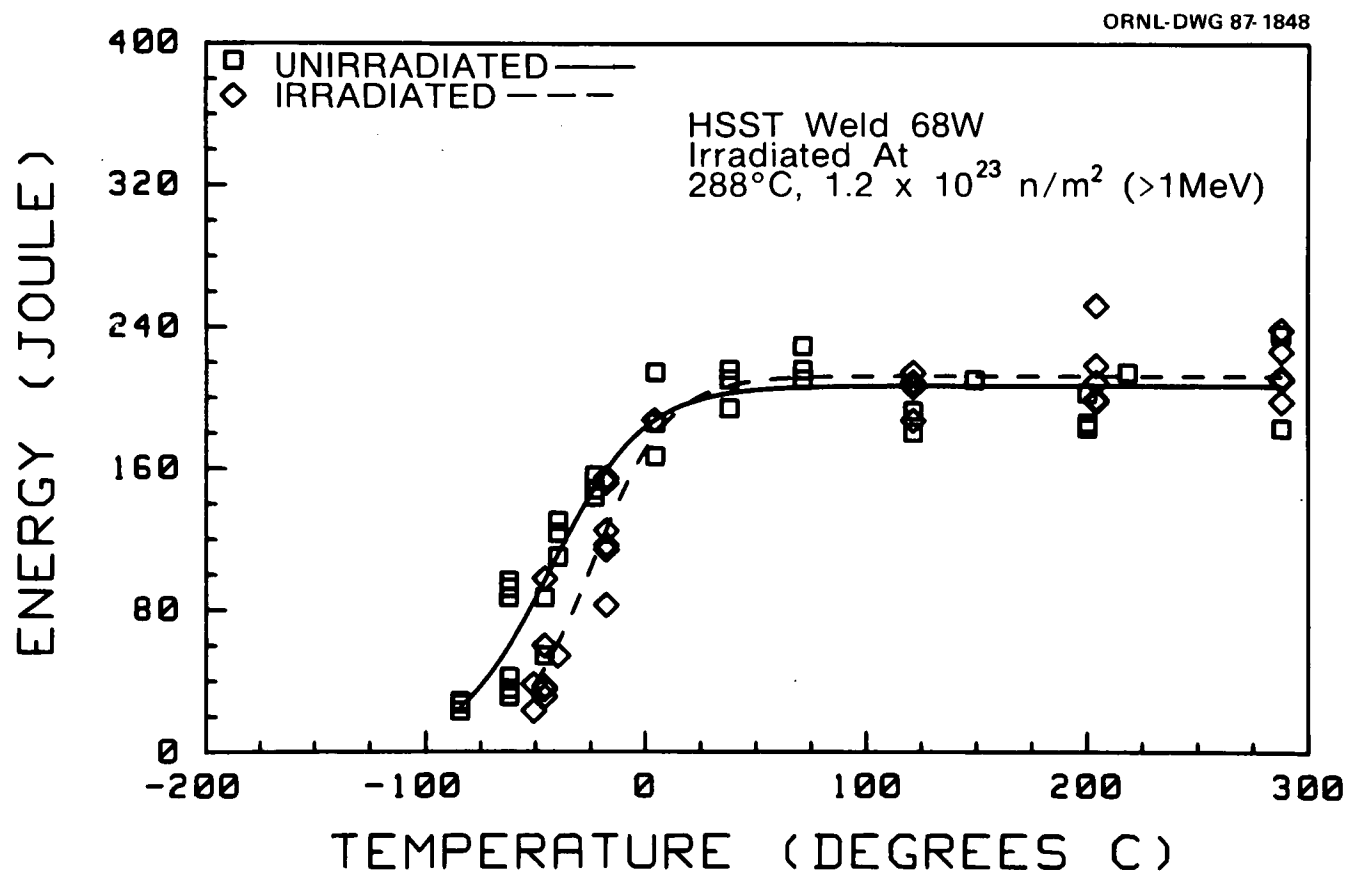

Fig. 18. Effects of irradiation on variation of Charpy V-notch energy with temperature for weld 68W.

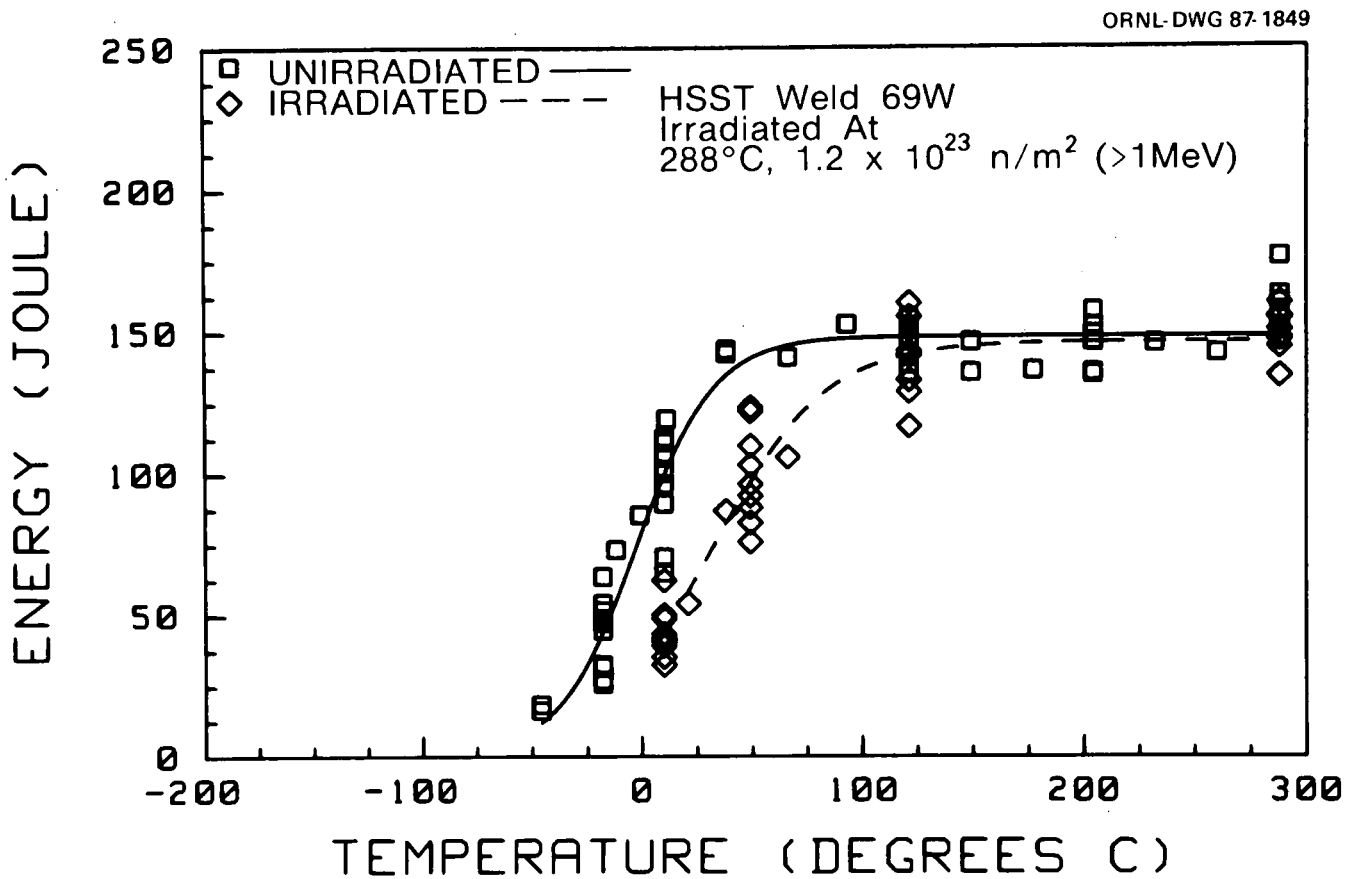

Fig. 19. Effects of irradiation on variation of Charpy V-notch energy with temperature for weld 69W.

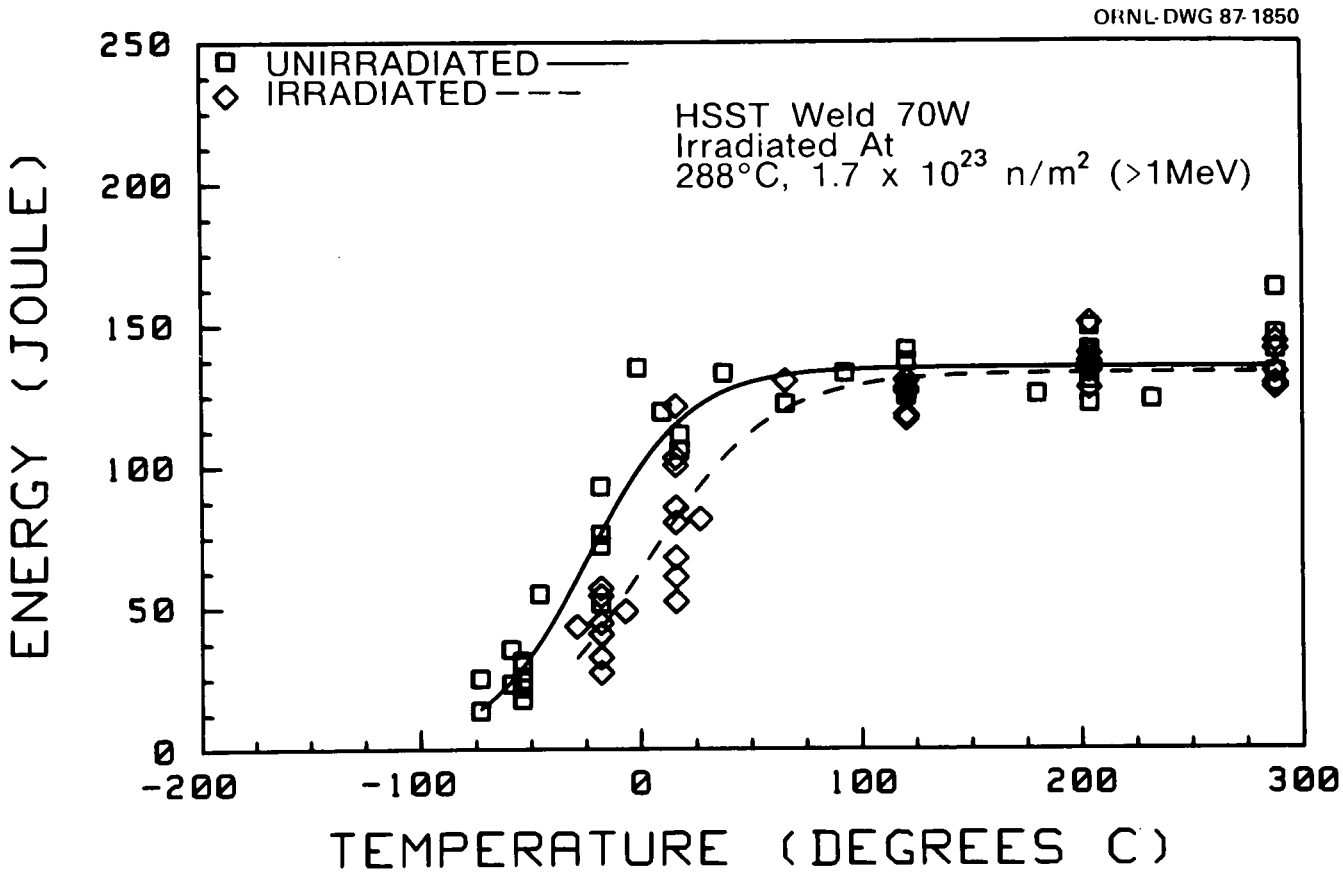

Fig. 20. Effects of irradiation on variation of Charpy V-notch energy with temperature for weld 70W.

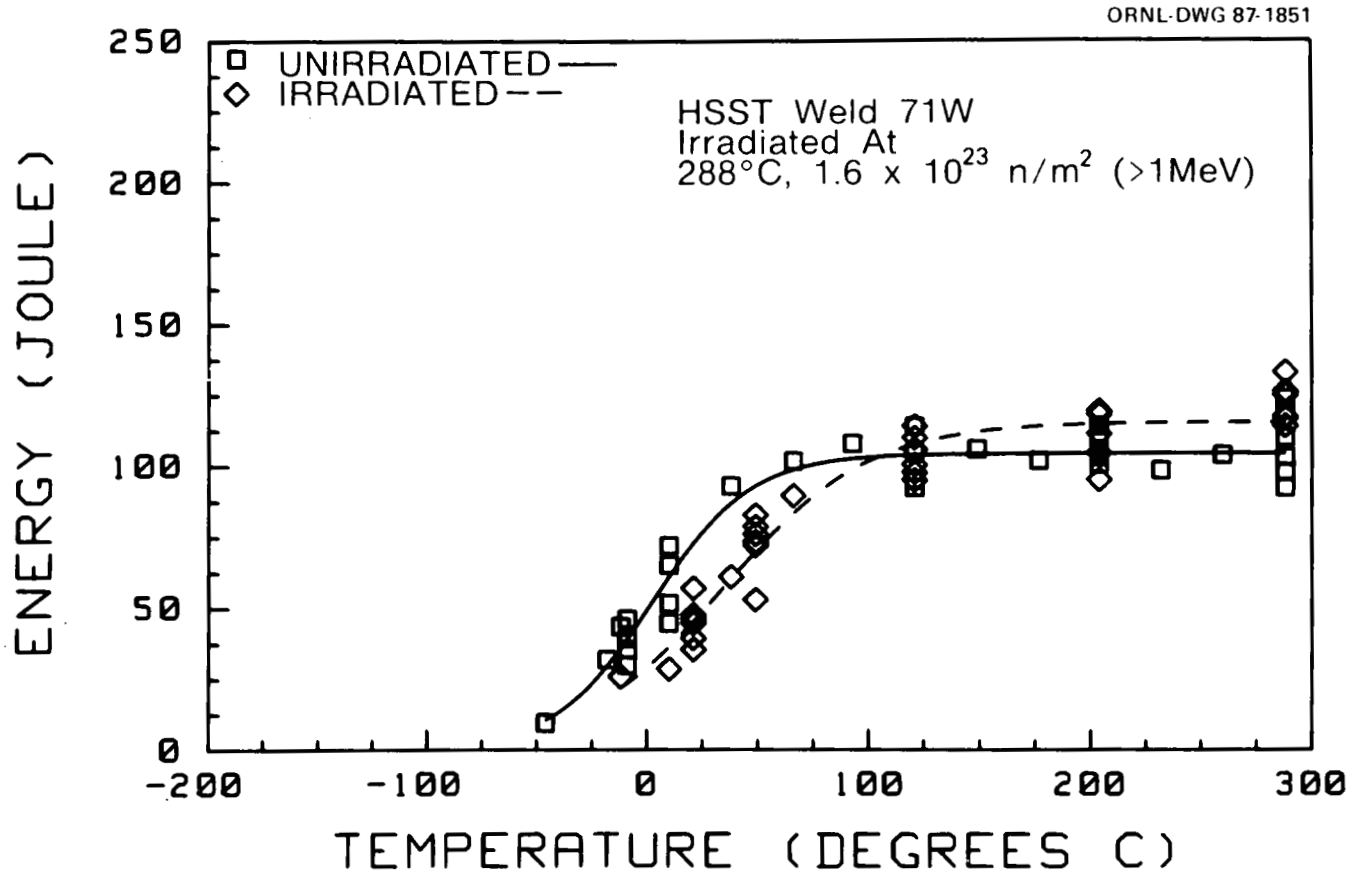

Fig. 21. Effects of irradiation on variation of Charpy V-notch energy with temperature for weld 71W.

Table 4. Comparison of Charpy impact energy for unirradiated pressure vessel plate and submerged-arc welds

Test temperature (°C)	Mean energy, J			Standard deviation, J			Number of tests	
	ORNL	MEA	Combined	ORNL	MEA	Combined	ORNL	MEA
A533 grade B class 1 (HSST-02)								
−7	31.5	28.7	30.1	5.0	5.7	5.5	5	5
21	64.8	61.3	63.0	7.9	7.2	7.7	5	5
66	119.7	116.9	118.5	8.2	8.9	8.6	6	5
149	143.0	135.6	139.6	5.8	4.9	6.6	6	5
204	138.4	138.3	138.3	5.1	10.6	8.1	6	5
288	137.9	145.9	141.5	10.6	3.9	9.2	6	5
Submerged-arc weld (HSST-68W)								
−62	36.2			5.5			3	
−46	70.5			23.0			2	
121	186.4			8.6			2	
200	190.5			10.7			3	
288	209.5			37.4			2	
Submerged-arc weld (HSST-69W)								
−18	41.9	41.2	41.6	12.7	10.5	11.7	6	5
10	98.7	98.2	98.4	14.5	17.8	16.4	5	6
121	144.0	148.9	146.4	6.1	4.7	6.0	5	5
204	143.0	151.2	146.7	6.7	4.0	6.9	5	4
288	147.8	161.3	154.6	1.5	8.5	9.1	5	5
Submerged-arc weld (HSST-70W)								
−54	25.8	24.4	24.9	4.1	5.5	5.0	2	3
−18	73.5	66.4	70.0	16.9	10.7	14.6	3	3
121	131.9	129.8	130.8	6.5	5.2	6.0	3	3
204	131.9	140.1	136.0	7.1	7.8	8.5	3	3
288	134.2	150.1	142.1	5.1	9.2	10.9	3	3
Submerged-arc weld (HSST-71W)								
−9	38.0	37.3	37.7	8.1	2.0	5.9	2	2
10	60.6	58.3	59.7	11.5	6.8	10.0	3	2
121	99.4	97.2	98.3	10.2	5.2	8.2	3	3
204	102.6	111.6	107.1	1.7	1.7	4.8	3	3
288	99.9	115.2	107.5	7.4	8.8	11.2	3	3

Table 5. Comparison of Charpy impact energy for irradiated pressure vessel plate and submerged-arc welds

Test temperature (°C)	Mean energy, J			Standard deviation, J			Number of tests	
	ORNL	MEA	Combined	ORNL	MEA	Combined	ORNL	MEA
A533 grade B class 1 (HSST-02)								
66	41.6	26.2	34.5	8.0	3.8	10.1	7	6
93	77.7	45.9	63.0	19.3	9.2	22.2	7	6
149	113.7	112.1	112.9	9.6	9.4	9.1	6	6
204	120.1	116.8	118.6	8.2	9.6	8.7	7	6
288	119.9	125.6	122.5	3.0	2.4	4.0	7	6
Submerged-arc weld (HSST-68W)								
−46	47.5	55.1	52.1	17.3	36.9	27.8	2	3
−18	137.0	98.3	124.1	19.2	22.1	26.7	4	2
121	211.5	200.2	204.7	3.8	11.4	10.3	2	3
204	226.4	198.6	215.3	22.8	1.0	22.2	3	2
288	224.4	211.9	216.9	20.1	14.3	15.8	2	3
Submerged-arc weld (HSST-69W)								
10	43.1	44.8	43.8	7.1	12.1	9.0	5	4
49	102.5	95.3	99.3	20.8	11.2	16.7	5	4
121	150.0	127.8	138.9	9.0	7.7	14.2	4	4
288	151.7	146.8	149.2	7.2	8.8	7.9	4	4
Submerged-arc weld (HSST-70W)								
−18	43.1	38.0	41.2	13.1	4.7	10.5	5	3
16	88.4	76.4	83.9	25.9	21.0	23.4	5	3
121	126.1	123.4	124.8	7.0	5.9	6.0	3	3
204	135.3	139.2	137.3	1.7	11.6	7.7	3	3
288	133.3	134.2	133.8	9.0	6.2	7.0	3	3
Submerged-arc weld (HSST-71W)								
21	46.5	39.8	43.6	8.8	4.7	7.7	4	3
49	77.6	66.0	72.6	4.1	11.4	9.5	4	3
121	106.8	100.3	104.0	7.0	5.5	6.8	4	3
204	112.2	111.2	111.2	6.8	14.1	9.9	3	3
288	122.2	118.9	120.8	8.4	6.4	7.2	4	3

two laboratories are generally within one standard deviation of each other, indicating good reproducibility between the laboratories. The standard deviations do not show any consistent trends with laboratory, material, or region of the curve. For irradiated specimens (Table 5), the means are also generally within one standard deviation of each other, with some exceptions for Plate 02 at the two lowest temperatures where the mean energy determined from MEA tests is significantly lower than the mean energy determined from ORNL tests. Extensive evaluation at ORNL of Charpy V-notch specimens conditioned in water baths indicate that at bath temperatures near 100°C, significant cooling of the specimen resulting from water evaporation occurs within 6 s after the specimen is out of the bath. This temperature drop is near 3°C at 66°C and 10°C at 93°C. This may explain to some degree the differences between the two data sets.

Some of the variation in impact energy is also due to fluence variations; to account for this, an adjustment on the test temperature axis can be made. In this procedure the unirradiated impact energy was fit with a hyperbolic tangent curve of the form

$$Y = A\{1 + \tanh[B(t - C)]\}/2 \ , \qquad (1)$$

where Y is energy, t is temperature, and A, B, and C are curve fit coefficients using nonlinear techniques developed by Marquardt.[11] Using this curve fit, the irradiation-induced temperature shift (δt) is determined for each specimen tested in the transition region. A power law is fit to the δt vs neutron fluence data (>1 MeV):

$$\delta t = D(\Phi^N) \ , \qquad (2)$$

where Φ is the fluence (>1 MeV) and D is a curve fit coefficient. Using Eq. (2), the temperature shift is corrected to the average fluence in the transition region for that material. Using this approach, the transition-region data of Plate 02 were corrected for fluence variation (using N = 0.5) and bath cooling; the resulting data are shown in Fig. 22 and listed in Table B14 of Appendix B. Although corrections of this type were tried on the welds, they were not effective.

Curve fits such as Eq. (1) were used to determine upper-shelf values and transition temperatures. Table 6 shows a summary of the transition temperature increases and the upper-shelf energy changes for all the materials as a consequence of irradiation. The most significant irradiation-induced change was for Plate 02 where the transition temperature increase was 68°C and the upper-shelf energy dropped 14%. This was expected because this material had the largest amounts of copper and nickel. All of the welds had relatively low levels of copper and, thus, smaller irradiation effects. In Table 7, the CVN transition temperature increases obtained in this study are compared to predictions from several trend curve formulations.[12-17] In making this comparison, several factors must be considered:

1. The predictions of the trend curve formulations are largely or wholly based on surveillance results (except for the MPC case for which both experimental and surveillance trends were used) and represent lower fluxes and much longer irradiation periods than for the present study.
2. The Regulatory Guide 1.99 (ref. 12) was meant to be conservative.
3. The values based on the Draft Regulatory Guide[13] do not include the "margin" specified in the draft.

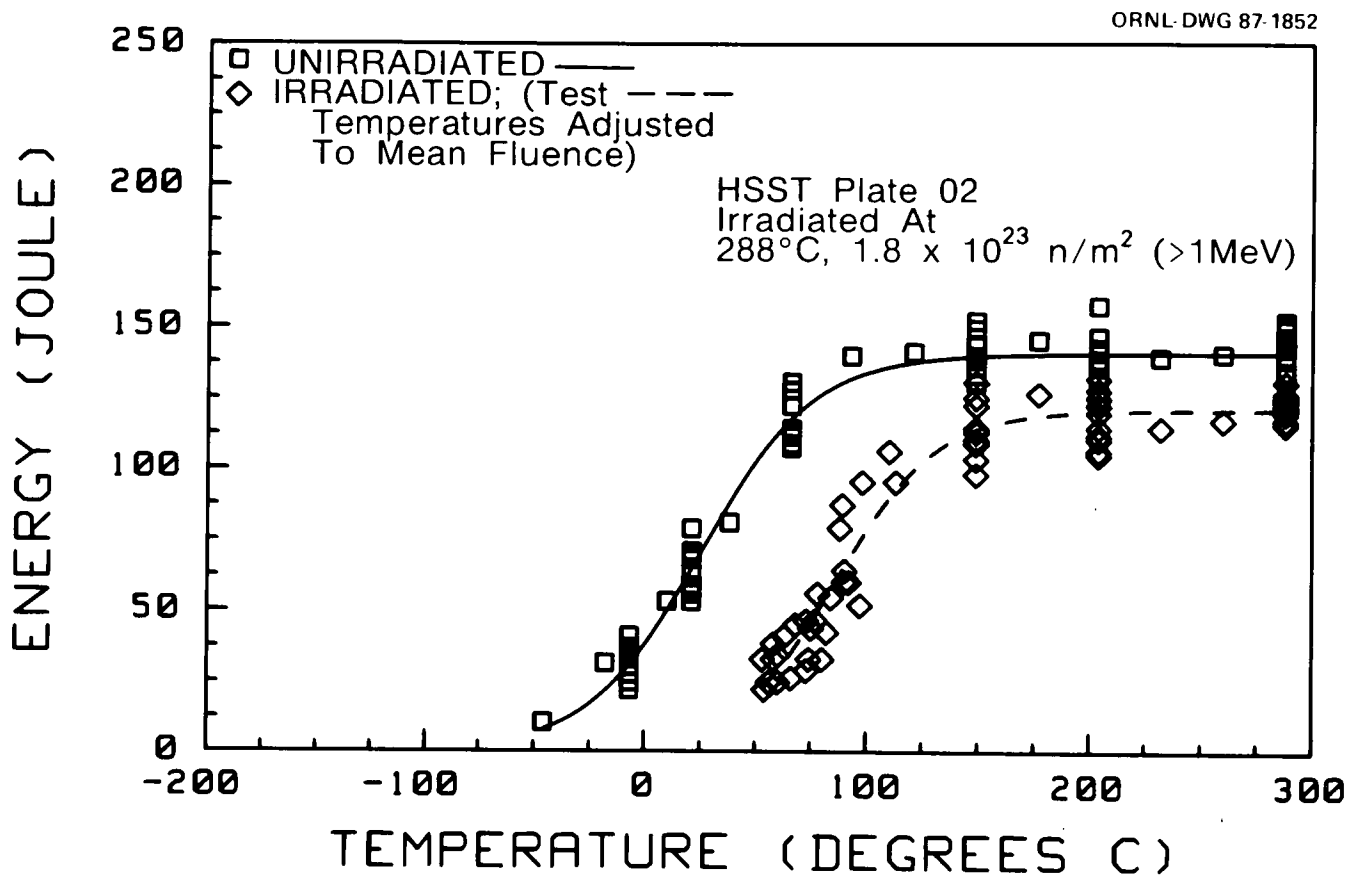

Fig. 22. Effects of irradiation on variation of Charpy V-notch energy with temperature for Plate 02; test temperatures adjusted to mean fluence of 1.77×10^{23} neutrons/m^2 (>1 MeV).

Table 6. Effect of irradiation on Charpy impact properties of plate and submerged-arc welds

Transition temperature increase at 41 J		Upper-shelf energy change			Copper (%)	Nickel (%)
Fluence, 10^{23} n/m^2 (>1 MeV)	Shift (°C)	Fluence, 10^{23} n/m^2 (>1 MeV)	Change J	Change %		
A533 grade B class 1 (HSST-02)						
1.77	68	1.79	−20	−14	0.14	0.67
Submerged-arc weld (HSST-68W)						
1.35	10	1.14	18	9	0.04	0.13
Submerged-arc weld (HSST-69W)						
1.22	27	1.18	−2	−1	0.12	0.10
Submerged-arc weld (HSST-70W)						
1.65	23	1.69	−2	−2	0.06	0.63
Submerged-arc weld (HSST-71W)						
1.65	23	1.64	11	10	0.05	0.63

Table 7. Comparison among several predictive expressions of Charpy impact transition temperature increase for pressure vessel plate and submerged-arc welds

Average fluence, 10^{23} n/m^2 (>1 MeV)	Charpy impact transition temperature increase, °C						
	Observed increase	RG 1.99[a]	Draft RG 1.99[b]	V-B[c]	P-W[d]	V-S-K[e]	MPC[f]
A533 grade B class 1 (HSST-02)							
1.77	68	78	65	72	59	66	72 (55)
Submerged-arc weld (HSST-68W)							
1.35	10	26	22	−44	20	17	−5 (13)
Submerged-arc weld (HSST-69W)							
1.22	27	55	36	23	35	29	34 (41)
Submerged-arc weld (HSST-70W)							
1.65	23	39	52	31	46	76	3 (21)
Submerged-arc weld (HSST-71W)							
1.65	23	39	43	26	38	74	−2 (17)

[a]"Effects of Residual Elements on Predicted Radiation Damage to Reactor Vessel Materials," *Regulatory Guide 1.99 (Rev. 1)*, U.S. Nuclear Regulatory Commission, Washington, D.C., April 1977.

[b]P. N. Randall, "Effects of Residual Elements on Predicted Radiation Damage to Reactor Vessel Materials," *Regulatory Guide 1.99 (Rev. 2 Draft)*, U.S. Nuclear Regulatory Commission, Washington, D.C., January 1984.

[c]J. D. Varsik and S. T. Byrne, "An Empirical Evaluation of the Irradiation Sensitivity of Reactor Pressure Vessel Materials," pp. 252–66 in *Effects of Radiation on Structural Materials, ASTM STP 683*, American Society for Testing and Materials, Philadelphia, 1979.

[d]J. S. Perrin, R. A. Wullaert, G. R. Odette, and P. M. Lombrozo, *Physically Based Regression Correlations of Embrittlement Data from Reactor Pressure Vessel Surveillance Programs*, EPRI NP-3319, Electric Power Research Institute, Palo Alto, Calif., January 1984.

[e]J. D. Varsik, S. M. Schloss, and J. J. Koziol, *Evaluation of Irradiation Response of Reactor Pressure Vessel Materials*, EPRI NP-2720, Electric Power Research Institute, Palo Alto, Calif., November 1982.

[f]Metal Properties Council Subcommittee 6 on Nuclear Materials, "Prediction of the Shift in the Brittle-Ductile Transition Temperature of Light-Water Reactor (LWR) Pressure Vessel Materials," *J. Test. Eval.* 11(4), 237–60 (July 1983); primary values shown are based on surveillance trend curves, whereas the values in parentheses are based on experimental trend curves, in both cases for plate or welds as applicable.

Considering the above factors, there is fairly good agreement of the present results with the several predictions. A notable exception would be the predictions of Varsik, Schloss, and Koziol;[16] this trend curve gives particularly poor predictions for welds 70W and 71W, both of which had low copper levels but high nickel levels. Reference 16 used formulations that add the effects of copper and nickel rather than multiply the effects of the two. The often-stated synergism between the two elements may be reflected in the observed differences. Note that the regulatory guides[12,13] are generally conservative. Also, the draft Regulatory Guide[13] (without "margin") overpredicts the shifts for welds 70W and 71W by a greater margin than for 68W and 69W. The draft guide incorporates nickel content whereas Rev. 1 of the guide does not. Thus, the draft guide predicts higher shifts for the two welds with higher nickel contents, 70W and 71W. Using the experimental trend curves of ref. 17, shown parenthetically in Table 7, the predictions increased for welds and decreased for Plate 02. Further information on Charpy impact testing can be found in ref. 18.

FRACTURE TOUGHNESS TESTING

Testing of compact specimens (CS) was performed by the single-specimen-compliance (SSC) technique, with each laboratory testing approximately one-half of the specimens. All compact specimens designated for ductile-shelf testing were side-grooved on each side by 10% of the specimen thickness. The SSC technique provides a method to determine the amount of specimen crack extension by means of small unloadings (<15% of maximum load) conducted at regular intervals throughout the test.

Values of the J-integral were calculated using the modified version of the J-integral, known as J_M, as proposed by Ernst.[18] Deformation theory J (J_D) is the formulation of the J-integral specified for use in the ASTM Standard Test for J_{Ic}, a measure of fracture toughness (E813-84), and in the tentative ASTM J-integral resistance (J-R) curve test procedure.[19] Modified J (J_M) was used in this program because Ernst has shown it to be more specimen-size independent when the crack extension exceeds the J-controlled crack growth regime.

A typical J-R curve produced with the SSC technique is illustrated in Fig. 23. The R curve format in Fig. 23 is in accordance with that of ASTM Standard E813, that is, J_{Ic} (the elastic-plastic initiation fracture toughness) is defined by the intersection of the blunting line with linear regression fit to the data between the 0.15- and the 1.5-mm exclusion lines. The tearing modulus, T, is defined as

$$T = (E/\sigma_f^2)dJ/da \ , \qquad (3)$$

where σ_f is flow stress, E is Young's modulus, and dJ/da is the slope of the J-R curve between the 0.15- and 1.5-mm exclusion lines from the linear regression for J_{Ic}; E is calculated from the formula E(GPa) = 207 − 0.057t(°C). As suggested by ref. 1, the value of J at J/T = 8.8 kJ/m^2 was calculated. This was done by fitting the entire J-R curve with a power law function:

$$J = C(\delta a)^N \qquad (4)$$

where C and N are constants of fit, δa is crack extension, and then

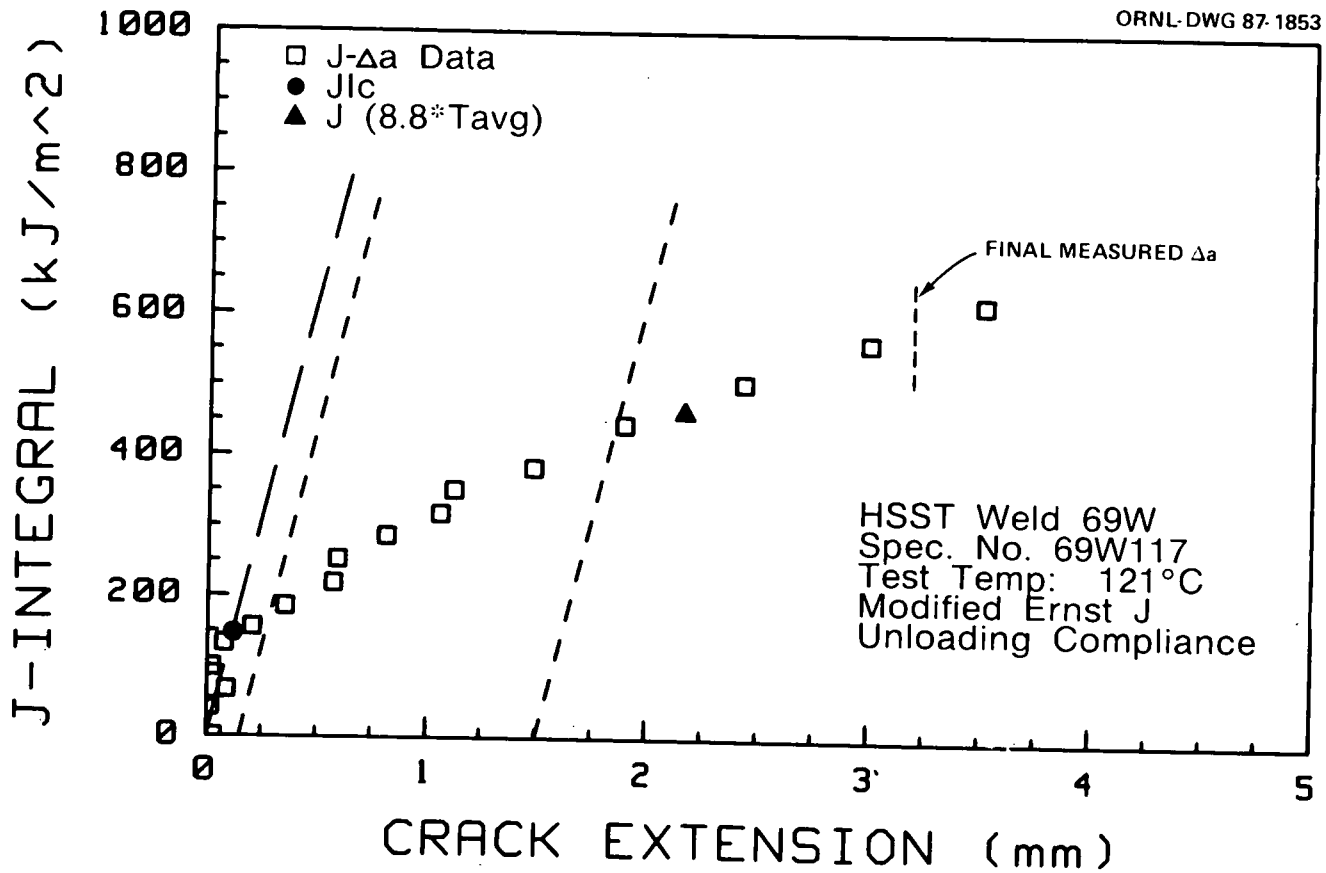

Fig. 23. Typical J-integral R-curve (weld 69W, 121°C, unirradiated), produced with the single-specimen unloading compliance technique.

solving Eqs. (3) and (4) for the J value for which $J/T = 8.8\ kJ/m^2$. In determining the curve fit, only J-δa pairs were used which satisfied the validity requirements of the draft ASTM J-R curve testing procedure.[19] To convert J_{Ic} to a quasi-elastic K_{Jc} value, the following relationship (suggested by ASTM Standard E813) was used:

$$K_{Jc} = (EJ_{Ic})^{0.5} \tag{5}$$

At toughness levels too great to allow measurement of a valid K_{Ic}, as specified in ASTM Standard E399 (ref. 20), K_{Jc} values can be determined using Eq. (5) with the value of the J-integral at the onset of cleavage; however, these data tend to be of greater magnitude than data obtained from larger specimens (valid by E399 criteria). A similar observation was made by Irwin[21] in that the plane stress fracture toughness (K_c) overestimates K_{Ic}. Irwin developed an empirical relationship from which K_{Ic} could be estimated once K_c was known. Recently, Merkle[22] has shown that reasonable estimates of K_{Ic} can be determined using K_{Jc} as a substitute for K_c. In this study, K_{Jc} values in the ductile-to-brittle transition region were corrected to $K_{\beta c}$ using the Irwin-Merkle β_{Ic} correction to provide another means of determining the shift to higher temperature of the ductile-to-brittle transition caused by irradiation.

A summary of all the transition-region fracture toughness results is presented in Table 8 for the five materials studied in the unirradiated condition, and a summary of all the ductile-shelf region fracture toughness results is presented in Table 9 for the five materials studied in the unirradiated condition. The variation of fracture toughness (K_{Jc}) with temperature for Plate 02 and welds 68W, 69W, 70W, and 71W in the unirradiated condition is shown in Figs. 24 through 28, respectively. The data scatter is generally small in the ductile-shelf and the low-transition regions, whereas it is higher in the upper transition region, due in some part to the ductile crack growth prior to cleavage. A summary of statistical information for the unirradiated plate and welds is shown in Table 10. Note that the agreement between the two laboratories for the mean K_{Jc} value is generally less than one standard deviation, independent of the temperature or material. Also note that the variations are similar for all the materials except weld 68W, which seems to have significantly higher variations in all regions. Variations of the β-corrected fracture toughness ($K_{\beta c}$) with temperature for Plate 02 and welds 68W, 69W, 70W, and 71W in the unirradiated condition are shown in Figs. 29 through 33, respectively. Although the magnitudes of the β-corrected fracture toughnesses ($K_{\beta c}$) are less than the uncorrected fracture toughnesses (K_{Jc}), the general behavior is similar.

The primary thrust of this irradiation program was to study the ductile-shelf behavior of "current practice" reactor pressure vessel welds. Of significant interest in that regard is the tearing modulus, T [defined in Eq. (3)], and the "J = 8.8T" value. Variations of the tearing modulus (T) with temperature for Plate 02 and welds 68W, 69W, 70W, and 71W in the unirradiated condition are shown in Figs. 34 through 38, respectively. The tearing modulus decreases with increasing test temperature and exhibits more scatter at the lower test temperatures. A summary of statistical information for the unirradiated plate and welds of the tearing modulus and J = 8.8T is shown in Table 11. Note that the coefficient of variation (CV = standard deviation/mean) is also listed in the table. Of the materials studied, weld 68W had the highest tearing

Table 8. Transition region 1TCS test data for unirradiated pressure vessel plate and submerged-arc welds

Specimen number	Laboratory	Side grooves (%)	Test temperature (°C)	(a/W)	Delta-a (mm)	J_c (KJ/m^2)	K_{Jc} (MPa$\sqrt{m}$)	K_{Ic} (MPa$\sqrt{m}$)	$K_{\beta c}$ (MPa$\sqrt{m}$)	Yield strength (MPa)	Young's modulus (GPa)
02G415	ORNL	0	−100	0.614	0.05	8.3	41.9	44.0	41.0	600	213
02G312	ORNL	0	−95	0.612	0.05	6.4	36.8	41.8	36.3	593	213
02G292	MEA	0	−95	0.617	0.05	8.8	43.2	44.4	42.1	593	213
02G308	MEA	0	−95	0.620	0.05	9.1	44.1	45.2	36.3	593	213
02G283	ORNL	0	−95	0.619	0.05	13.3	53.2	57.2	50.4	593	213
02G300	MEA	0	−95	0.623	0.05	15.6	57.6	58.7	53.8	593	213
02G350	ORNL	0	−80	0.622	0.05	13.3	53.1	50.3	50.1	574	212
02G296	ORNL	0	−40	0.617	0.05	22.8	69.1	*a*	59.5	529	209
02G361	ORNL	0	−40	0.620	0.05	23.6	70.3	*a*	60.2	529	209
02G301	ORNL	0	−40	0.621	0.05	26.6	74.6	*a*	62.6	529	209
02G347	MEA	0	−40	0.620	0.05	37.6	88.8	*a*	69.4	529	209
02G355	MEA	0	−40	0.622	0.07	39.3	90.8	*a*	70.2	529	209
02G352	MEA	0	−40	0.622	0.05	59.7	91.6	*a*	70.6	529	209
02G297	MEA	0	−5	0.619	0.06	74.2	124.1	*a*	79.5	496	207
02G405	ORNL	0	−5	0.612	0.07	74.3	124.2	*a*	79.6	496	207
02G313	MEA	0	−5	0.619	0.10	81.8	130.3	*a*	81.3	496	207
02G304	MEA	0	−5	0.619	0.09	90.6	137.2	*a*	83.2	496	207
02G367	ORNL	0	0	0.622	0.05	75.1	124.7	*a*	79.4	492	207
02G417	ORNL	0	0	0.606	0.10	75.9	125.4	*a*	79.6	492	207
02G322	MEA	20	22	0.622	0.22	251.8	227.8	*a*	99.7	475	206
02G343	MEA	20	22	0.631	0.55	317.2	255.6	*a*	104.1	475	206
02G341	MEA	0	23	0.623	0.28	209.5	207.8	*a*	96.1	474	206
02G309	ORNL	0	23	0.617	0.56	277.0	238.9	*a*	101.4	474	206
02G293	ORNL	0	23	0.619	1.06	248.6	280.1	*a*	107.6	474	206
02G408	ORNL	20	24	0.609	0.17	206.9	206.4	*a*	89.4	473	206

Table 8. (Continued)

Specimen number	Laboratory	Side grooves (%)	Test temperature (°C)	(a/W)	Delta-a (mm)	J_c (KJ/m^2)	K_{Jc} (MPa$\sqrt{m}$)	K_{Ic} (MPa$\sqrt{m}$)	$K_{\beta c}$ (MPa$\sqrt{m}$)	Yield strength (MPa)	Young's modulus (GPa)
68WEB	ORNL	0	−135	0.597	0.05	7.6	40.4	40.2	40.0	776	215
68WJE	MEA	0	−125	0.603	0.05	29.4	79.4	*a*	72.9	757	214
68WHA	MEA	0	−120	0.599	0.05	16.2	58.9	59.8	56.9	749	214
68WJC	MEA	0	−95	0.597	0.05	40.2	92.5	*a*	79.6	707	213
68WCB	ORNL	0	−80	0.601	0.05	16.2	58.6	59.5	55.9	684	212
68WKD	ORNL	0	−80	0.604	0.07	71.3	122.9	*a*	93.0	684	212
68WHE	MEA	0	−80	0.608	0.15	107.3	150.8	*a*	103.3	684	212
68WAE	MEA	0	−40	0.600	0.53	421.8	296.9	*a*	131.0	627	209
68WDD	ORNL	0	−30	0.616	0.26	215.7	212.3	*a*	113.3	615	209
68WAC	MEA	0	−30	0.596	0.66	410.0	292.7	*a*	128.7	615	209
69W109	ORNL	0	−100	0.597	0.05	7.8	40.8	40.7	40.5	779	213
69W135	MEA	0	−100	0.592	0.05	9.6	45.1	46.6	44.6	779	213
69W103	ORNL	0	−100	0.595	0.05	9.9	45.9	42.6	45.3	779	213
69W134	MEA	0	−100	0.593	0.05	16.1	58.6	60.1	56.9	779	213
69W140	ORNL	0	−60	0.587	0.05	12.3	50.8	55.8	49.6	726	211
69W130	MEA	0	−60	0.599	0.05	12.8	51.9	54.1	50.6	725	211
69W136	ORNL	0	−60	0.596	0.05	16.2	58.4	60.8	56.2	726	211
69W138	ORNL	0	−60	0.612	0.05	21.1	66.6	68.4	62.9	726	211
69W104	MEA	0	−60	0.597	0.05	30.6	80.3	*a*	72.7	725	211
69W124	ORNL	0	−20	0.605	0.05	58.3	110.2	*a*	87.4	680	208
69W111	MEA	0	−5	0.604	0.05	39.4	90.5	*a*	76.8	665	207
69W170	ORNL	0	−5	0.605	0.05	44.0	95.5	*a*	79.5	665	207
69W128	ORNL	0	−5	0.599	0.06	44.4	95.9	*a*	79.7	665	207
69W152	MEA	0	−5	0.601	0.05	69.1	119.8	*a*	90.6	665	207

Table 8. (Continued)

Specimen number	Laboratory	Side grooves (%)	Test temperature (°C)	(a/W)	Delta-a (mm)	J_c (KJ/m^2)	K_{Jc} (MPa$\sqrt{m}$)	K_{Ic} (MPa$\sqrt{m}$)	$K_{\beta c}$ (MPa$\sqrt{m}$)	Yield strength (MPa)	Young's modulus (GPa)
69W158	MEA	0	−5	0.600	0.05	84.4	132.4	[a]	95.5	665	207
69W164	MEA	0	20	0.593	0.06	92.9	138.4	[a]	95.9	642	206
69W174	MEA	0	20	0.595	0.06	103.2	143.4	[a]	97.6	642	206
69W151	ORNL	0	20	0.600	0.10	118.4	156.2	[a]	101.6	642	206
69W133	MEA	0	23	0.589	1.99	179.6	192.3	[a]	111.3	639	206
69W175	ORNL	0	24	0.599	0.10	136.3	167.5	[a]	104.6	639	206
69W132	ORNL	0	24	0.592	7.92	183.2	228.5	[a]	119.7	640	206
70W103	ORNL	0	−135	0.550	0.05	5.5	34.2	35.9	34.0	652	215
70W127	ORNL	0	−135	0.549	0.05	10.0	46.4	47.3	45.3	652	215
70W109	MEA	0	−115	0.546	0.05	8.3	42.0	44.1	41.2	625	214
70W102	MEA	0	−115	0.544	0.05	21.5	67.8	[a]	61.7	625	214
70W121	MEA	0	−65	0.546	0.05	32.8	83.2	[a]	68.6	566	211
70W149	ORNL	0	−65	0.546	0.05	56.0	108.7	[a]	79.8	566	211
70W143	ORNL	0	−65	0.546	0.05	58.1	110.7	[a]	80.5	566	211
70W122	MEA	0	−65	0.548	0.12	73.0	124.1	[a]	85.2	566	211
70W120	ORNL	0	−40	0.552	0.05	59.3	111.4	[a]	79.0	540	209
70W141	MEA	0	−35	0.566	0.08	89.5	136.9	[a]	86.7	535	209
71W132	MEA	0	−95	0.550	0.05	16.8	59.8	[a]	55.4	593	213
71W113	MEA	0	−95	0.548	0.05	17.7	61.4	[a]	56.5	593	213
71W105	ORNL	0	−90	0.547	0.05	12.6	51.7	47.8	50.0	656	212
71W107	ORNL	0	−50	0.544	0.05	35.1	85.8	[a]	68.6	541	210
71W102	MEA	0	−50	0.546	0.05	43.4	95.5	[a]	72.9	541	210
71W114	ORNL	0	−10	0.553	0.05	58.8	110.6	[a]	75.8	502	208
71W135	ORNL	0	−10	0.551	0.45	202.2	205.0	[a]	99.0	502	208

[a]Test did not provide valid K_{Ic} value by ASTM E399.

Table 9. Ductile-shelf region 1TCS test data for unirradiated pressure vessel plate and submerged-arc welds

Specimen number	Laboratory	Side grooves (%)	Test temperature (°C)	(a/W)	Delta-a (mm)	J_{max} (KJ/m^2)	J_{Ic} (KJ/m^2)	K_{JIc} (MPa$\sqrt{m}$)	Tearing modulus	J = 8.8T (KJ/m^2)	Flow strength (MPa)	Young's modulus (GPa)
02G374	ORNL	0	40	0.623	3.84	450.5	0.0	0.0	0	0.0	538	205
02G410	ORNL	20	50	0.627	2.95	339.8	118.8	155.8	197	1194.0	531	204
02G400	MEA	20	50	0.615	8.37	347.7	192.2	198.2	164	812.8	531	204
02G364	MEA	20	50	0.633	2.62	319.8	194.1	199.2	154	611.1	531	204
02G299	ORNL	20	50	0.620	3.09	265.5	207.6	206.0	141	663.8	531	204
02G323	MEA	20	50	0.619	8.91	337.3	221.7	212.8	153	763.7	531	204
02G325	ORNL	24	121	0.622	4.11	282.5	114.5	151.5	156	688.0	500	200
02G294	MEA	20	121	0.623	8.95	335.8	141.6	168.4	178	752.6	500	200
02G302	MEA	20	121	0.618	6.01	307.0	167.0	182.9	147	746.3	500	200
02G310	MEA	20	121	0.622	6.00	293.8	173.9	186.6	133	696.0	500	200
02G303	ORNL	20	121	0.620	3.06	233.1	177.0	188.3	138	595.8	500	196
02G306	MEA	20	204	0.620	10.31	246.6	139.8	165.3	118	558.4	498	196
02G326	ORNL	20	204	0.623	5.73	250.0	142.5	166.9	99	439.1	498	196
02G320	MEA	20	204	0.623	10.96	279.9	147.3	169.7	115	535.6	498	196
02G315	MEA	20	204	0.623	10.40	309.7	148.5	170.4	113	459.0	498	196
02G321	ORNL	20	204	0.626	3.09	248.2	191.4	193.5	100	425.3	498	191
02G319	MEA	20	288	0.622	8.73	184.1	121.3	152.1	81	431.1	534	191
02G333	MEA	20	288	0.626	5.84	189.7	121.6	152.3	73	475.4	534	191
02G324	MEA	20	288	0.622	8.50	188.5	128.0	156.3	92	509.7	534	191
02G327	ORNL	20	288	0.632	6.01	168.9	132.2	158.8	73	337.8	534	191
02G357	ORNL	20	288	0.627	3.73	200.1	143.7	165.6	89	414.3	534	206
68WKA	ORNL	20	23	0.604	2.78	423.2	160.9	182.0	219	1321.3	600	200
68WMC	MEA	20	121	0.606	8.01	351.5	156.1	176.8	204	1054.8	542	200
68WHB	ORNL	20	121	0.607	3.12	355.5	203.3	201.8	204	1070.5	542	196
68WHD	MEA	20	200	0.606	4.07	273.3	236.1	215.0	111	575.9	533	191
68WJD	MEA	20	288	0.604	7.09	187.0	131.5	158.4	132	651.0	561	191
68WAA	ORNL	20	288	0.598	3.21	348.6	206.8	198.6	138	769.8	562	191

Table 9. (Continued)

Specimen number	Laboratory	Side grooves (%)	Test temperature (°C)	(a/W)	Delta-a (mm)	J_{max} (KJ/m^2)	J_{Ic} (KJ/m^2)	K_{JIc} (MPa$\sqrt{m}$)	Tearing modulus	J = 8.8T (KJ/m^2)	Flow strength (MPa)	Young's modulus (GPa)
69W176	MEA	20	50	0.608	11.01	231.5	144.7	172.0	87	492.2	664	204
69W125	ORNL	20	50	0.591	2.72	215.3	149.8	174.9	80	454.2	664	204
69W129	MEA	20	50	0.604	10.81	219.6	165.6	184.0	70	434.8	664	204
69W162	MEA	20	121	0.598	9.72	243.6	144.2	169.9	89	493.2	630	200
69W117	ORNL	20	121	0.598	3.18	231.7	146.4	171.2	93	460.6	630	200
69W110	MEA	20	121	0.603	9.98	229.9	147.3	171.8	82	466.9	630	200
69W141	ORNL	20	121	0.595	3.20	219.6	164.0	181.3	88	466.5	630	200
69W150	MEA	20	200	0.602	4.69	262.6	184.3	190.0	54	323.1	623	196
69W145	ORNL	20	204	0.603	3.66	225.2	104.5	143.0	76	369.3	623	196
69W168	MEA	20	204	0.607	9.98	226.4	124.0	155.9	61	343.0	623	196
69W180	MEA	20	288	0.605	10.80	190.2	97.2	136.2	56	296.3	651	191
69W127	MEA	20	288	0.601	10.50	210.4	102.0	139.5	49	299.7	651	191
69W154	ORNL	20	288	0.598	3.31	216.6	112.5	146.5	56	302.6	651	191
69W161	ORNL	20	288	0.598	3.93	226.1	140.2	163.6	56	301.6	651	191
70W150	ORNL	20	50	0.543	2.99	255.0	107.5	148.2	188	925.4	526	204
70W134	MEA	20	50	0.549	11.53	236.7	180.0	191.8	163	852.0	526	204
70W135	ORNL	20	121	0.548	2.98	224.2	131.6	162.4	159	751.5	494	200
70W105	MEA	20	121	0.547	10.59	247.8	135.4	164.7	148	684.5	494	200
70W114	ORNL	20	121	0.552	3.27	190.4	147.6	171.9	140	617.4	494	200
70W146	MEA	20	204	0.548	9.95	202.8	109.3	146.2	108	480.1	486	196
70W144	ORNL	20	204	0.553	2.81	159.2	118.4	152.2	133	566.3	487	196
70W147	ORNL	20	204	0.553	3.01	216.9	128.8	158.7	110	445.0	487	196
70W151	MEA	20	288	0.552	9.98	165.8	95.5	135.0	79	380.7	511	191
70W152	ORNL	20	288	0.545	3.05	184.7	114.6	147.8	93	403.9	511	191
70W116	ORNL	20	288	0.553	3.80	188.9	115.0	148.2	88	398.7	511	191

Table 9. (Continued)

Specimen number	Laboratory	Side grooves (%)	Test temperature (°C)	(a/W)	Delta-a (mm)	J_{max} (KJ/m^2)	J_{Ic} (KJ/m^2)	K_{JIc} ($MPa\sqrt{m}$)	Tearing modulus	J = 8.8T (KJ/m^2)	Flow strength (MPa)	Young's modulus (GPa)
71W145	MEA	0	−10	0.555	1.43	176.6	0.0	0.0	0	0.0	567	208
71W137	MEA	0	−5	0.556	3.13	230.5	0.0	0.0	0	0.0	563	207
71W130	ORNL	0	30	0.547	3.29	285.3	128.8	162.7	186	1019.9	535	205
71W124	ORNL	20	50	0.549	3.01	228.4	99.2	142.3	144	763.7	521	204
71W109	MEA	20	50	0.563	11.96	205.7	122.5	158.2	98	529.2	521	204
71W152	MEA	20	121	0.553	10.08	214.0	114.4	151.4	153	705.5	489	200
71W103	ORNL	20	121	0.556	3.33	188.0	130.8	161.9	105	424.8	489	200
71W136	MEA	20	121	0.554	11.94	206.8	135.2	164.6	155	750.8	489	200
71W106	MEA	20	204	0.544	10.48	148.7	82.1	126.7	66	291.3	482	196
71W129	MEA	20	204	0.555	10.94	153.0	89.7	132.4	87	355.5	482	196
71W125	ORNL	20	204	0.553	3.19	158.4	122.1	154.5	90	344.6	482	196
71W104	MEA	20	288	0.565	10.11	134.5	69.9	115.5	72	296.9	508	191
71W148	MEA	20	288	0.545	11.05	151.4	83.8	126.5	71	347.2	508	191
71W127	ORNL	20	288	0.553	3.87	155.1	86.9	128.8	61	247.5	508	191

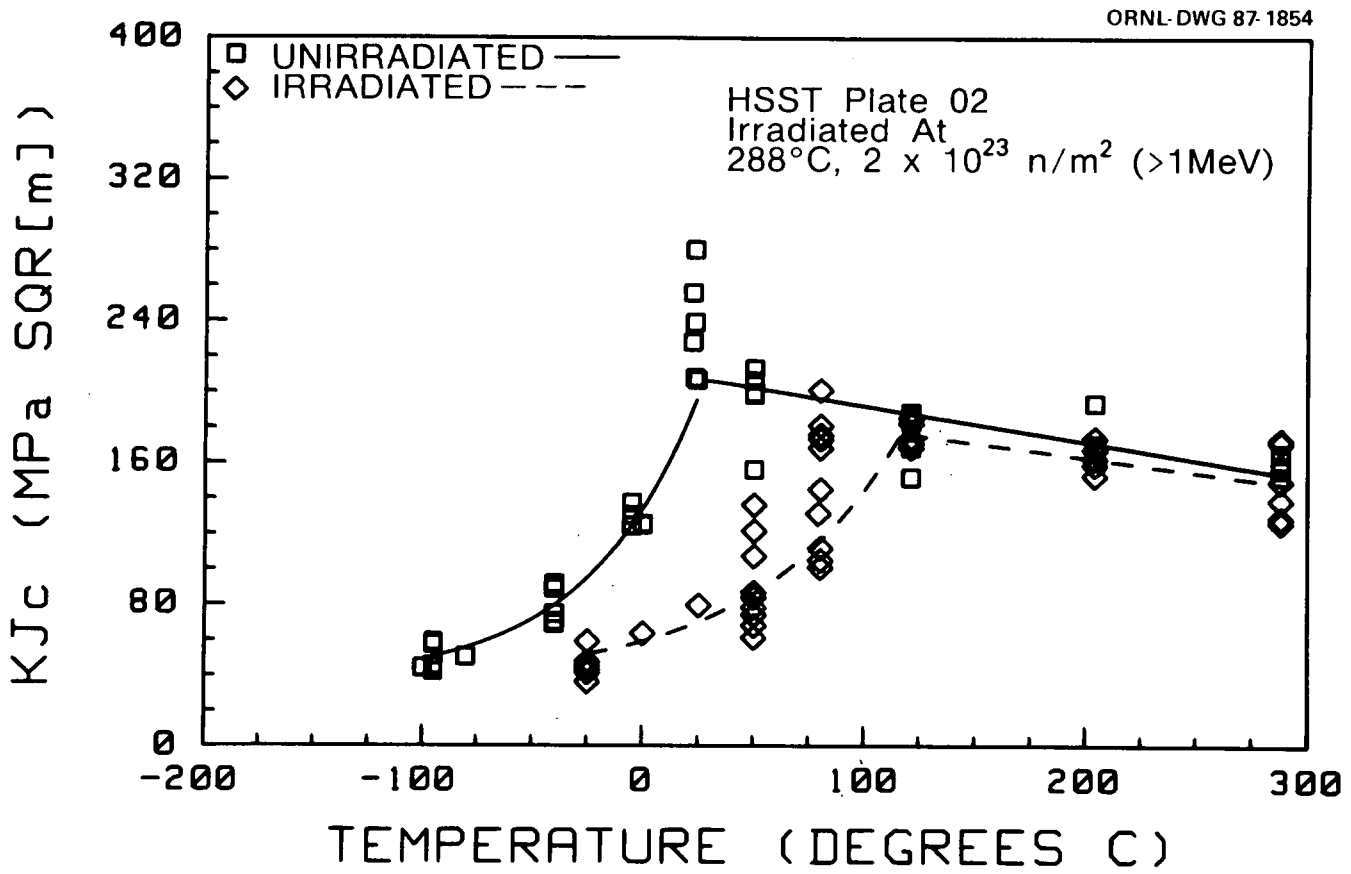

Fig. 24. Effects of irradiation on variation of fracture toughness with temperature for Plate 02.

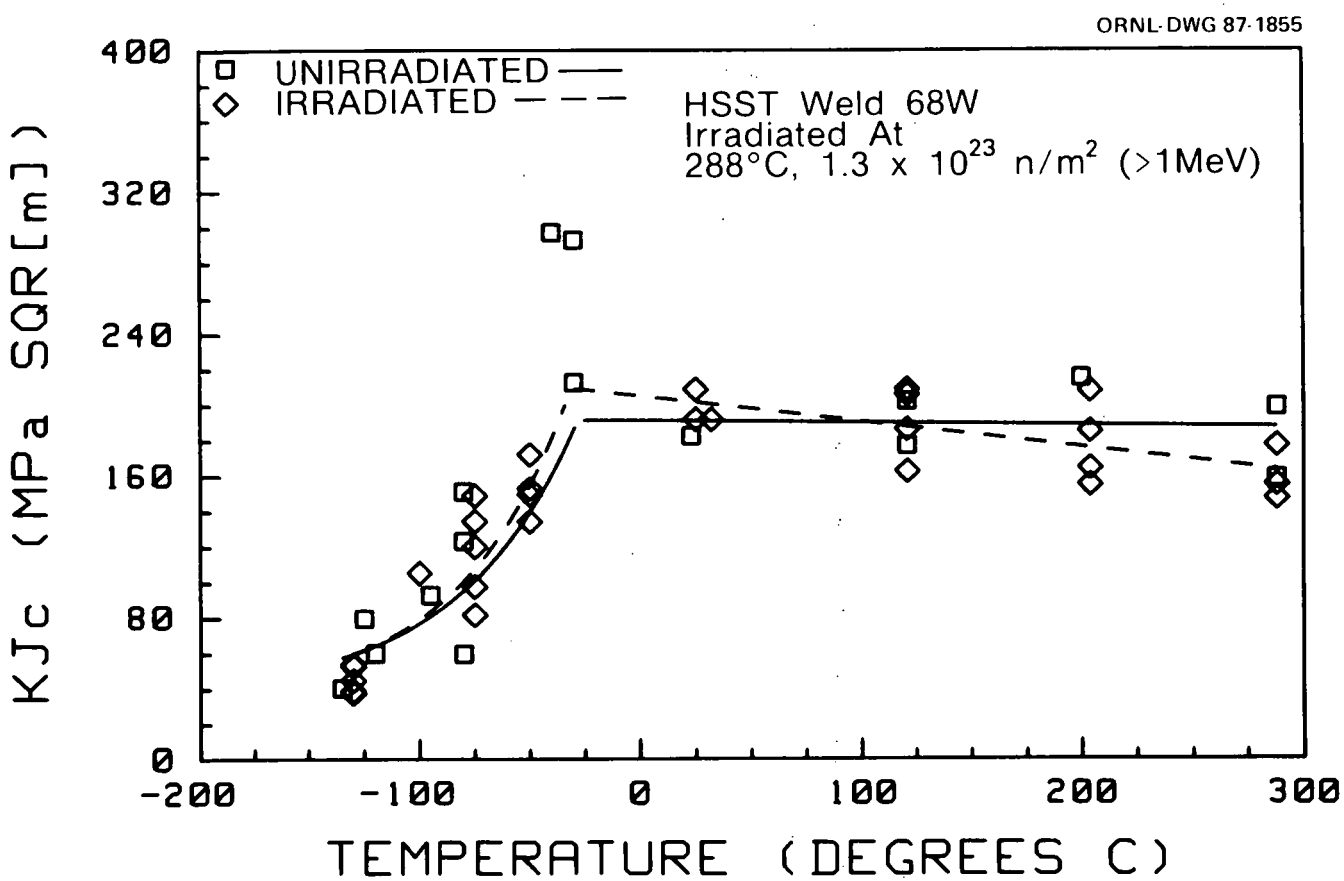

Fig. 25. Effects of irradiation on variation of fracture toughness with temperature for weld 68W.

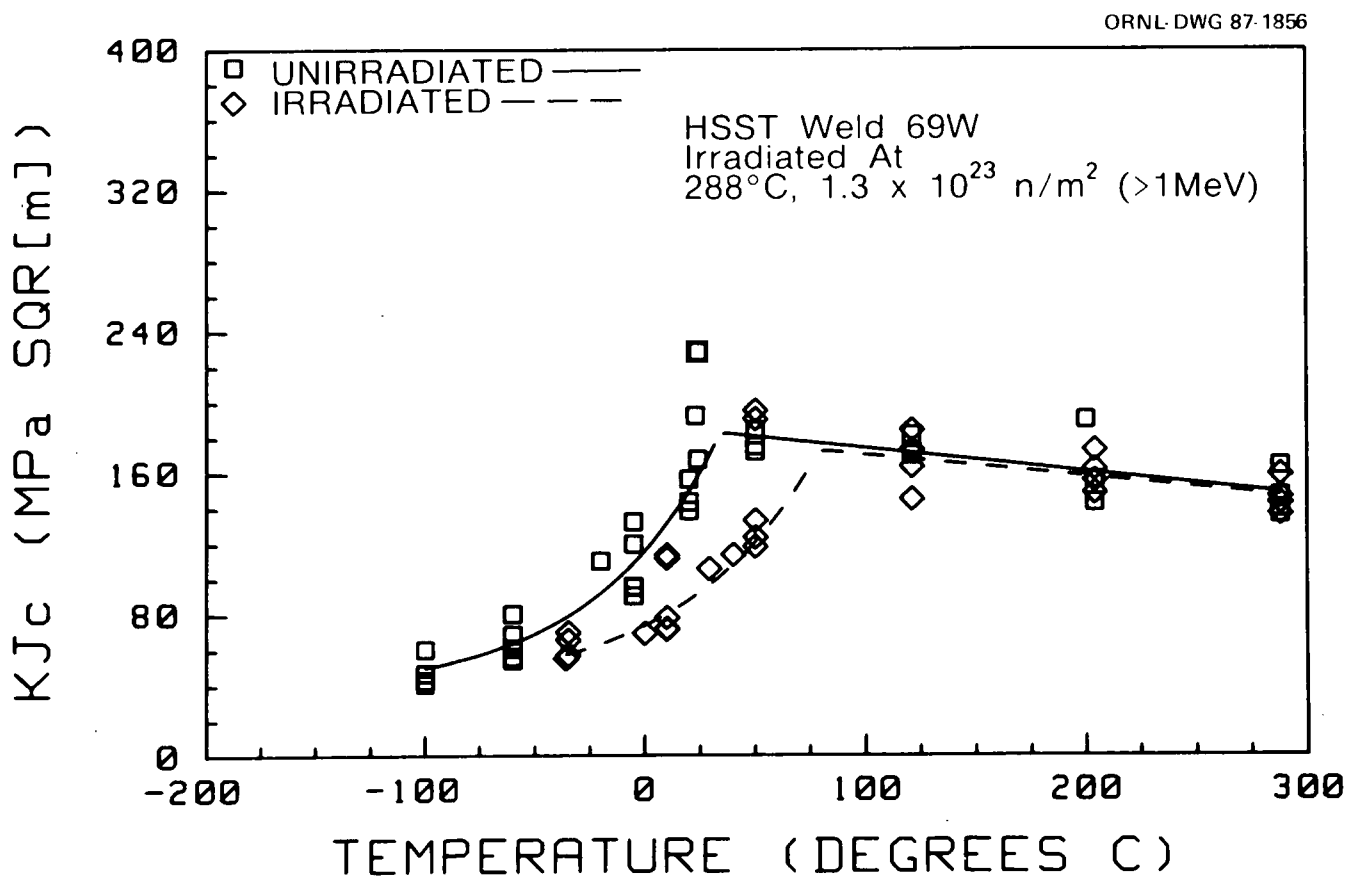

Fig. 26. Effects of irradiation on variation of fracture toughness with temperature for weld 69W.

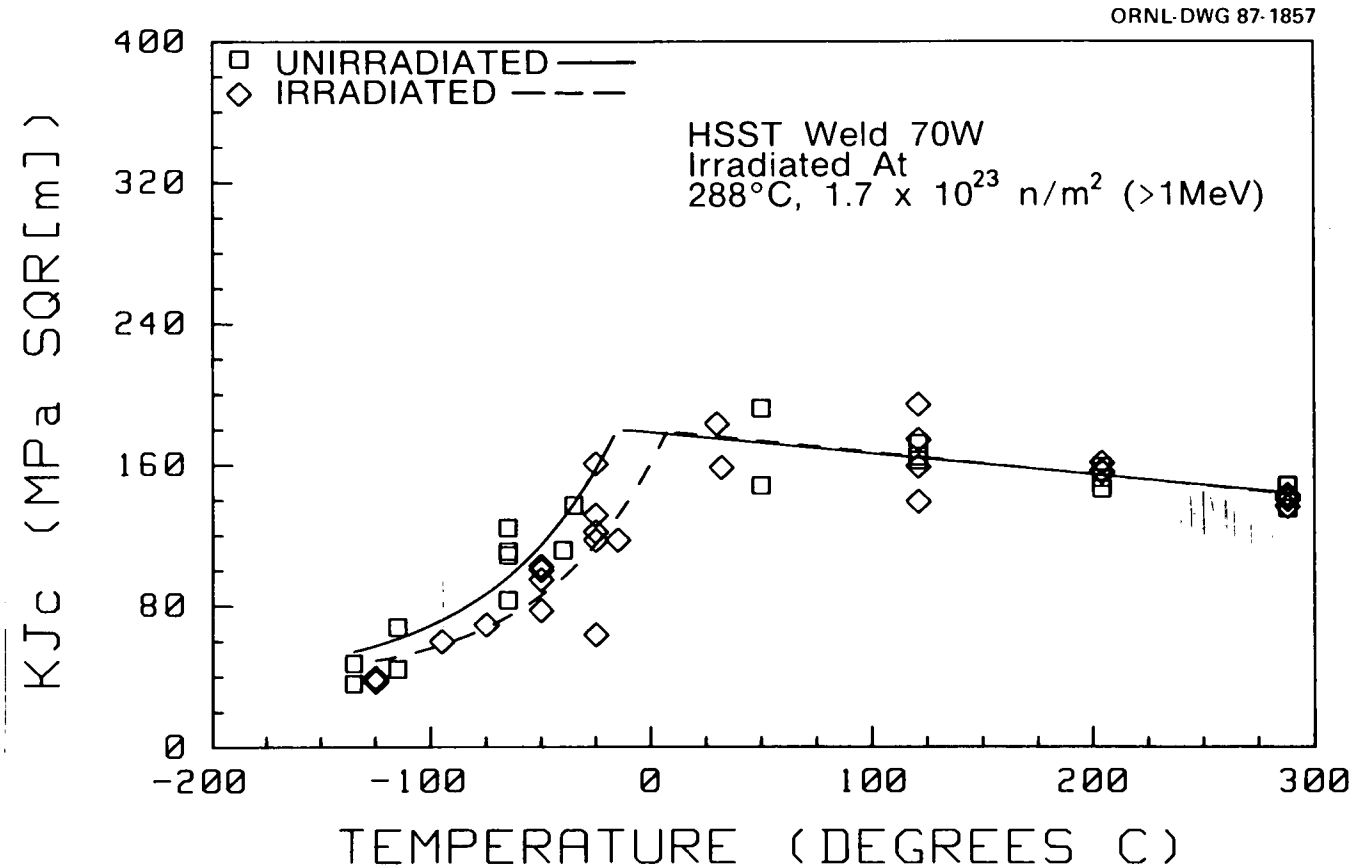

Fig. 27. Effects of irradiation on variation of fracture toughness with temperature for weld 70W.

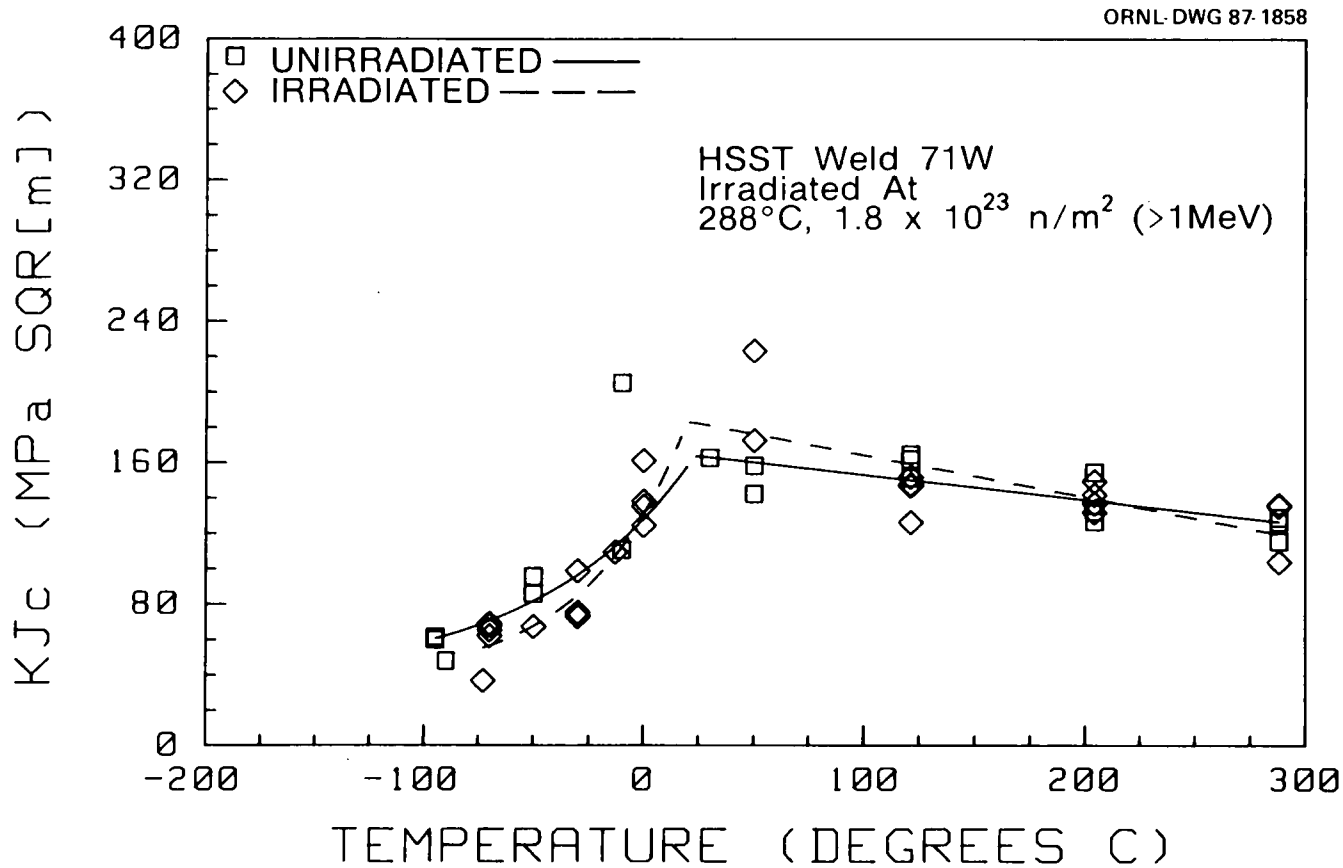

Fig. 28. Effects of irradiation on variation of fracture toughness with temperature for weld 71W.

Table 10. Statistical comparison of 1TCS K_{Jc} results for unirradiated pressure vessel plate and submerged-arc welds

Test temperature (°C)	Mean K_{Jc}, MPa$\sqrt{m}$			Standard deviation, MPa$\sqrt{m}$			Number of tests	
	ORNL	MEA	Combined	ORNL	MEA	Combined	ORNL	MEA
A533 grade B class 1 (HSST-02)								
−95	49.5	49.4	49.5	10.9	8.0	7.9	2	3
−40	71.3	90.4	80.9	2.9	1.4	10.6	3	3
−5	124.2	130.5	129.0		6.6	6.2	1	3
23	241.8	230.4	236.1	36.9	24.0	28.6	3	3
50	180.9	203.4	194.4	35.5	8.2	22.4	2	3
121	169.9	179.3	175.5	26.0	9.6	15.6	2	3
204	180.2	168.5	173.2	18.8	2.8	11.6	2	3
288	162.2	153.6	157.0	4.8	2.4	5.6	2	3
Submerged-arc weld (HSST-68W)								
−80	90.8	150.8	110.8	45.5		47.3	2	1
−30	212.3	292.7	252.5			56.9	1	1
121	201.8	176.8	189.3			17.7	1	1
288	198.6	158.4	178.5			28.4	1	1
Submerged-arc weld (HSST-69W)								
−100	41.7	53.4	47.5	1.3	9.5	8.8	2	2
−60	61.7	67.2	63.9	6.3	18.5	10.7	3	2
−5	95.7	114.2	106.8	0.3	21.5	18.3	2	3
22	184.1	158.0	171.1	38.9	29.8	34.1	3	3
50	174.9	178.0	177.0		8.5	6.3	1	2
121	176.3	170.9	173.6	7.1	1.3	5.2	2	2
203	143.0	173.0	163.0		24.1	24.3	1	2
288	155.1	137.9	146.5	12.1	2.3	12.2	2	2
Submerged-arc weld (HSST-70W)								
−135	41.6			8.1			2	
−115		56.0			16.8			2
−65	109.7	103.7	106.7	1.4	28.9	17.1	2	2
50	148.2	191.8	170.0			30.8	1	1
121	167.2	164.7	166.3	6.7		5.0	2	1
204	155.5	146.2	152.4	4.6		6.3	2	1
288	148.0	135.0	143.7	0.3		7.5	2	1
Submerged-arc weld (HSST-71W)								
−93	47.8	60.6	56.3		1.1	7.4	1	2
−50	85.8	95.5	90.7			6.9	1	1
−10	157.8			66.8			2	
50	142.3	158.2	150.3			11.2	1	1
121	161.9	158.0	159.3		9.3	7.0	1	2
204	154.5	129.6	137.9		4.0	14.7	1	2
288	128.8	121.0	123.6		7.8	7.1	1	2

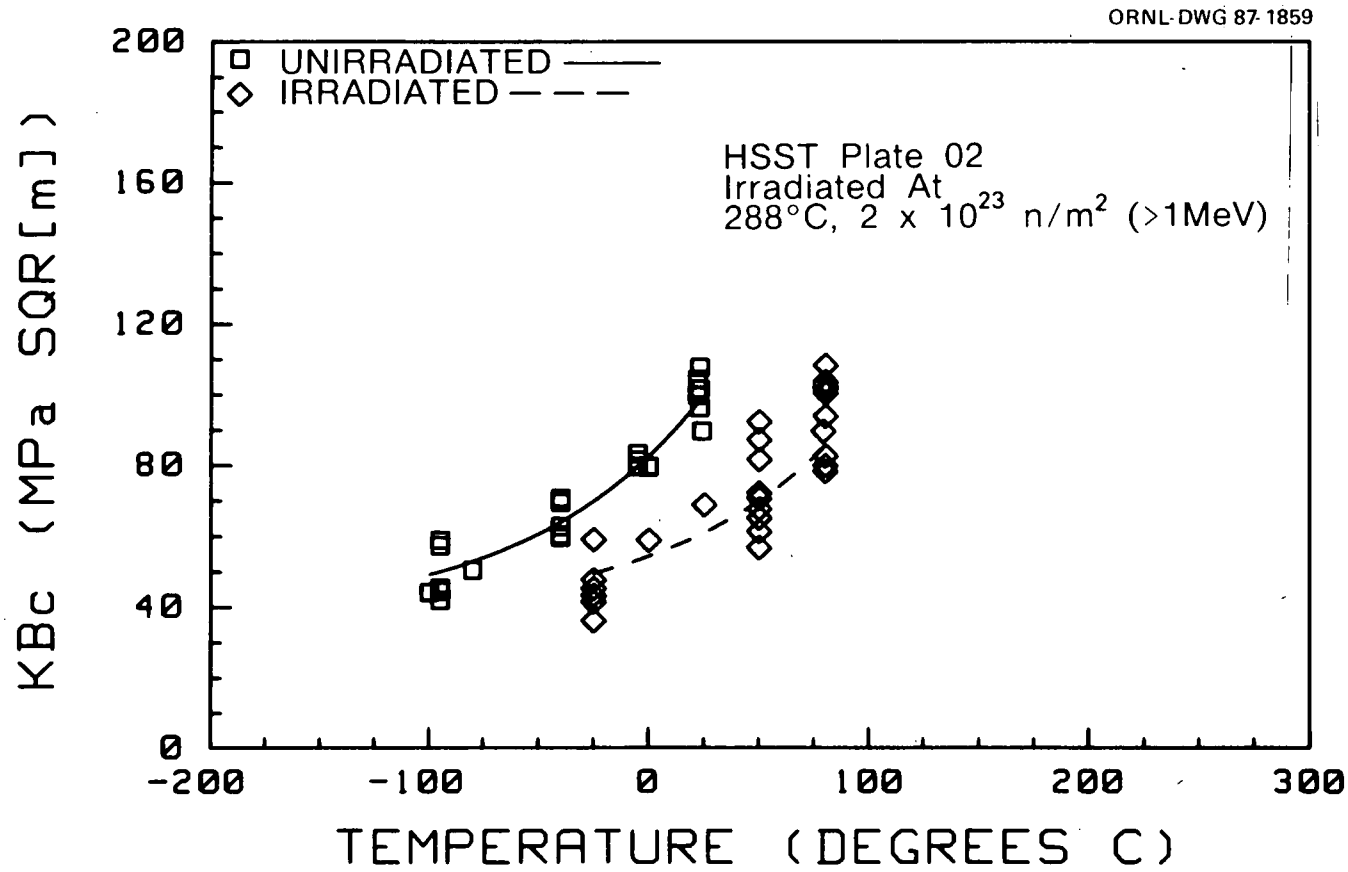

Fig. 29. Effects of irradiation on variation of β-corrected fracture toughness with temperature for Plate 02.

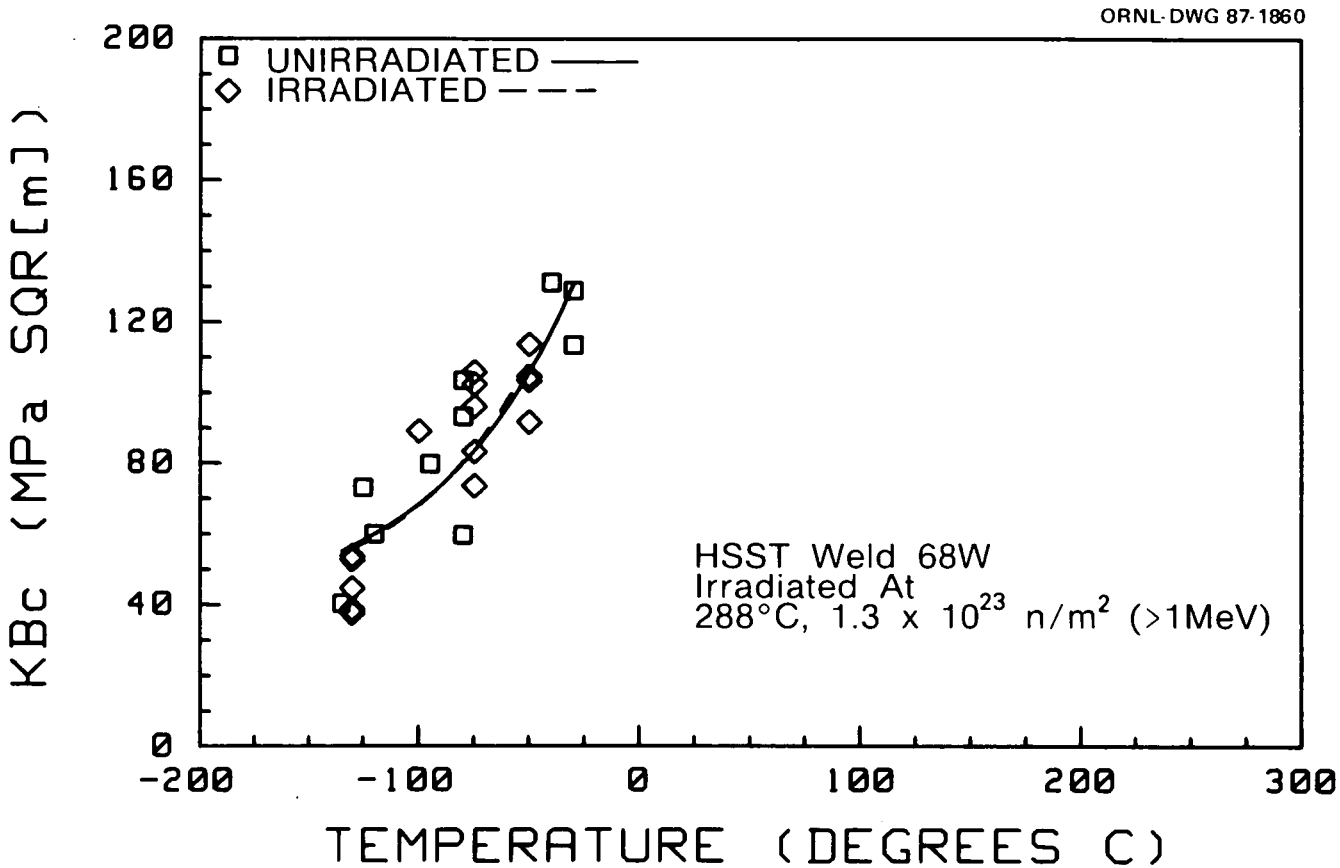

Fig. 30. Effects of irradiation on variation of β-corrected fracture toughness with temperature for weld 68W.

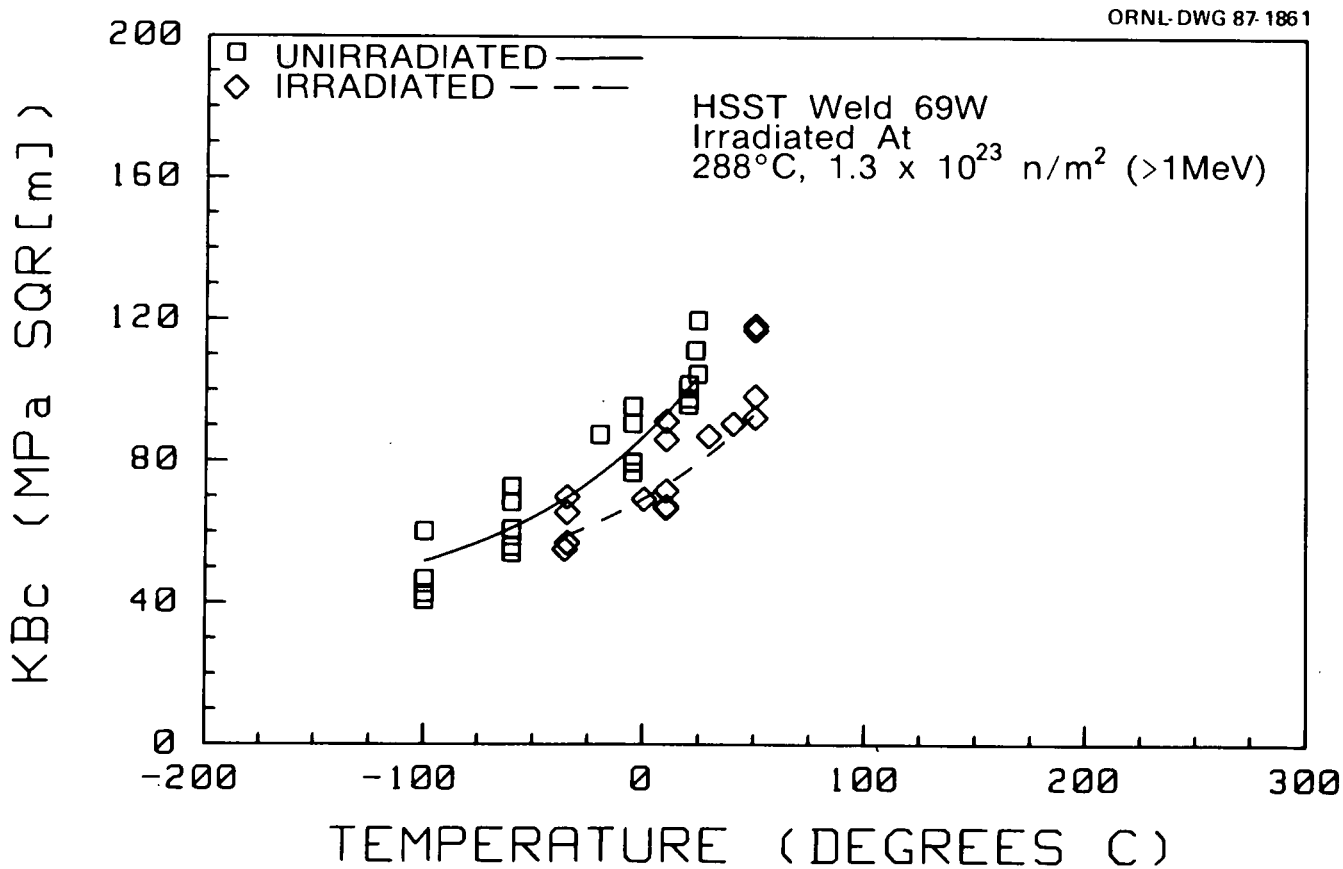

Fig. 31. Effects of irradiation on variation of β-corrected fracture toughness with temperature for weld 69W.

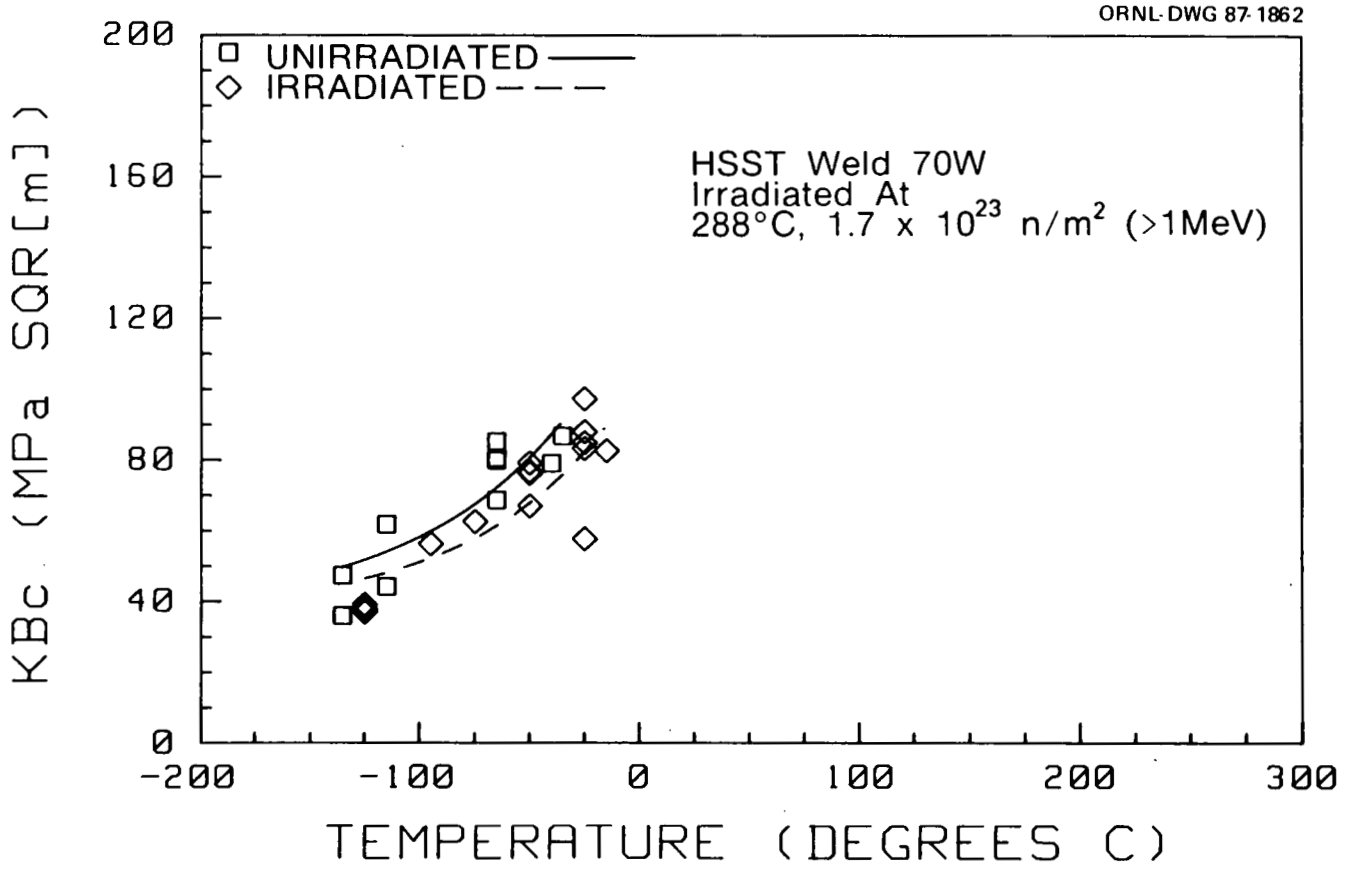

Fig. 32. Effects of irradiation on variation of β-corrected fracture toughness with temperature for weld 70W.

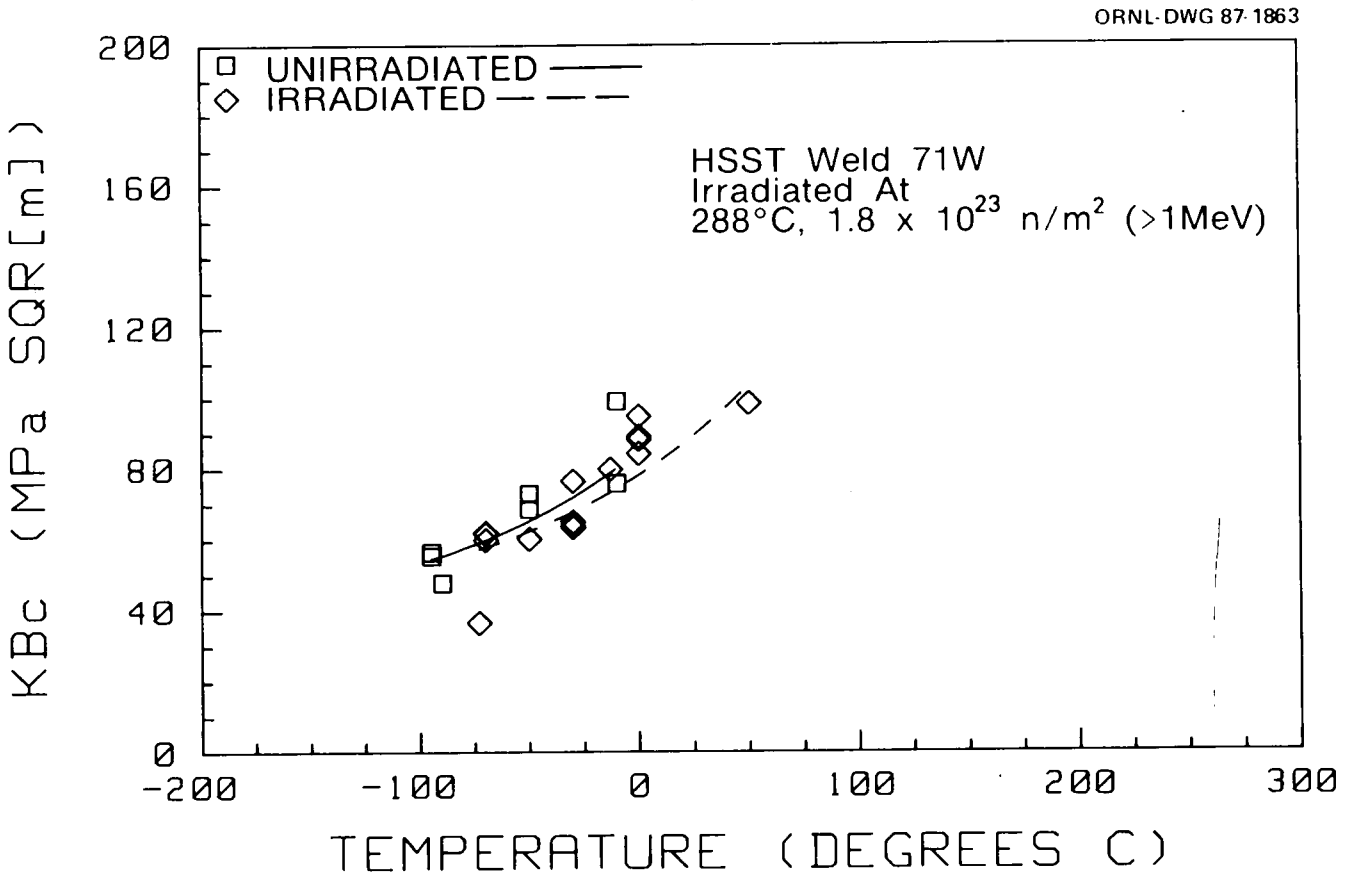

Fig. 33. Effects of irradiation on variation of β-corrected fracture toughness with temperature for weld 71W.

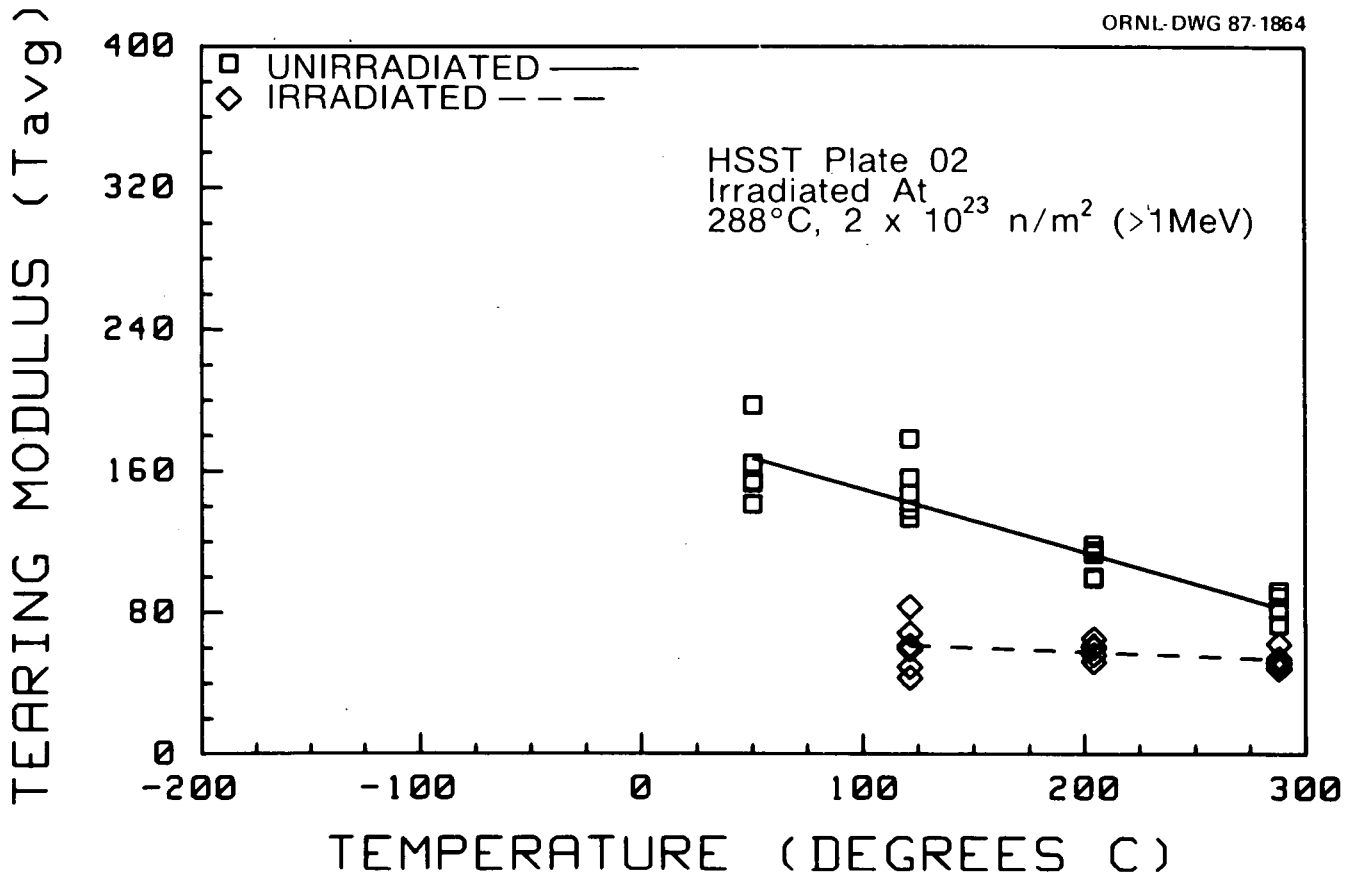

Fig. 34. Effects of irradiation on variation of tearing modulus with temperature for Plate 02.

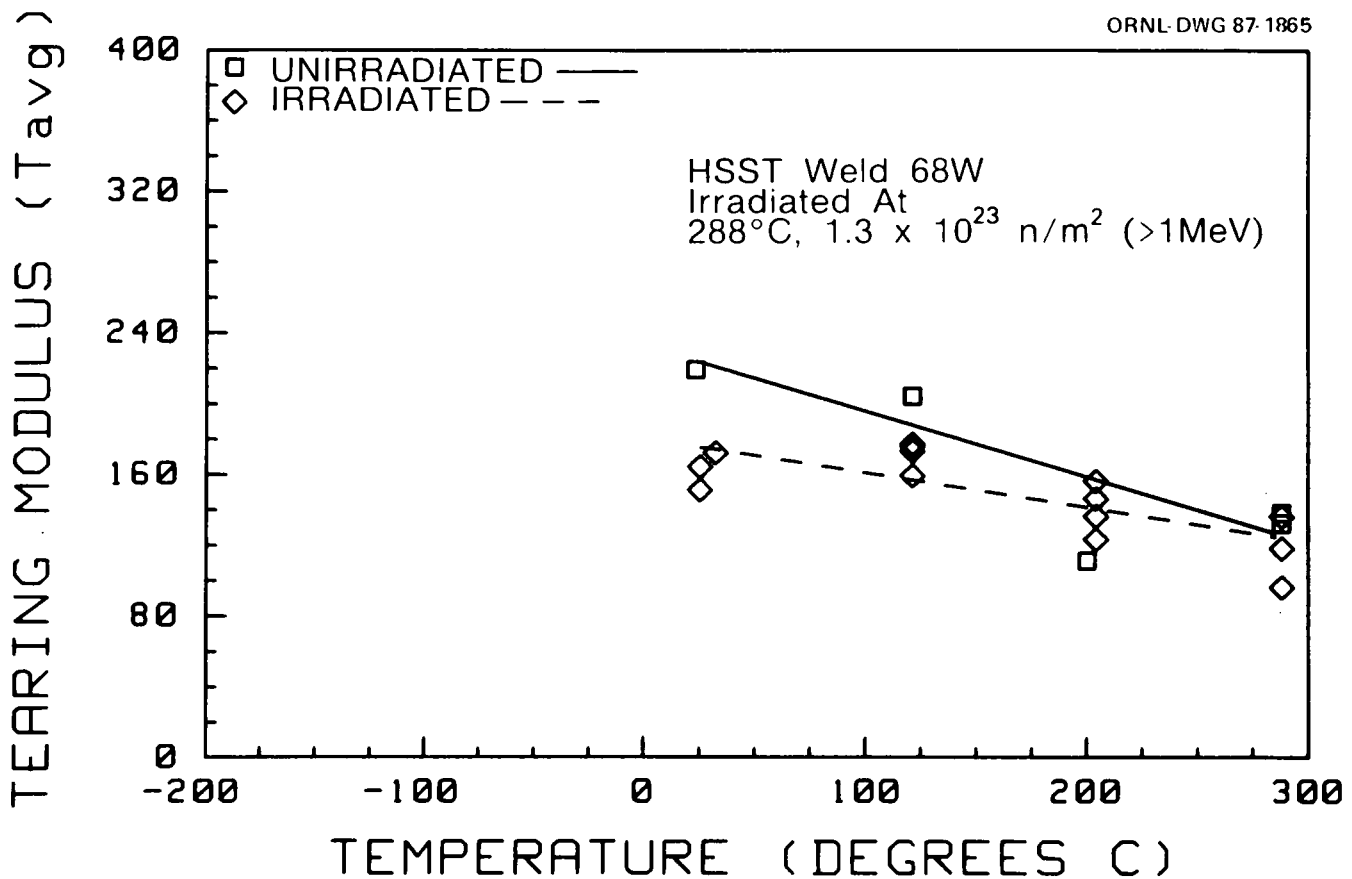

Fig. 35. Effects of irradiation on variation of tearing modulus with temperature for weld 68W.

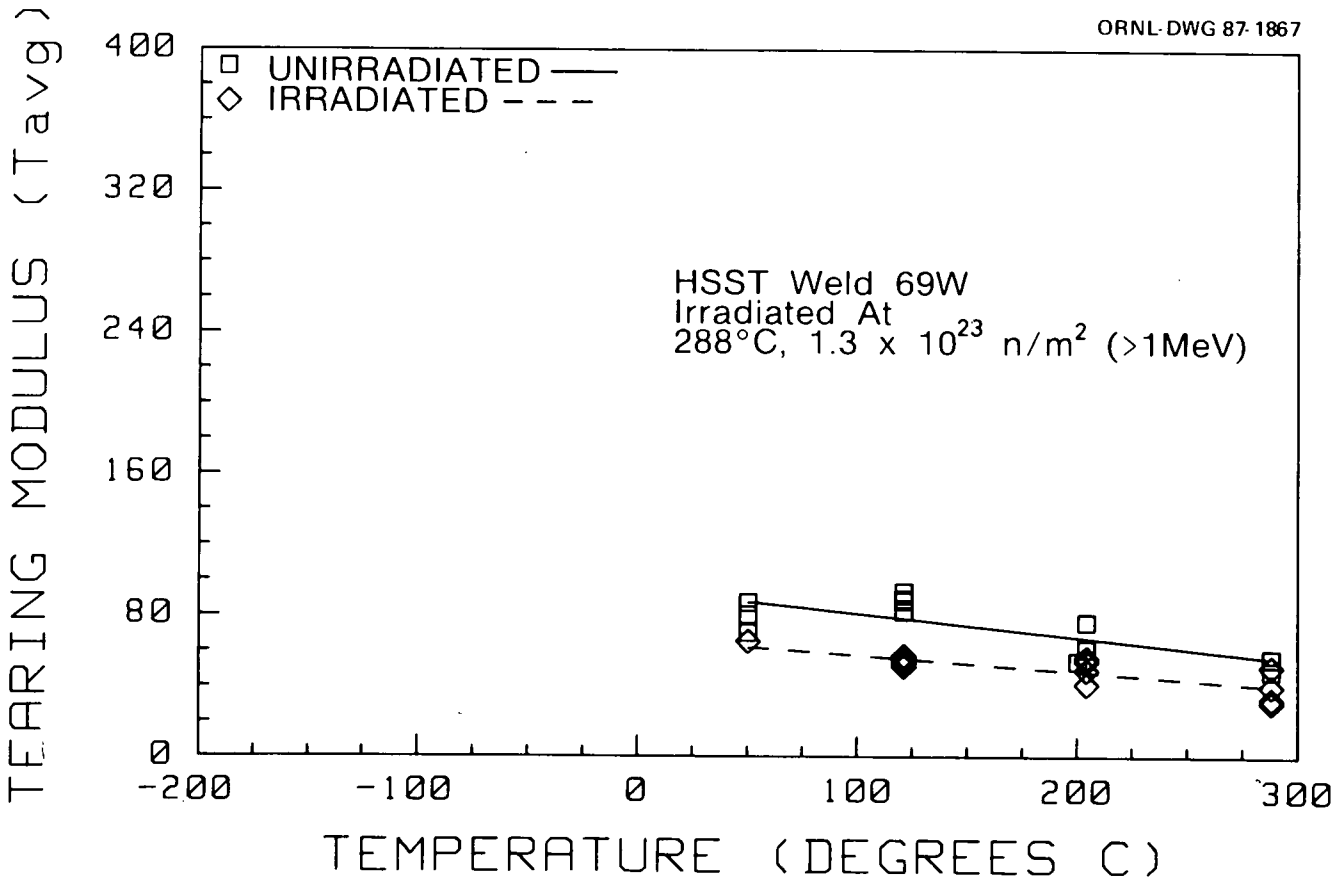

Fig. 36. Effects of irradiation on variation of tearing modulus with temperature for weld 69W.

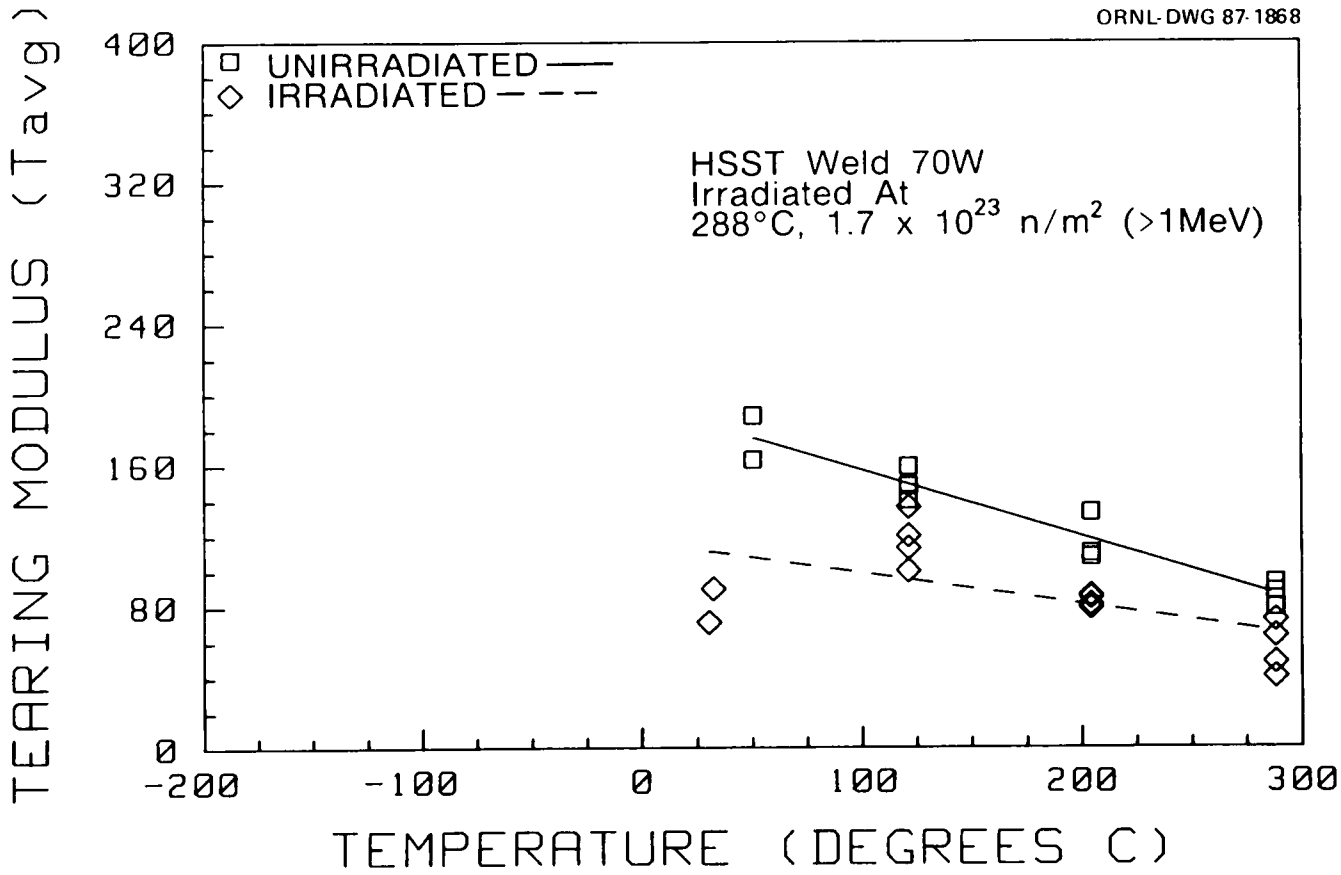

Fig. 37. Effects of irradiation on variation of tearing modulus with temperature for weld 70W.

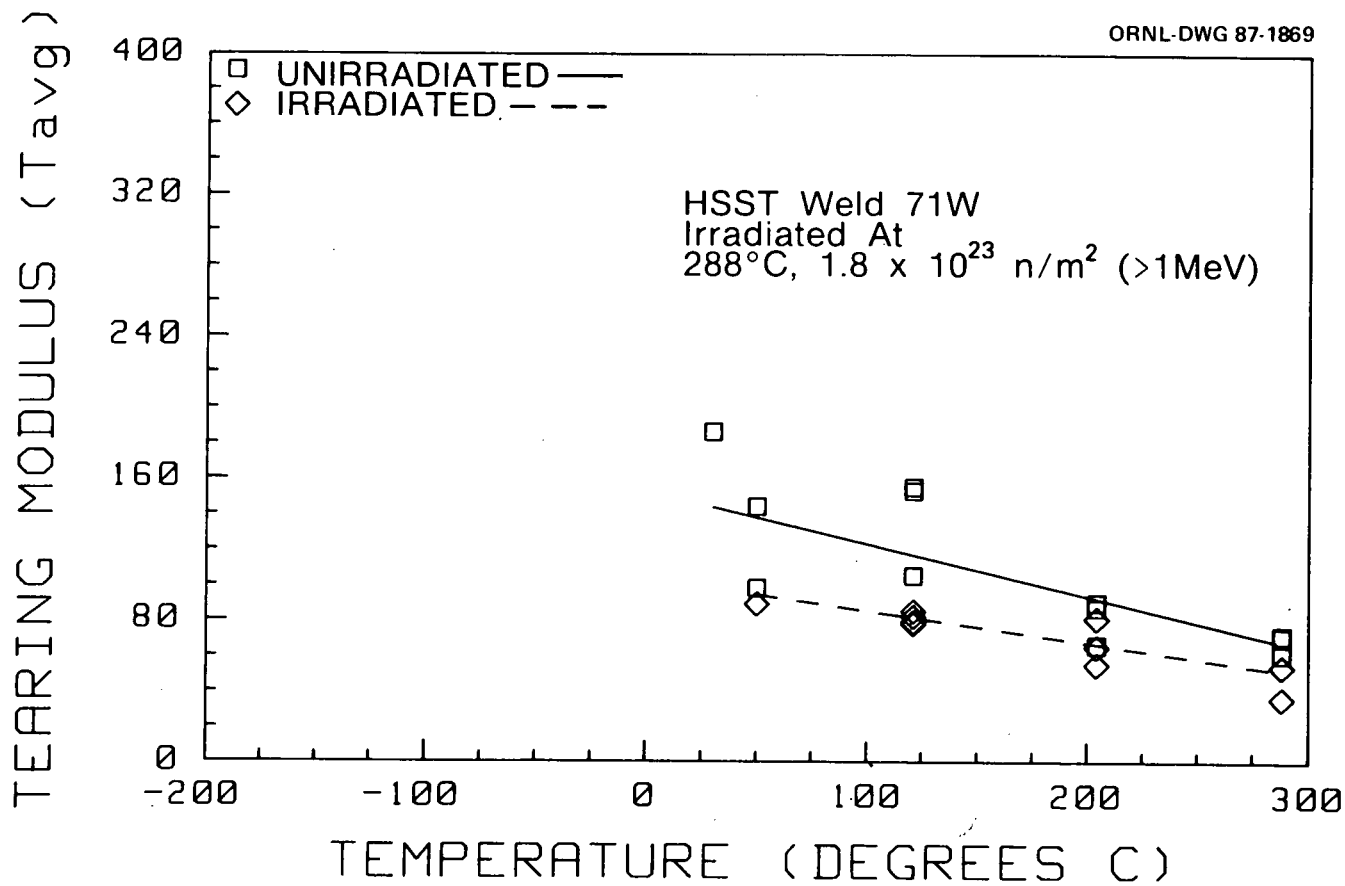

Fig. 38. Effects of irradiation on variation of tearing modulus with temperature for weld 71W.

Table 11. Statistical comparison of 1TCS mean tearing modulus and mean J = 8.8T value with temperature for unirradiated plate and submerged-arc welds

Test temperature (°C)	Tearing modulus			J = 8.8T, KJ/m^2			Number of tests
	Mean	Standard deviation	CV	Mean	Standard deviation	CV	
A533 grade B class 1 (HSST-02)							
50	162	21	0.132	809	229	0.284	5
121	150	18	0.118	696	63	0.090	5
204	109	9	0.082	484	60	0.124	5
288	82	9	0.108	434	65	0.151	5
Submerged-arc weld (HSST-68W)							
121	204	0	0.000	1063	11	0.010	2
288	135	4	0.031	710	84	0.118	2
Submerged-arc weld (HSST-69W)							
50	79	9	0.108	460	29	0.063	3
121	88	5	0.051	472	15	0.031	4
204	64	11	0.176	345	23	0.067	3
288	54	4	0.064	300	3	0.009	4
Submerged-arc weld (HSST-70W)							
50	176	18	0.101	889	52	0.058	2
121	149	10	0.064	685	67	0.098	3
204	117	14	0.119	497	62	0.126	3
288	87	7	0.082	394	12	0.031	3
Submerged-arc weld (HSST-71W)							
50	121	33	0.269	647	166	0.256	2
121	138	28	0.206	627	177	0.282	3
204	81	13	0.162	331	34	0.104	3
288	68	6	0.090	297	50	0.168	3

modulus and weld 69W had the lowest. The largest scatter in the tearing modulus was seen in weld 71W, and the lowest in weld 68W. Of the materials studied, weld 68W had the largest values of J = 8.8T and weld 69W had the smallest. The scatter in the J = 8.8T value was higher at lower temperatures, with weld 71W having the highest scatter and weld 69W the lowest. (Appendix C* contains load-displacement and J-R curves for unirradiated 1TCS specimens tested by MEA. Appendix D contains load-displacement curves, J-R curves, and photographs of the fracture surfaces for unirradiated 1TCS specimens tested by ORNL.)

Tables 12 and 13 provide summaries of the transition region and ductile-shelf region fracture toughness results, respectively, for the five materials tested in the irradiated condition. Variations of the fracture toughness (K_{Jc}) with temperature for Plate 02 and welds 68W, 69W, 70W, and 71W in the irradiated condition are shown in Figs. 24 through 28, respectively. The data scatter is generally small in the ductile-shelf and low-transition regions. The data scatter is higher in the upper-transition region, due in some part to variations in fluence and to ductile crack growth prior to cleavage. A statistical summary for K_{Jc} of the plate and welds is shown in Table 14. Note that the agreement between the two laboratories for the irradiated mean K_{Jc} value is generally less than one standard deviation, independent of the temperature or material. Also note that the variations are similar for all materials. Variations of the β-corrected fracture toughness ($K_{\beta c}$) with temperature for Plate 02 and welds 68W, 69W, 70W, and 71W in the irradiated condition are shown in Figs. 29 through 33, respectively. Although the magnitudes of the β-corrected fracture toughnesses ($K_{\beta c}$) are less than the uncorrected fracture toughnesses (K_{Jc}), the general behavior is similar. To reduce the scatter in the transition-region K_{Jc} and $K_{\beta c}$ data, the test temperature was shifted slightly to account for fluence variations. In this procedure the unirradiated transition-region K_{Jc} data were fit with an exponential curve of the following form:

$$K_{Jc} = A + e^{(Bt+C)} , \qquad (6)$$

where t is the temperature in °C, and A, B, and C are curve fit coefficients. [Note that in making the fit to Eq. (6), no data points were used that had ductile crack growth greater than 0.15 mm.] Using this curve fit, the irradiation-induced temperature shift (δt) was determined for each specimen. Using Eq. (2), a power law was fit to the δt vs fluence data. As with the CVN data, the temperature shift was corrected to the average fluence in the transition region for that material. This approach was pursued for each material; however, as with the CVN data, only in the case of Plate 02 was a successful result obtained. For Plate 02, the power N was determined to be 0.73. A summary of the 1TCS data after accounting for fluence effects is shown in Table 15. The resulting K_{Jc} and $K_{\beta c}$ data after correction are shown in Figs. 39 and 40, respectively. Note that the scatter in the irradiated data is much reduced and is similar to the unirradiated data.

Variations of the tearing modulus (T) with temperature for Plate 02 and welds 68W, 69W, 70W, and 71W in the irradiated condition are shown in

*Appendixes C through F are included in ORNL/TM-10387/V2, available to those listed in Distribution Category RF by contacting ORNL.

Table 12. Transition-region 1TCS test data for irradiated pressure vessel plate and submerged-arc welds

Specimen number	Fluence, 10^{23} n/m^2 (>1 MeV)	Laboratory	Side grooves (%)	Test temperature (°C)	(a/W)	Delta-a (mm)	J_{max} (KJ/m^2)	K_{Jc} (MPa$\sqrt{m}$)	K_{Ic} (MPa$\sqrt{m}$)	$K_{\beta c}$ (MPa$\sqrt{m}$)	Yield strength (MPa)	Young's modulus (GPa)
02G414	2.14	ORNL	0	−25	0.592	0.05	6.9	38.0	36.0	37.5	647	209
02G368	2.34	MEA	0	−25	0.625	0.05	7.4	39.3	41.3	38.8	643	209
02G360	2.68	MEA	0	−25	0.622	0.05	8.2	41.3	43.1	40.6	643	209
02G423	1.23	MEA	0	−25	0.610	0.05	10.0	45.8	47.5	44.7	643	209
02G406	1.90	ORNL	0	−25	0.602	0.05	14.3	54.6	45.1	52.2	647	209
02G401	1.23	ORNL	0	−25	0.609	0.05	16.6	58.8	58.9	55.6	647	209
02G403	1.63	MEA	0	0	0.608	0.05	19.4	63.4		58.7	630	207
02G280	0.96	MEA	0	25	0.621	0.05	30.6	79.3		68.7	617	206
02G407	2.00	ORNL	0	50	0.611	0.05	18.3	61.1		56.6	604	204
02G365	2.57	ORNL	0	50	0.624	0.05	22.5	67.8		61.2	604	204
02G358	2.65	MEA	0	50	0.619	0.05	26.6	73.8		65.0	604	204
02G416	2.08	MEA	0	50	0.610	0.05	26.7	73.9		65.0	604	204
02G353	2.34	ORNL	0	50	0.618	0.05	29.8	78.0		67.5	604	204
02G411	2.15	MEA	0	50	0.612	0.05	34.3	83.7		70.6	604	204
02G404	1.77	ORNL	0	50	0.609	0.05	36.7	86.6		72.1	604	204
02G348	1.74	MEA	0	50	0.618	0.07	55.9	107.0		81.5	604	204
02G402	1.41	MEA	0	50	0.615	0.05	71.9	121.2		87.1	604	204
02G282	1.44	ORNL	0	50	0.618	0.05	90.3	135.9		92.2	604	204
02G288	2.08	ORNL	0	79	0.624	0.12	84.7	131.1		89.5	591	203
02G316	2.36	ORNL	0	80	0.619	0.05	50.1	100.7		78.1	590	203
02G413	2.18	MEA	0	80	0.600	0.05	54.1	104.7		79.8	590	203
02G335	2.36	MEA	0	80	0.617	0.06	61.3	111.5		82.5	590	203
02G342	1.44	MEA	0	80	0.615	0.26	103.4	144.8		93.8	590	203
02G349	2.00	MEA	0	80	0.626	0.24	139.4	168.1		100.3	590	203
02G331	2.56	MEA	0	80	0.620	0.15	147.8	173.1		101.6	590	203
02G344	1.00	ORNL	0	80	0.607	0.25	152.0	175.5		102.2	590	203
02G329	2.56	ORNL	0	80	0.612	0.51	161.1	180.7		103.5	590	203
02G421	1.74	ORNL	0	80	0.603	0.44	138.1	200.7		108.1	590	203

Table 12. (Continued)

Specimen number	Fluence, 10^{23} n/m^2 (>1 MeV)	Laboratory	Side grooves (%)	Test temperature (°C)	(a/W)	Delta-a (mm)	J_{max} (KJ/m^2)	K_{Jc} (MPa$\sqrt{m}$)	K_{Ic} (MPa$\sqrt{m}$)	$K_{\beta c}$ (MPa$\sqrt{m}$)	Yield strength (MPa)	Young's modulus (GPa)
68WMB	1.74	ORNL	0	−130	0.598	0.05	6.5	37.4	37.4	37.2	833	215
68WED	1.39	MEA	0	−130	0.603	0.05	6.5	37.4	38.5	37.2	817	215
68WCD	1.46	MEA	0	−130	0.594	0.05	9.5	45.3	44.5	44.9	817	215
68WEA	1.52	MEA	0	−130	0.605	0.05	12.9	52.3	53.6	51.4	817	215
68WHC	1.16	ORNL	0	−130	0.601	0.05	13.5	53.9	52.5	52.9	833	215
68WEE	1.27	MEA	0	−100	0.623	0.05	51.8	105.1		88.9	765	213
68WLD	1.89	MEA	0	−75	0.596	0.05	31.3	81.4		73.4	726	211
68WCC	1.38	MEA	0	−75	0.597	0.05	44.8	97.3		83.1	726	211
68WLC	1.82	ORNL	0	−75	0.597	0.05	67.7	119.6		95.9	757	211
68WBB	1.03	ORNL	0	−75	0.593	0.05	84.9	134.0		102.2	757	211
68WBA	0.89	MEA	0	−75	0.596	0.05	104.3	148.5		105.7	726	211
68WJB	1.04	MEA	0	−50	0.603	0.05	85.3	133.9		91.5	691	210
68WLA	1.41	MEA	0	−50	0.611	0.18	105.8	149.1		103.3	691	210
68WBD	1.29	MEA	0	−50	0.597	0.07	110.6	152.4		104.4	691	210
68WAD	0.75	ORNL	0	−50	0.608	0.25	140.3	171.7		113.5	727	210
69W142	1.35	ORNL	0	−36	0.594	0.05	12.9	52.0	55.0	51.1	785	209
69W119	1.52	ORNL	0	−35	0.593	0.05	15.2	56.4	56.9	55.0	784	209
69W159	1.73	MEA	0	−35	0.589	0.05	21.3	66.7	65.4	63.6	774	209
69W149	0.89	ORNL	0	−35	0.581	0.05	24.1	71.1	69.8	67.2	784	209
69W108	1.00	MEA	0	0	0.598	0.05	22.4	68.1	69.2	64.1	730	207
69W121	1.54	ORNL	0	10	0.603	0.05	24.7	71.4		66.7	739	207
69W114	1.34	ORNL	0	10	0.598	0.05	25.0	71.9		67.1	739	207
69W173	1.07	ORNL	0	10	0.604	0.05	29.5	78.1		71.6	739	207
69W106	0.87	MEA	0	10	0.610	0.27	60.2	111.6		86.1	724	207
69W166	1.81	MEA	0	10	0.594	0.34	62.3	113.5		91.3	724	207
69W113	1.25	ORNL	0	29	0.617	0.05	54.3	105.7		87.0	714	206
69W112	1.15	MEA	0	40	0.618	0.13	63.1	113.7		90.5	708	205
69W143	1.23	ORNL	0	50	0.597	0.05	68.5	118.3		92.3	703	204
69W120	1.54	MEA	0	50	0.600	0.19	86.5	133.0		98.3	703	204
69W137	1.42	MEA	0	50	0.595	3.91	177.8	190.4		116.9	703	204
69W172	1.38	ORNL	0	50	0.572	0.64	186.4	195.2		118.2	703	204

Table 12. (Continued)

Specimen number	Fluence, 10^{23} n/m^2 (>1 MeV)	Laboratory	Side grooves (%)	Test temperature (°C)	(a/W)	Delta-a (mm)	J_{max} (KJ/m^2)	K_{Jc} (MPa$\sqrt{m}$)	K_{Ic} (MPa$\sqrt{m}$)	$K_{\beta c}$ (MPa$\sqrt{m}$)	Yield strength (MPa)	Young's modulus (GPa)
70W126	2.12	ORNL	0	−125	0.546	0.05	6.2	36.4	37.9	36.1	691	214
70W140	1.65	ORNL	0	−125	0.541	0.05	6.3	36.7	36.9	36.4	691	214
70W129	2.05	MEA	0	−125	0.550	0.05	6.3	36.8	37.3	36.4	683	214
70W111	1.19	MEA	0	−125	0.544	0.05	7.0	38.7	39.0	38.3	683	214
70W125	1.99	MEA	0	−95	0.540	0.05	16.7	59.6		56.2	644	213
70W137	1.89	MEA	0	−75	0.548	0.05	22.5	69.1		62.5	621	211
70W124	2.37	ORNL	0	−50	0.543	0.05	28.4	77.2		66.9	603	210
70W106	0.97	ORNL	0	−50	0.544	0.05	42.7	94.7		76.1	603	210
70W133	1.96	MEA	0	−50	0.550	0.05	47.6	100.1		76.7	572	210
70W138	1.70	MEA	0	−50	0.551	0.05	49.8	102.3		79.0	594	210
70W123	2.05	ORNL	0	−25	0.538	0.05	19.3	63.4		57.6	579	209
70W113	1.86	MEA	0	−25	0.544	0.07	65.5	117.0		83.1	570	209
70W128	2.45	MEA	0	−25	0.542	0.10	71.0	121.7		84.8	570	209
70W112	1.60	MEA	0	−25	0.548	0.23	82.6	131.3		87.9	570	209
70W148	1.35	ORNL	0	−25	0.538	0.05	123.3	160.4		97.2	579	209
70W119	1.80	MEA	0	−15	0.549	0.08	65.9	117.1		82.5	561	208
71W143	1.80	ORNL	0	−73	0.548	0.05	5.6	34.3	36.6	33.8	566	211
71W116	1.74	ORNL	0	−70	0.544	0.05	15.7	57.6	61.9	54.2	622	211
71W108	1.20	ORNL	0	−70	0.544	0.05	20.1	65.2		59.9	622	211
71W141	1.86	ORNL	0	−70	0.548	0.05	21.7	67.7		61.6	622	211
71W138	2.03	MEA	0	−70	0.548	0.05	22.2	68.6		61.8	609	211
71W131	2.12	MEA	0	−50	0.553	0.05	21.4	67.1		60.2	587	210
71W151	1.18	MEA	0	−30	0.553	0.05	25.3	72.8		63.4	578	209
71W139	2.35	MEA	0	−30	0.550	0.05	25.9	73.6		63.9	578	209
71W111	1.40	ORNL	0	−30	0.542	0.05	27.1	75.3		65.0	579	209
71W142	2.15	ORNL	0	−30	0.546	0.05	46.6	98.7		76.5	579	209
71W122	1.90	ORNL	0	−13	0.546	0.09	57.4	109.3		79.8	563	208
71W133	2.45	ORNL	0	0	0.537	0.16	74.5	124.3		84.2	552	207
71W115	1.36	MEA	0	0	0.545	0.14	88.0	135.1		88.1	558	207
71W112	1.62	MEA	0	0	0.548	0.25	91.8	138.0		89.0	558	207
71W144	1.56	ORNL	0	0	0.540	0.18	125.1	161.0		94.8	552	207
71W146	1.80	ORNL	20	50	0.522	1.45	155.9	223.2		98.4	526	204

Table 13. Ductile-shelf region 1TCS test data for irradiated pressure vessel plate and submerged-arc welds

Specimen number	Fluence, 10^{23} n/m^2 (>1 MeV)	Laboratory	Side grooves (%)	Test temperature (°C)	(a/W)	Delta-a (mm)	J_{max} (KJ/m^2)	J_{Ic} (KJ/m^2)	K_{JIc} (MPa$\sqrt{m}$)	Tearing modulus	J = 8.8T (KJ/m^2)	Yield strength (MPa)	Young's modulus (GPa)
02G285	1.66	ORNL	20	121	0.626	3.54	204.1	141.6	168.4	68	376.5	639	200
02G362	2.68	ORNL	20	121	0.622	4.30	192.2	146.3	171.2	49	246.2	639	200
02G298	2.23	ORNL	20	121	0.623	4.50	209.1	146.3	171.2	61	337.8	639	200
02G419	1.90	MEA	20	121	0.622	8.79	197.5	150.6	173.7	59	345.5	639	200
02G356	2.59	MEA	20	121	0.622	9.87	194.3	165.2	181.9	43	351.3	639	200
02G375	1.03	MEA	20	121	0.626	7.00	263.9	171.1	185.1	83	475.1	639	200
02G340	1.66	ORNL	20	204	0.622	2.99	177.1	118.8	152.4	65	310.2	617	196
02G363	2.64	ORNL	20	204	0.623	2.20	175.8	128.5	158.5	60	309.4	617	196
02G354	2.47	MEA	20	204	0.617	10.66	196.2	134.3	162.0	61	318.7	617	196
02G412	2.18	MEA	20	204	0.612	9.83	199.7	143.0	167.2	56	323.4	617	196
02G345	1.26	MEA	20	204	0.623	9.88	221.6	154.6	173.8	52	353.6	617	196
02G332	2.52	MEA	20	288	0.616	11.56	135.6	83.3	126.1	49	280.8	613	191
02G287	1.91	MEA	20	288	0.609		150.5	86.8	128.7	54	288.5	613	191
02G373	0.81	MEA	20	288	0.624	11.58	173.9	100.9	138.7	48	279.1	613	191
02G338	2.04	ORNL	20	288	0.622	1.91	196.7	116.8	149.3	62	299.6	613	191
02G422	1.41	ORNL	20	288	0.607	4.73	195.5	153.8	171.3	52	293.9	613	191
02G328	2.53	ORNL	20	288	0.613	4.50	192.4	157.0	173.1	51	282.6	613	191
68WME	1.23	MEA	20	25	0.607	4.04	335.3	178.1	191.4	164	981.6	650	206
68WDE	1.56	MEA	20	25	0.610	3.90	364.0	210.7	208.3	151	932.4	650	206
68WMD	1.51	ORNL	20	32	0.606	6.75	346.7	178.3	191.3	172	1113.1	610	205
68WDC	1.59	ORNL	20	121	0.601	2.81	313.1	131.2	162.1	177	1090.0	575	200
68WKE	1.06	ORNL	20	121	0.601	2.62	342.3	172.6	185.9	159	903.8	575	200
68WEC	1.46	MEA	20	121	0.605	4.35	350.7	210.8	205.5	176	990.1	576	200
68WAB	0.59	MEA	20	121	0.603	4.10	360.4	217.0	208.5	173	983.7	576	200
68WKB	0.90	ORNL	20	204	0.602	2.28	278.0	122.3	154.7	136	730.4	572	196
68WDA	1.57	ORNL	20	204	0.600	2.47	275.1	137.9	164.2	156	839.5	572	196
68WMA	1.86	MEA	20	204	0.602	5.22	287.4	175.1	185.0	146	783.8	572	196
68WLB	1.64	MEA	20	204	0.605	5.26	280.7	201.0	207.8	123	738.5	572	196
68WCE	1.53	ORNL	20	288	0.606	2.08	295.6	113.4	147.1	136	778.6	593	191
68WBC	1.18	MEA	20	288	0.602	7.47	264.6	125.8	154.9	96	542.9	591	191
68WKC	0.70	ORNL	20	288	0.598	2.31	306.5	164.1	176.9	118	657.4	593	191

Table 13. (Continued)

Specimen number	Fluence, 10^{23} n/m^2 (>1 MeV)	Laboratory	Side grooves (%)	Test temperature (°C)	(a/W)	Delta-a (mm)	J_{max} (KJ/m^2)	J_{Ic} (KJ/m^2)	K_{JIc} (MPa$\sqrt{m}$)	Tearing modulus	J = 8.8T (KJ/m^2)	Yield strength (MPa)	Young's modulus (GPa)
69W165	1.89	ORNL	0	50	0.592	2.26	191.2	74.5	123.4	65	411.6	739	204
69W116	1.42	ORNL	0	52	0.580	0.89	171.6	0.0	0.0	0	0.0	702	204
69W126	1.48	ORNL	20	121	0.597	3.15	206.0	105.0	145.0	57	303.1	712	200
69W102	0.57	ORNL	20	121	0.603	2.43	204.3	133.4	163.4	53	296.7	675	200
69W157	1.53	MEA	20	121	0.593	10.33	245.6	149.3	172.9	55	349.6	712	200
69W146	1.01	MEA	20	121	0.597	9.26	227.5	169.3	184.1	51	346.4	712	200
69W160	1.87	ORNL	20	204	0.602	2.08	194.9	112.8	148.5	54	298.1	698	196
69W122	1.52	MEA	20	204	0.595	11.68	199.3	123.7	155.5	49	282.4	698	196
69W153	1.22	ORNL	20	204	0.606	2.26	195.8	134.4	162.1	56	296.2	698	196
69W148	0.88	MEA	20	204	0.611	10.81	214.7	152.7	172.8	41	290.5	698	196
69W144	1.13	ORNL	20	288	0.608	2.17	190.9	97.6	136.4	51	297.4	704	191
69W118	1.49	MEA	20	288	0.555		216.3	106.6	142.6	33	199.9	705	191
69W105	0.72	MEA	20	288	0.606	11.79	162.5	112.1	146.2	31	212.1	705	191
69W167	1.65	ORNL	20	288	0.602	2.00	190.6	132.0	158.7	40	238.1	704	191
70W115	1.55	MEA	20	30	0.555	11.57	238.8	163.0	183.0	71	442.5	600	205
70W139	1.97	ORNL	20	32	0.547	8.66	157.1	121.9	158.2	90	456.4	590	205
70W110	1.42	ORNL	20	121	0.551	4.35	204.8	96.3	138.9	113	571.4	550	200
70W136	2.26	ORNL	20	121	0.544	5.27	238.4	126.0	158.9	120	610.1	550	200
70W132	2.02	MEA	20	121	0.545	8.55	250.6	151.4	174.1	136	633.4	550	200
70W104	0.84	MEA	20	121	0.541	10.06	225.6	187.9	194.0	100	537.9	550	200
70W131	2.41	MEA	20	204	0.556	11.46	188.4	123.9	155.7	85	412.0	535	196
70W145	1.61	MEA	20	204	0.552	11.55	194.0	124.1	155.7	81	410.9	535	196
70W108	1.23	ORNL	20	204	0.551	2.05	196.5	124.7	156.1	86	384.0	535	196
70W118	2.15	ORNL	20	204	0.556	2.50	169.5	132.5	160.9	79	371.5	535	196
70W107	0.81	ORNL	20	288	0.549	2.05	163.0	97.0	136.0	63	251.4	543	191
70W130	2.09	MEA	20	288	0.565	11.05	134.7	102.6	139.9	48	287.8	543	191
70W117	1.86	ORNL	20	288	0.551	1.83	164.8	105.0	141.5	72	287.4	543	191
70W142	1.40	MEA	20	288	0.550	11.94	130.6	106.7	142.7	40	249.0	543	191

Table 13. (Continued)

Specimen number	Fluence, 10^{23} n/m^2 (>1 MeV)	Laboratory	Side grooves (%)	Test temperature (°C)	(a/W)	Delta-a (mm)	J_{max} (KJ/m^2)	J_{Ic} (KJ/m^2)	K_{JIc} (MPa$\sqrt{m}$)	Tearing modulus	J = 8.8T (KJ/m^2)	Yield strength (MPa)	Young's modulus (GPa)
71W140	1.97	ORNL	0	16	0.553	0.71	139.7	0.0	0.0	0	0.0	603	206
71W128	2.03	MEA	20	50	0.555	10.53	222.5	145.7	172.5	89	478.2	570	204
71W101	1.04	ORNL	20	121	0.555	2.94	165.7	79.5	126.2	85	357.5	546	200
71W150	1.41	MEA	20	121	0.546	12.01	171.1	107.4	146.7	78	365.0	546	200
71W134	2.05	ORNL	20	121	0.539	2.30	167.4	108.7	147.6	79	335.1	546	200
71W121	2.27	MEA	20	121	0.547	11.33	191.0	115.0	151.8	82	383.0	546	200
71W149	1.22	MEA	20	204	0.551	13.12	156.8	89.0	131.9	81	305.6	527	196
71W120	1.96	MEA	20	204	0.562	12.70	212.4	95.7	136.8	81	374.3	527	196
71W126	2.43	ORNL	20	204	0.551	2.26	164.7	102.9	141.8	65	265.2	527	198
71W119	1.69	ORNL	20	204	0.546	2.34	160.2	114.1	149.4	55	276.9	527	196
71W117	2.02	MEA	20	288	0.551	0.85	0.0	0.0	0.0	0	0.0	533	191
71W110	1.00	MEA	20	288	0.554	12.10	140.5	56.4	103.7	36	169.0	533	191
71W147	1.51	ORNL	20	288	0.547	2.31	155.8	95.9	135.2	54	234.1	533	191
71W123	2.10	ORNL	20	288	0.552	2.16	156.9	97.0	136.1	54	222.4	533	191

Table 14. Statistical comparison of 1TCS K_{Jc} results for irradiated pressure vessel plate and submerged-arc welds

Test temperature (°C)	Mean K_{Jc}, MPa$\sqrt{m}$			Standard deviation, MPa$\sqrt{m}$			Number of tests	
	ORNL	MEA	Combined	ORNL	MEA	Combined	ORNL	MEA
A533 grade B class 1 (HSST-02)								
−25	46.7	44.0	45.3	11.5	3.2	7.7	3	2
50	85.9	91.9	88.9	29.6	21.2	24.5	5	5
80	157.7	140.4	149.1	40.8	31.5	35.5	5	5
121	170.3	180.2	175.3	1.6	5.9	6.7	3	3
204	155.5	167.7	162.8	4.3	5.9	8.2	2	3
288	164.6	131.2	147.9	13.3	6.7	20.6	3	3
Submerged-arc weld (HSST-68W)								
−130	45.0	45.5	45.3	10.7	7.6	7.6	2	3
−75	126.8	109.1	116.2	10.2	35.1	27.1	2	3
−50	171.7	145.1	151.8		9.9	15.5	1	3
25		199.9			12.0			2
121	174	207	190.5	16.8	2.1	21.4	2	2
204	159.5	196.4	177.9	6.7	16.1	23.6	2	2
288	162	154.9	159.6	21.1		15.5	2	1
Submerged-arc weld (HSST-69W)								
−35	60.6	65.4	61.8	8.1		7.0	3	1
10	73.8	112.6	89.3	3.7	1.3	21.4	3	2
50	156.8	161.7	159.2	54.4	40.6	39.3	2	2
121	154.2	178.5	166.4	13.0	7.9	16.6	2	2
204	155.3	164.2	159.7	9.6	12.2	10.3	2	2
288	147.6	144.4	146.0	15.8	2.5	9.4	2	2
Submerged-arc weld (HSST-70W)								
−125	37.4	38.2	37.8	0.7	1.2	0.9	2	2
−50	86.0	101.2	93.6	12.4	1.6	11.4	2	2
−25	111.9	123.3	118.8	68.6	7.3	35.2	2	3
31	183.0	158.2	170.6			17.5	1	1
121	148.9	184.1	166.5	14.1	14.1	23.3	2	2
204	158.5	155.7	157.1	3.4	0.0	2.5	2	2
288	138.8	140.7	139.7	3.9	1.1	2.6	2	2
Submerged-arc weld (HSST-71W)								
−70	64.9	68.6	65.9	2.9		3.0	4	1
−30	87.0	73.2	80.1	16.5	0.6	12.4	2	2
0	142.7	136.6	139.6	26.0	2.1	15.4	2	2
121	136.9	149.3	143.1	15.1	3.6	11.5	2	2
204	145.6	134.4	140.0	5.4	3.5	7.5	2	2
288	135.7	103.7	125.0	0.6		18.5	2	1

Table 15. Transition-region 1TCS test data for irradiated Plate 02; test temperature adjusted for mean fluence = 1.95×10^{23} neutrons/m^2 (>1 MeV)

Specimen number	Fluence, 10^{23} n/m^2 (>1 MeV)	Test temperature (°C)		K_{Jc} (MPa$\sqrt{m}$)	K_{Ic} (MPa$\sqrt{m}$)	$K_{\beta c}$ (MPa$\sqrt{m}$)
		Actual	Adjusted			
02G414	2.14	−25	−25	38.0	36.0	37.5
02G368	2.34	−25	−38	39.3	41.3	38.8
02G360	2.68	−25	−43	41.3	43.1	40.6
02G423	1.23	−25	1	45.8	47.5	44.7
02G406	1.90	−25	−24	54.6	45.1	52.2
02G401	1.23	−25	−10	58.8	58.9	55.6
02G403	1.63	0	7	63.4		58.7
02G280	0.96	25	65	79.3		68.7
02G407	2.00	50	48	61.1		56.6
02G365	2.57	50	32	67.8		61.2
02G358	2.65	50	32	73.8		65.0
02G416	2.08	50	46	73.9		65.0
02G353	2.34	50	39	78.0		67.5
02G411	2.15	50	44	83.7		70.6
02G404	1.77	50	56	86.6		72.1
02G348	1.74	50	55	107.0		81.5
02G402	1.41	50	65	121.2		87.1
02G282	1.44	50	62	135.9		92.2
02G288	2.08	79	75	131.1		89.5
02G316	2.36	80	67	100.7		78.1
02G413	2.18	80	73	104.7		79.8
02G335	2.36	80	68	111.5		82.5
02G342	1.44	80	99	144.8		93.8
02G349	2.00	80	79	168.1		100.3
02G331	2.56	80	68	173.1		101.6
02G344	1.00	80	121	175.5		102.2
02G329	2.56	80	69	180.7		103.5
02G421	1.74	80	85	200.7		108.1

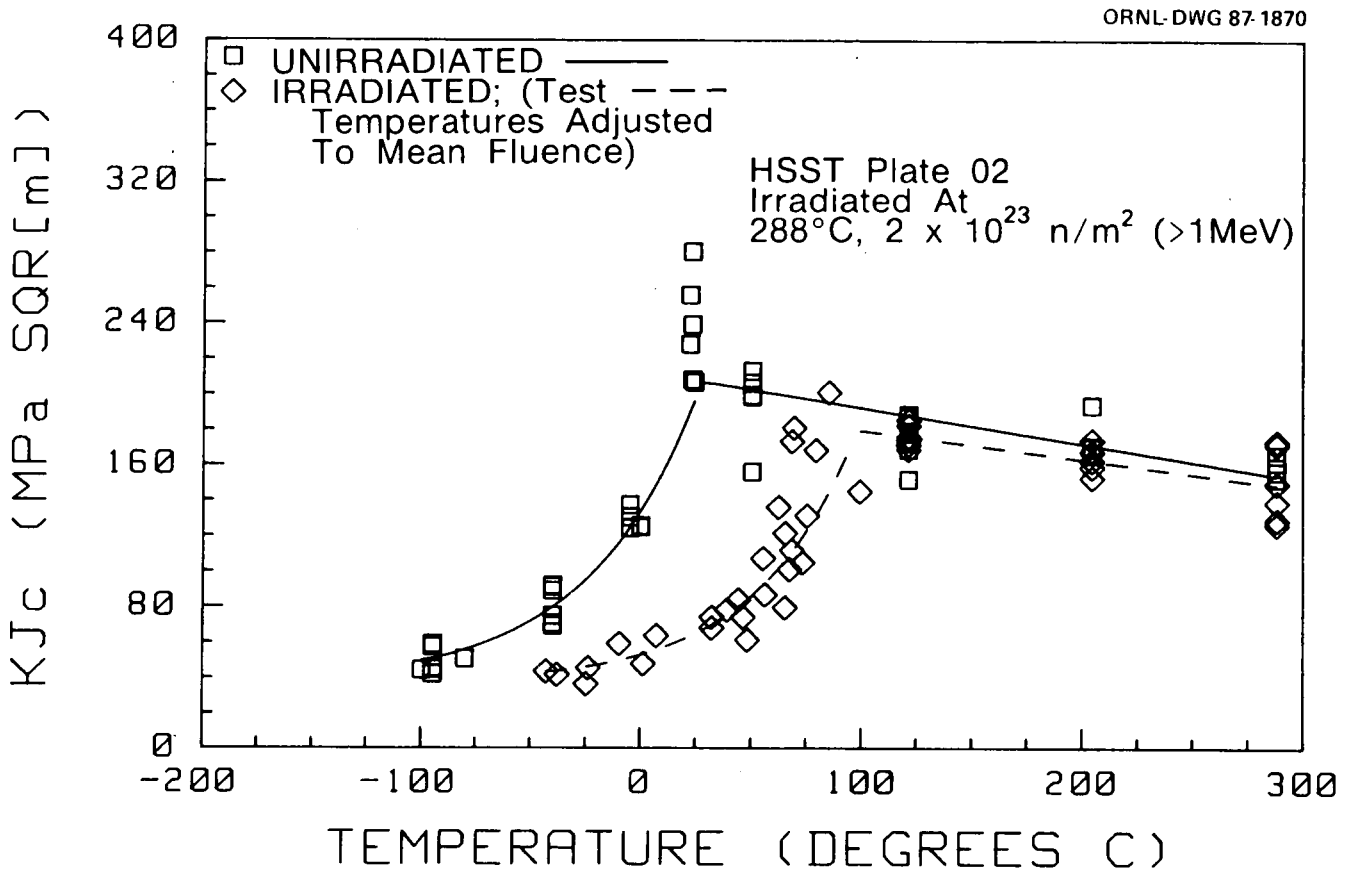

Fig. 39. Effects of irradiation on variation of fracture toughness with temperature for Plate 02, test temperatures adjusted to mean fluence of 1.95×10^{23} neutrons/m^2 (>1 MeV).

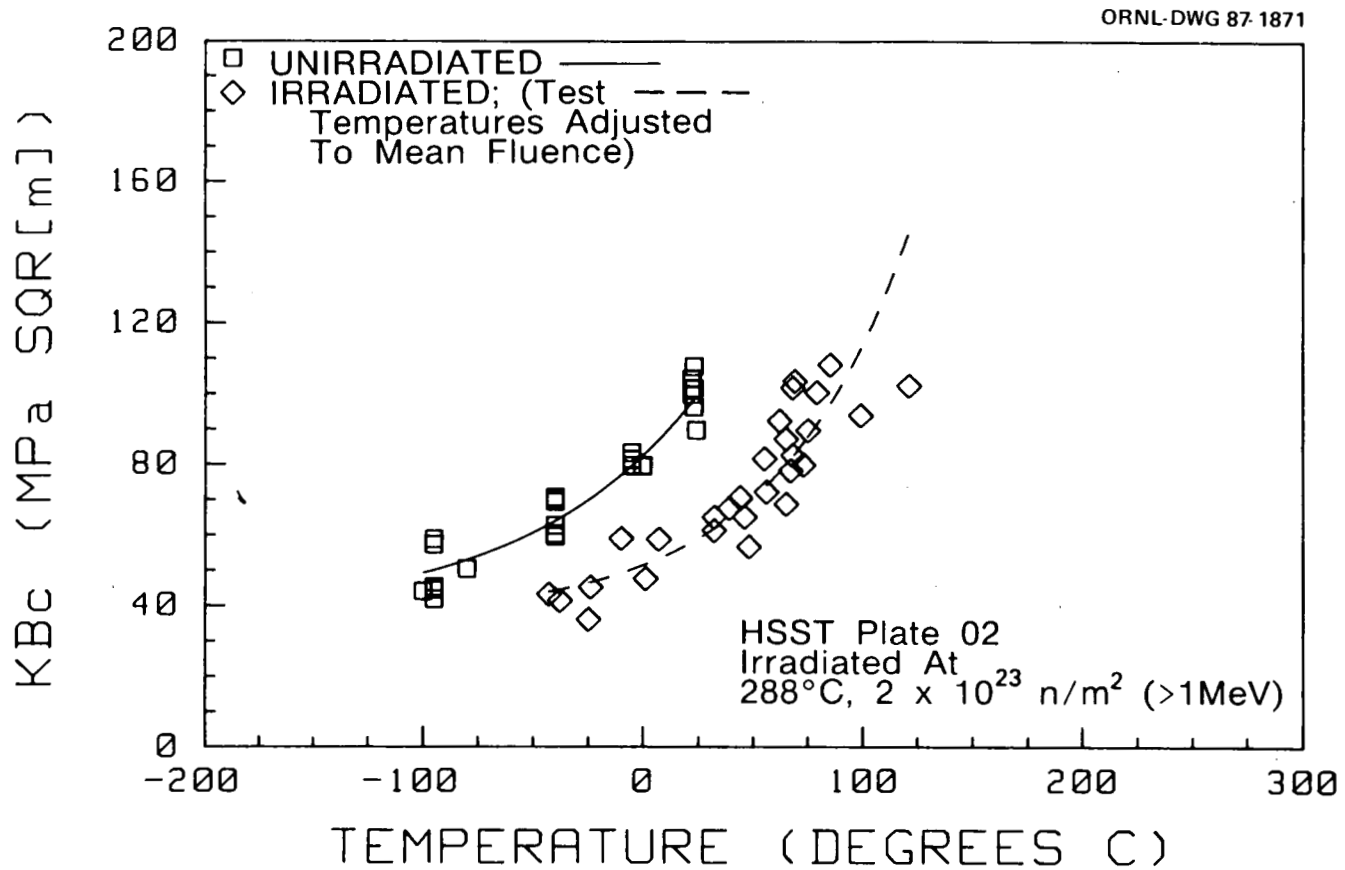

Fig. 40. Effects of irradiation on variation of β-corrected fracture toughness with temperature for Plate 02, test temperatures adjusted to mean fluence of 1.95×10^{23} neutrons/m^2 (>1 MeV).

Figs. 34 through 38, respectively. The value of the tearing modulus decreases linearly with temperature. A statistical summary for tearing modulus and J = 8.8T of the plate and welds is shown in Table 16. Note that the coefficient of variation (CV = standard deviation/mean) is also listed in the table. Of the irradiated materials studied, weld 68W had the highest tearing modulus and weld 69W had the lowest. The scatter in tearing modulus was similar for all the materials investigated. Of the irradiated materials studied, weld 68W had the largest values of J = 8.8T and weld 69W had the lowest, the same ranking as observed for the unirradiated case. Weld 68W had generally higher scatter than the other materials. (Appendix E contains load-displacement and J-R curves for irradiated 1TCS specimens tested by MEA. Appendix F contains load-displacement curves, J-R curves, and photographs of the fracture surfaces for irradiated 1TCS specimens tested by ORNL.)

COMPARISON OF RESULTS AND STATISTICAL ANALYSES

It is common practice to estimate the irradiated transition-region fracture toughness by shifting the unirradiated results by the Charpy V-notch 41-J shift temperature. A comparison of the transition temperature shifts for the five materials in the study is listed in Table 17 and shown in Fig. 41. Both the K_{Jc} and the $K_{\beta c}$ shifts correlate qualitatively with the CVN shifts; the correlation coefficients of linear fits are over 0.9. A comparison of J_{Ic} at 204°C and Charpy V-notch upper-shelf energy is listed in Table 18 and shown in Fig. 42. The change in J_{Ic} is not significant (±10%) and does not correlate well with the CVN upper-shelf energy change (correlation coefficient of 0.5). A comparison between T and J = 8.8T, both at 204°C, is listed in Table 18 and shown in Fig. 43. The value of the tearing modulus is heavily influenced by flow stress [Eq. (3)]; therefore, there is good correlation between the flow stress and the tearing modulus and between the flow stress and the J = 8.8T values (correlation coefficient of ~0.9). The decreases in the tearing moduli and the J = 8.8T values are generally about double the increases of the flow stresses.

A procedure was developed jointly by the Pressure Vessel Research Committee (PVRC) and the Materials Properties Council (MPC)[23] to correlate fracture toughness with Charpy V-notch energy. In the statistically based procedure, the entire CVN energy curve is used to determine the full fracture toughness behavior. Hyperbolic tangent temperature models were assumed for both the fracture toughness and CVN energy. Using the PVRC-MPC method, the fracture toughness transition temperature shifts and the ductile-shelf changes were calculated for the five materials in this study. A comparison of those predictions and actual observations are listed in Table 19 and shown in Figs. 44 and 45 for transition temperature shift and ductile-shelf change, respectively.

The predicted PVRC-MPC shifts show general agreement (within about 25°C) with the experimentally determined shifts. Note, however, that three of the predicted shifts are about 20°C, whereas the observed K_{Jc} shifts for those three materials were −6, 25, and 47°C. The correlation coefficient of a linear fit was 0.84. The upper-shelf fracture toughness changes predicted by the PVRC-MPC study show reasonable agreement with the experimentally determined changes; both indicate nonsignificant changes (±10%).

Table 16. Statistical comparison of 1TCS mean tearing modulus and mean J = 8.8T value with temperature for irradiated plate and submerged-arc welds

Test temperature (°C)	Tearing modulus			J = 8.8T			Number of tests
	Mean	Standard deviation	CV	Mean (KJ/m^3)	Standard deviation (KJ/m^2)	CV	
A533 grade B class 1 (HSST-02)							
121	61	14	0.235	355	74	0.207	6
204	59	5	0.085	323	18	0.056	6
288	53	5	0.095	287	8	0.028	6
Submerged-arc weld (HSST-68W)							
121	171	8	0.048	992	76	0.077	4
204	140	14	0.100	773	50	0.065	4
288	117	20	0.171	660	118	0.179	3
Submerged-arc weld (HSST-69W)							
121	54	3	0.048	324	28	0.086	4
204	50	7	0.134	292	7	0.024	4
288	39	9	0.232	237	43	0.183	4
Submerged-arc weld (HSST-70W)							
121	117	15	0.128	588	42	0.072	4
204	83	3	0.040	395	20	0.051	4
288	56	14	0.258	269	22	0.080	4
Submerged-arc weld (HSST-71W)							
121	81	3	0.040	360	20	0.055	4
204	71	13	0.182	306	49	0.160	4
288	48	10	0.217	209	35	0.166	3

Table 17. Comparison of Charpy V-notch and 1TCS transition temperature shifts due to irradiation

Copper (wt %)	Nickel (wt %)	Charpy V-notch		1TCS		
		Fluence, 10^{23} n/m^2 (>1 MeV)	CVN at 41 J (°C)	Fluence, 10^{23} n/m^2 (>1 MeV)	K_{Jc} at 125 MPa$\sqrt{m}$ (°C)	$K_{\beta c}$ at 90 MPa$\sqrt{m}$ (°C)
		A533 grade B class 1 (HSST-02)				
0.14	0.67	1.77	68	1.95	81	66
		Submerged-arc weld (HSST-68W)				
0.04	0.13	1.35	10	1.34	−6	−2
		Submerged-arc weld (HSST-69W)				
0.12	0.10	1.22	27	1.32	47	39
		Submerged-arc weld (HSST-70W)				
0.06	0.63	1.65	23	1.81	25	21
		Submerged-arc weld (HSST-71W)				
0.05	0.63	1.65	23	1.78	−1	16

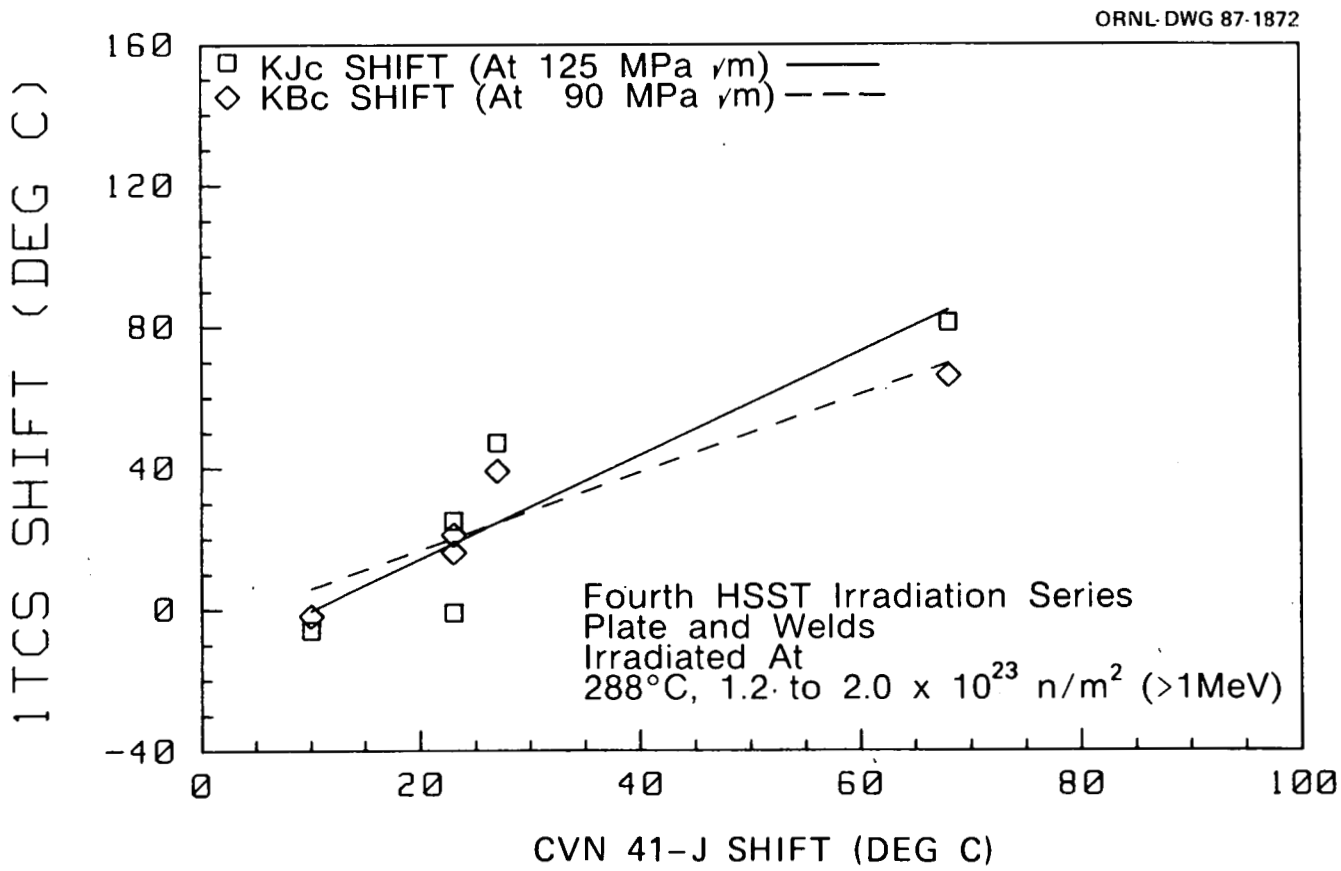

Fig. 41. Correlation of radiation-induced Charpy V-notch 41-J transition temperature shift with radiation-induced fracture toughness (K_{Jc} at 125 MPa$\sqrt{m}$) shift and with radiation-induced β-corrected fracture toughness ($K_{\beta c}$ at 90 MPa$\sqrt{m}$) shift.

Table 18. Comparison of Charpy V-notch and 1TCS ductile shelf changes due to irradiation

Copper (wt %)	Nickel (wt %)	Charpy V-notch		1TCS				Tensile	
		Fluence, 10^{23} n/m^2 (>1 MeV)	Upper shelf energy change (%)	Fluence, 10^{23} n/m^2 (>1 MeV)	Change, %, at 204°C			Fluence, 10^{23} n/m^2 (>1 MeV)	Flow stress change at 204°C (%)
					J_{Ic}	T	J = 8.8T		
A533 grade B class 1 (HSST-02)									
0.14	0.67	1.79	–14	1.97	–12	–46	–33	1.85	24
Submerged-arc weld (HSST-68W)									
0.04	0.13	1.14	9	1.31	–6	–17	–13	1.30	7
Submerged-arc weld (HSST-69W)									
0.12	0.10	1.18	–1	1.31	-4	–22	–15	1.31	12
Submerged-arc weld (HSST-70W)									
0.06	0.63	1.69	–2	1.69	6	–29	–21	1.64	10
Submerged-arc weld (HSST-71W)									
0.05	0.63	1.64	10	1.76	4	–12	–8	1.66	9

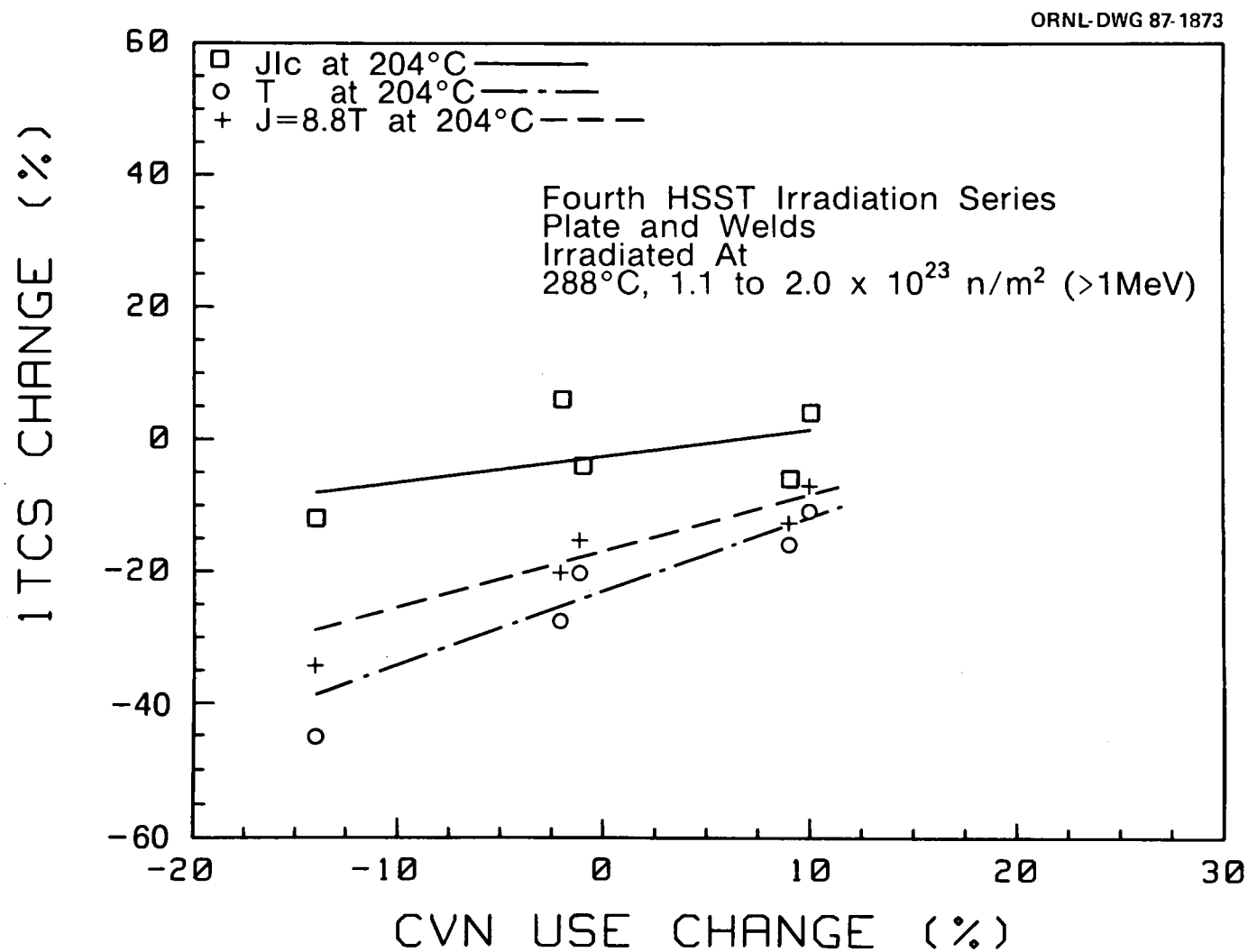

Fig. 42. Correlation of radiation-induced Charpy V-notch upper-shelf energy change with radiation-induced 1TCS-J_{Ic} change (at 204°C).

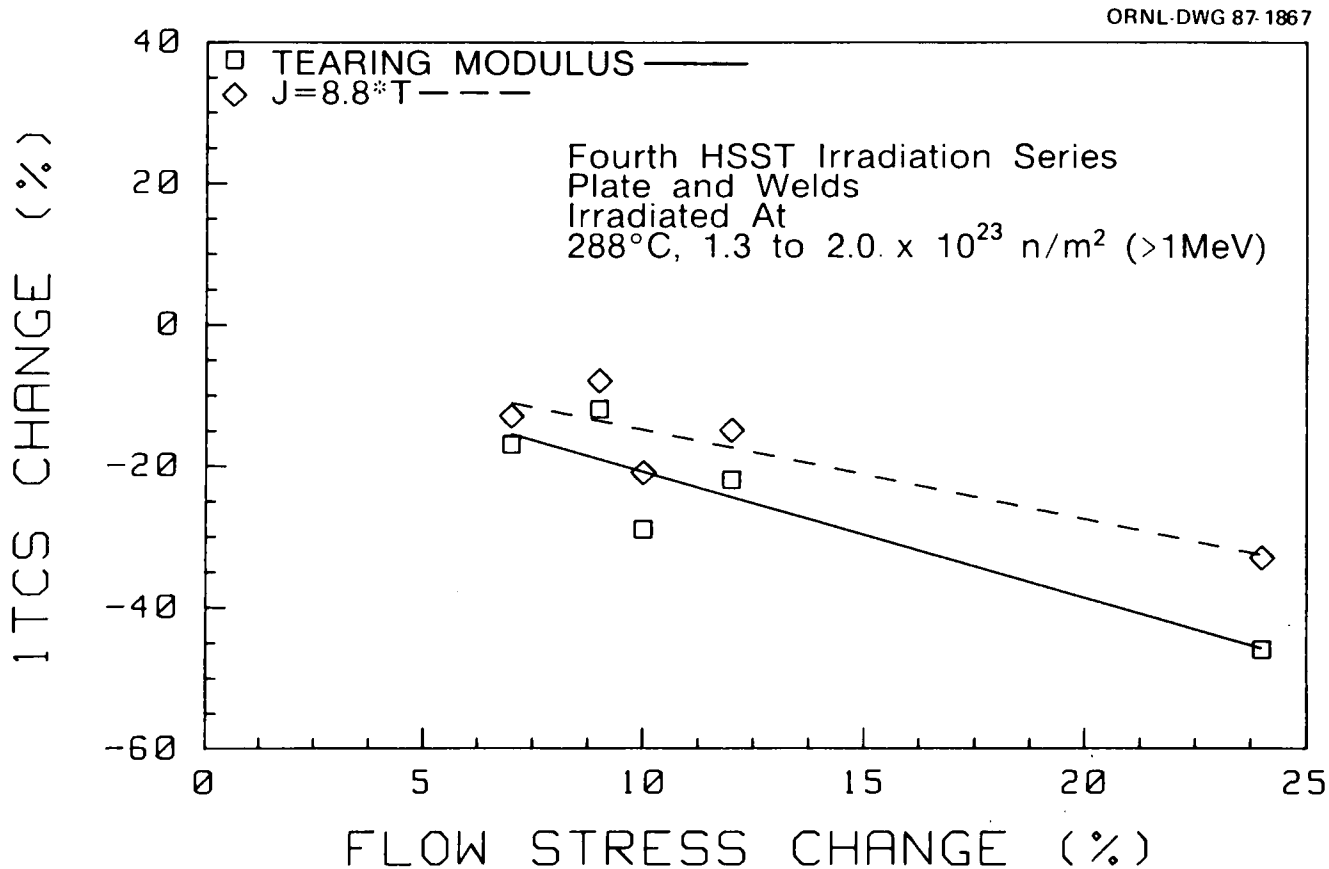

Fig. 43. Correlation of radiation-induced flow stress change (at 204°C) with radiation-induced 1TCS-tearing-modulus change (at 204°C) and with radiation-induced 1TCS-J = 8.8*T change (at 204°C).

Table 19. Comparison of PVRC-MPC predicted fracture toughness behavior and experimentally determined behavior

Copper (wt %)	Nickel (wt %)	Fluence, 10^{23} n/m^2 (>1 MeV)	K_{Jc} transition temperature shift at 125 MPa$\sqrt{m}$ (°C)		K_{Jc} ductile-shelf change at 204°C (%)	
			PVRC-MPC prediction	This study	PVRC-MPC prediction	This study
		A533 grade B class 1 (HSST-02)				
0.14	0.67	1.95	76	81	−8	−6
		Submerged-arc weld (HSST-68W)				
0.04	0.13	1.34	19	−6	5	−3
		Submerged-arc weld (HSST-69W)				
0.12	0.10	1.32	19	47	−1	−2
		Submerged-arc weld (HSST-70W)				
0.06	0.63	1.81	20	25	−1	3
		Submerged-arc weld (HSST-71W)				
0.05	0.63	1.78	10	−1	5	2

Table 20 provides a comparison of the coefficients of variation observed for unirradiated CVN and K_{Jc} results. The values (shown in the table) for each material in the transition region are averages of all transition temperature results. Similarly, averages are reflected for the ductile shelf. Except for the case of weld 68W, for which the number of fracture toughness specimens was very limited, the variations of CVN energy and K_{Jc} results in the transition region are comparable. The variations in K_{Jc} are somewhat greater than those for CVN energy on the ductile shelf. The table amplifies, however, previous observations that variations are much greater in the transition region than on the ductile shelf. This is expected because of the random nature of the cleavage fracture phenomenon that occurs in the transition region.

Table 21 compares variations in fracture toughness results for unirradiated and irradiated K_{Jc} in HSST Plate 02 in the transition region and on the ductile shelf. Variations at lower temperatures, in the transition region, are much greater for the irradiated tests. On the ductile shelf, there appears to be slightly more variation for the irradiated tests.

Table 22 shows a comparison of the statistical confidence associated with the mean transition temperature increases of all materials for both CVN and K_{Jc} test results. The 95% confidence intervals for fracture toughness are generally greater than those for the Charpy impact energy.

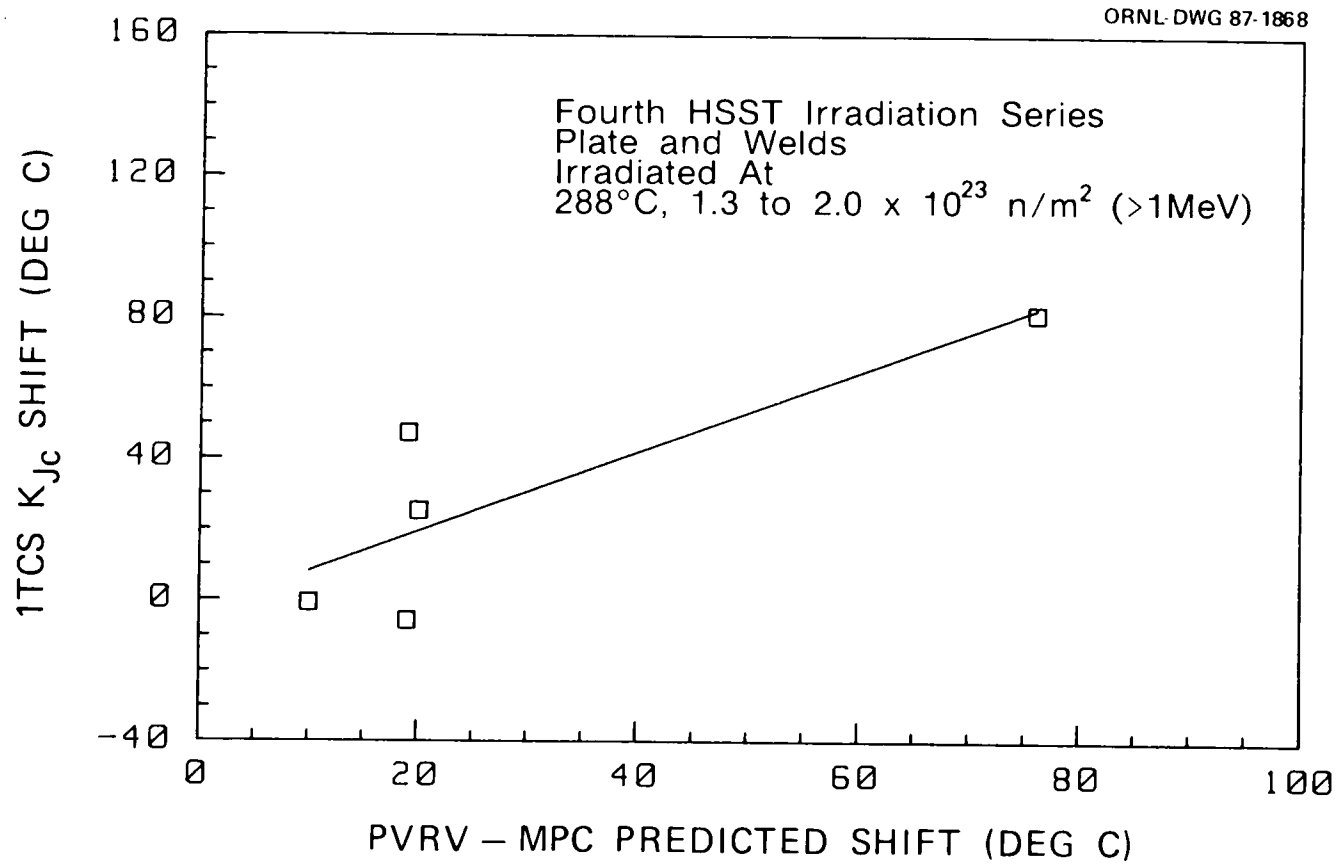

Fig. 44. Comparison of radiation-induced fracture toughness transition temperature shift (K_{Jc} at 125 MPa$\sqrt{m}$) with PVRC-MPC predictions.

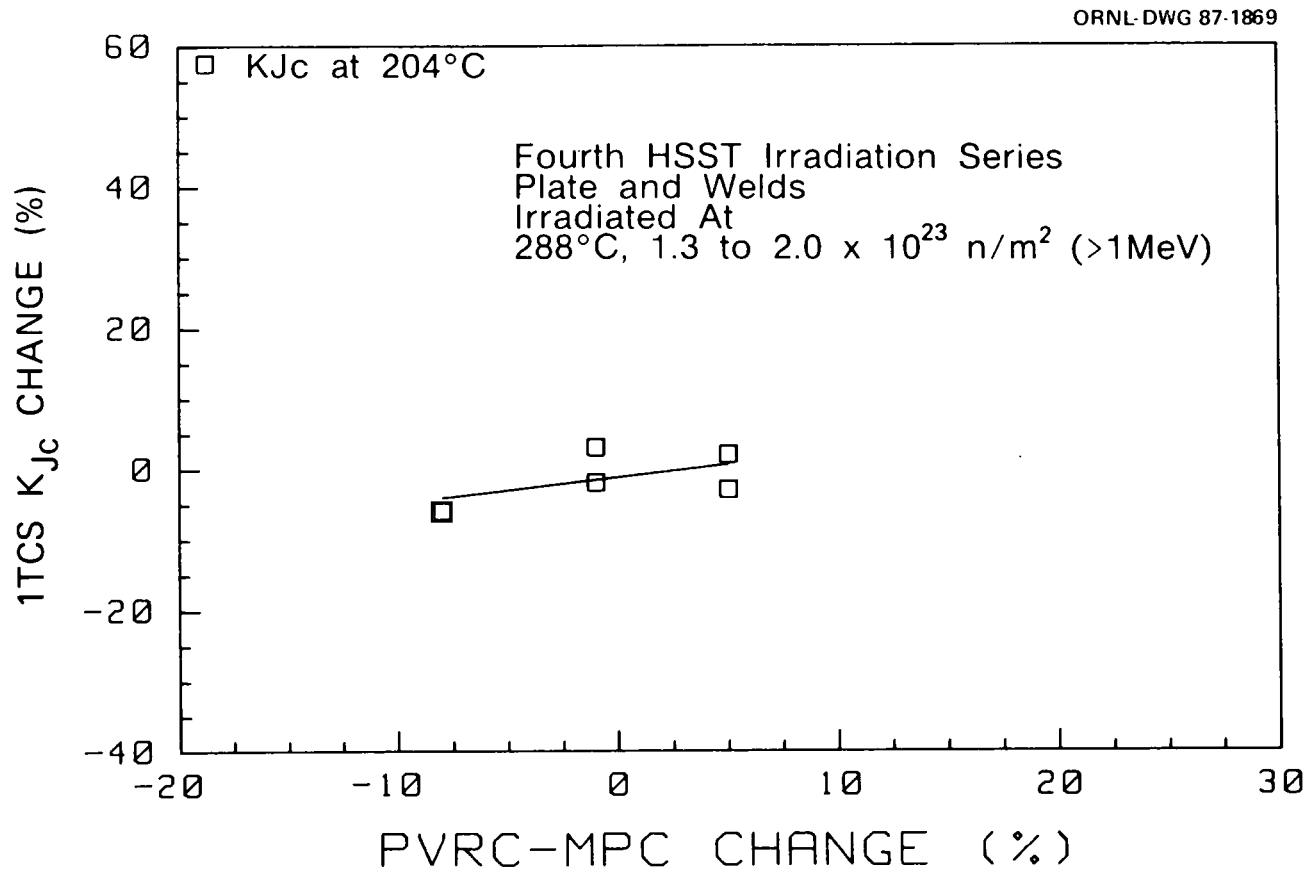

Fig. 45. Comparison of radiation-induced upper-shelf fracture toughness changes (K_{Jc} at 204°C) with PVRC-MPC predictions.

Table 20. Coefficients of variation for unirradiated Charpy impact and fracture toughness tests

Material	Coefficients of variation, %			
	Charpy impact		Fracture toughness	
	Transition region	Ductile shelf	Transition region	Ductile shelf
Plate 02	16	6	11	9
68W	24	10	43	16
69W	22	5	18	8
70W	20	6	22	8
71W	17	7	21	7

DISCUSSION

It is clear that transition temperature shifts measured by both K_{Jc} and CVN are reduced by decreasing both the copper and the nickel contents. Reducing either one separately does not produce as substantial a change in the shift as reducing both. Only the welds can be compared directly. The highest shift is evidenced by the results from weld 69W, with the highest copper and lowest nickel, indicating that copper alone has a substantial effect. However, increased nickel with lowered copper levels (welds 70W and 71W) also produced a substantial but lesser shift. The lowest shift was produced by weld 68W, where both the copper and nickel levels were low. Although the magnitude of the transition temperature shifts (K_{Jc}, $K_{\beta c}$, or CVN) varies somewhat, all three support these observations.

There are at least four factors that could obscure the conclusions regarding effects of composition. One factor is the fluence difference between the various welds. To evaluate the sensitivity of results to neutron fluence, the method of ref. 13 was used to calculate predicted shifts for weld 69W, assuming the higher fluence experienced by welds 70W and 71W. Those methods predict a shift of only 3 to 4°C greater than that at the actual fluence. Thus, the difference in fluence for the welds of this study do not substantially obscure the observations. A second factor is material condition before irradiation. The welds were fabricated with various fluxes and weld wires and were given different postweld heat treatments, which resulted in quite different unirradiated strengths. The room temperature yield strengths of welds 68W, 69W, 70W, and 71W were about 542, 638, 478, and 469 MPa, respectively. The ratios of ultimate strength to yield strength at room temperature were about 1.16, 1.13, 1.24, and 1.28, respectively. Third, other than the differences in copper and nickel contents, the silicon contents of 70W and 71W were substantially higher than those for 68W and 69W. Fourth, the scatter of results

Table 21. Statistical variations in fracture toughness results for HSST Plate 02

Test temperature (°C)	Number of tests	Mean K_{Jc} (MPa$\sqrt{m}$)	Standard deviation (MPa$\sqrt{m}$)	Coefficient of variation (%)
		HSST Plate 02, unirradiated		
−95	5	50	7.9	16
−40	6	81	10.6[a]	13
23	6	236	28.6	12
121	5	175	15.6	9
288	5	157	5.6[b]	4
		HSST Plate 02, irradiated		
−25	5	45	7.7	17
50	10	89	24.5	28
80	10	149	35.5[b]	24
121	6	175	6.7	4
288	6	148	20.6[a]	14

[a]Difference between ORNL and MEA mean K_{Jc} values greater than two standard deviations.

[b]Difference between ORNL and MEA mean K_{Jc} values greater than one standard deviation.

Table 22. Comparison of 95% confidence intervals for transition temperature shifts of Charpy impact and fracture toughness tests

Material	Transition temperature increase, °C			
	CVN		K_{Jc}	
	At 41 J	95% confidence interval	at 125 MPa$\sqrt{m}$	95% confidence interval
Plate 02	68	±4	81	±8
Weld 68W	10	±13	−6	±10
Weld 69W	27	±11	47	±10
Weld 70W	23	±8	25	±18
Weld 71W	23	±10	−1	±25

in the transition region for both CVN and fracture toughness tests is quite large, and the number of specimens tested at any given temperature is small relative to that required for a comprehensive statistical evaluation.

Thus, curve fits can be significantly skewed, resulting in large changes in the calculated shifts. The K_{Jc} shift for weld 70W, for example, does not compare well with the CVN shift. The curve for unirradiated K_{Jc} data of weld 71W, shown in Fig. 28, has a much lower slope than the curve fits for the other welds. Large scatter and few data points have skewed the curve toward that for the irradiated data, resulting in no indicated shift at 125 MPa$\sqrt{m}$. It is believed that differences of 15°C in K_{Jc} curve shift determinations in this program could be expected.

Primarily, the J-integral results have indicated that reduced levels of copper and nickel will reduce the degradation of the ductile-shelf tearing modulus, although there will likely be decreases in the tearing modulus because of the increase in the yield stress [see Eq. (3)].

CONCLUSIONS

1. There was good agreement between the Charpy V-notch and 1TCS results from the two laboratories, ORNL and MEA.

2. Ductile-shelf elastic-plastic initiation fracture toughness (J_{Ic}) is essentially insensitive to neutron radiation [~2×10^{22} neutrons/cm^2 (>1 MeV)] for the relatively low copper, current production practice welds evaluated in this study.

3. Transition temperature shifts to higher temperature resulting from irradiation are directly related to the copper and nickel content of the material, with copper producing the larger effect.

4. Ductile-shelf fracture toughness, J_{Ic}, and tearing modulus, T, are inversely proportional to temperature.

5. The degradation of tearing modulus with radiation is directly related to radiation-induced increases in flow stress.

6. Radiation-induced transition temperature shifts, indicated by the CVN data indexed at 41 J, agree qualitatively with transition temperature shifts determined from fracture toughness data (K_{Jc} at 125 MPa$\sqrt{m}$ or $K_{\beta c}$ at 90 MPa$\sqrt{m}$) for welds that exhibit CVN shifts from 10 to 27°C.

7. Radiation-induced upper-shelf CVN energy changes correlated poorly with upper-shelf fracture toughness (J_{Ic}) changes.

8. The variation in fracture toughness, K_{Jc}, with small specimens in the transition region is similar to that observed with Charpy impact tests.

9. Variations in both fracture toughness, K_{Jc}, and CVN energy are substantially greater in the transition region than on the ductile shelf.

ACKNOWLEDGMENTS

The authors wish to acknowledge and thank many people at ORNL whose contributions were invaluable to the successful execution of this program: D. A. Canonico (now with Combustion Engineering) for guidance and leadership in formulating and initiating the program; R. G. Berggren (now retired) for planning, coordinating, testing, and analysis activities; T. N. Jones for tensile and Charpy testing and hot cell coordination; R. L. Swain for fracture mechanics testing and test system developments; D. L. Thomas and J. T. Hutton for computer-interactive test system development; K. K. Chipley of the Engineering Division for capsule design; J. W. Woods (now retired) and D. W. Heatherly of the Engineering Technology Division for assembly, installation, operation, removal, and disassembly of capsules; A. A. Shourbaji of the Instrumentation and Controls Division for instrumentation design and data reduction; and C. A. Baldwin and F. B. K. Kam of the Operations Division for dosimetry and aid in the thermal shield design.

Our appreciation is also extended to B. H. Menke, J. R. Hawthorne, F. J. Loss, and K. Miller of Materials Engineering Associates, Inc., for invaluable discussions of test procedures, timely production of high quality test data and analyses, and coordination of this program. We also thank G. D. Whitman (former HSST Program Manager, now retired), and C. E. Pugh, current HSST Program Manager, for their guidance and support, and M. Vagins of the U.S. Nuclear Regulatory Commission for guidance and financial support.

Finally, in preparation of the report, we express our thanks to J. L. Bishop for manuscript preparation, S. K. Iskander and W. R. Corwin for technical review, and B. Q. Atkinson and D. L. Balltrip for preparation of the final document.

REFERENCES

1. R. Johnson, *Resolution of the Task A-11 Reactor Vessel Materials Toughness Safety Issue*, NUREG-0744, Vols. 1 and 2, Rev. 1, U.S. Nuclear Regulatory Commission, Washington, D.C., October 1982.

2. A. L. Hiser, F. J. Loss, and B. H. Menke, *J-R Curve Characterization of Irradiated Low Upper Shelf Welds*, NUREG/CR-3506 (MEA-2028), U.S. Nuclear Regulatory Commission, Washington, D.C., April 1984.

3. C. E. Childress, *Fabrication History of the First Two 12-inch Thick ASTM A533 Grade B, Class 1 Steel Plates of the Heavy Section Steel Technology Program, Documentary Report 1*, ORNL-4313 (February 1969).

4. T. V. Marston et al., *Fracture Toughness of Ferritic Materials in Light-Water Reactor Vessels*, MML-75-152, Combustion Engineering, Inc., Chattanooga, Tenn., October 1975, pp. 47–48.

5. A. L. Lowe, Jr., and J. I. Qureshi, *Fabrication of Weldments Using Linde 80 and Linde 124 Weld Fluxes for HSST Irradiation Program*, Babcock and Wilcox Nuclear Power Group, Lynchburg, Va., June 1981.

6. "Standard Test Method for J_{Ic}, A Measure of Fracture Toughness," E813-81, *1985 Annual Book of ASTM Standards*, Vol. 03.01, American Society for Testing and Materials, Philadelphia, July 1985.

7. C. A. Baldwin, *Neutron Spectral Characterization Calculations for the Fourth Nuclear Regulatory Commission Heavy Section Steel Technology 1T-CT Irradiation Experiments*, NUREG/CR-3311 (ORNL/TM-8782), June 1983.

8. F. W. Stallman, C. A. Baldwin, and F. B. K. Kam, *Neutron Spectral Characterization Calculations for the Fourth Nuclear Regulatory Commission Heavy Section Steel Technology 1T-CT Irradiation Experiments: Dosimetry and Uncertainty Analysis*, NUREG/CR-3333 (ORNL/TM-8789), July 1983.

9. J. J. McGowan, *Tensile Properties of Irradiated Nuclear Grade Pressure Vessel Plate and Welds for the Fourth HSST Irradiation Series*, NUREG/CR-4086 (ORNL/TM-9516), January 1985.

10. "Standard Methods for Notched Bar Impact Testing of Metallic Materials," E23-82, *1985 Annual Book of ASTM Standards*, vol. 03.01, American Society for Testing and Materials, Philadelphia, July 1985.

11. D. Marquardt, "An Algorithm for Least Squares Estimation of Nonlinear Parameters," *J. Soc. Ind. and Appl. Math.* **11**(2), 1963.

12. "Effects of Residual Elements on Predicted Radiation Damage to Reactor Vessel Materials," *Regulatory Guide 1.99 (Rev. 1)*, U.S. Nuclear Regulatory Commission, Washington, D.C., April 1977.

13. P. N. Randall, "Effects of Residual Elements on Predicted Radiation Damage to Reactor Vessel Materials," *Regulatory Guide 1.99 (Rev. 2 Draft)*, U.S. Nuclear Regulatory Commission, Washington, D.C., January 1984.

14. J. D. Varsik and S. T. Byrne, "An Empirical Evaluation of the Irradiation Sensitivity of Reactor Pressure Vessel Materials," pp. 252–66 in *Effects of Radiation on Structural Materials, ASTM STP 683*, American Society for Testing and Materials, Philadelphia, 1979.

15. J. S. Perrin, R. A. Wullaert, G. R. Odette, and P. M. Lombrozo, *Physically Based Regression Correlations of Embrittlement Data from Reactor Pressure Vessel Surveillance Programs*, EPRI NP-3319, Electric Power Research Institute, Palo Alto, Calif., January 1984.

16. J. D. Varsik, S. M. Schloss, and J. J. Koziol, *Evaluation of Irradiation Response of Reactor Pressure Vessel Materials*, EPRI NP-2720, Electric Power Research Institute, Palo Alto, Calif., November 1982.

17. Metal Properties Council Subcommittee 6 on Nuclear Materials, "Prediction of the Shift in the Brittle-Ductile Transition Temperature of Light-Water Reactor (LWR) Pressure Vessel Materials," *J. Test. Eval.* **11**(4), 237–60 (July 1983).

18. R. G. Berggren, J. R. Hawthorne, and R. K. Nanstad, "Analysis of Charpy V-notch Impact Toughness of Irradiated A533-B Class 1 Plate and

Four Submerged-Arc Welds," pp. 1094–1110 in *Effects of Radiation on Materials: Twelfth International Symposium, ASTM STP 870*, American Society for Testing and Materials, Philadelphia, 1985.

19. P. Albrecht et al., "Tentative Test Procedure for Determining the Plane Strain J_I-R Curve," *J. Test. Eval.* **10**(6), 245–51 (November 1982).

20. "Standard Test Method for Plane-Strain Fracture Toughness of Metallic Materials," E399-83, *1985 Annual Book of ASTM Standards*, vol. 03.01, American Society for Testing and Materials, Philadelphia, July 1985.

21. G. R. Irwin, "Fracture Mode Transition for a Crack Traversing a Plate," *J. Basic Eng.* **82**(2), 417–25 (1960).

22. J. G. Merkle, *An Examination of the Size Effects and Data Scatter Observed in Small-Specimen Cleavage Fracture Toughness Testing*, NUREG/CR-3672 (ORNL/TM-9088), April 1984.

23. W. Bamford, W. Oldfield, and T. Marston, "An Improved Reference Fracture Toughness Procedure for Pressure Vessel Steels," pp. 932–65 in *Proceedings of the Fifth International Conference on Pressure Vessel Technology, Vol. II, Materials and Manufacturing*, American Society of Mechanical Engineers, New York, September 1984.

Appendix A

SPECIMEN LOADINGS AND IRRADIATION FACILITIES

Appendix A

SPECIMEN LOADINGS AND IRRADIATION FACILITIES

The locations of all thermocouples and the specimen irradiation positions for all three capsules are shown in Fig. A1. The location of each specimen irradiated in this series is listed in Tables A1 through A6.

The capsules were irradiated at the Bulk Shielding Reactor (BSR), a 2-MW open-pool-type, light-water moderated and cooled reactor located at ORNL. After initial operation with the first capsule in this series, it was found necessary to place gamma shields between the capsules and the reactor to reduce the gamma heating rate to a level that would permit acceptable temperature control characteristics. A cross-sectional view of the BSR core showing the capsule irradiation positions and the gamma shields is presented in Fig. A2. The axial positions of the experiments relative to the reactor are not well defined. Based on a comparison of experiment drawings with reactor drawings, the axial centerline of the capsules should be 4.9 mm above the reactor centerline. However, when rough measurements were made at the BSR, it appeared that this distance was about 13 mm.

The capsule support structure consists of an aluminum platform assembly with adjustable feet resting on the floor of the BSR pool. Bolted to the platform are two capsule stand-and-carriage assemblies. The carriage assemblies provide clamping for the capsules and provide a means to insert or retract the capsules from the reactor faces. This motion is accomplished by manually rotating a shaft on the carriage.

Both capsule positions have a common water supply system consisting of a centrifugal pump and a two-valve manifold to provide coolant water flow on the front face of each capsule. The pump is mounted on the instrument bridge of the BSR about 3 ft above the minimum water level. Reactor pool water is drawn directly into the pump through stainless steel pipe to the manifold. The bottom of the coolant water gap on the front face of each capsule is open to allow the water to return to the reactor pool.

A binary gas system provides a variable mixture of helium and nitrogen to the gas gap region of each capsule. The resultant variation in gap thermal resistance provides the primary source for temperature control. One selected thermocouple in each capsule is connected to a recorder-controller that adjusts the nitrogen flow rate to the appropriate capsule. The helium flow rate is set manually to maintain a minimum gas flow rate through the capsule. After flowing through the capsules, the gas is directed to the building off-gas system. A complete capsule flow diagram is presented in Fig. A3.

To trim the temperature distribution throughout each capsule, electrical power is supplied by variable transformers (Variacs) to the 12 heater zones in the heater plate at the front of each capsule. These Variacs were set manually at the beginning of each reactor cycle and required only minimal adjustment during the cycle.

All thermocouples were connected to a Fluke data logger. This system allowed "on-demand" printing of all data on paper tape and was programmed to record the thermocouple readings on magnetic tape every 30 min.

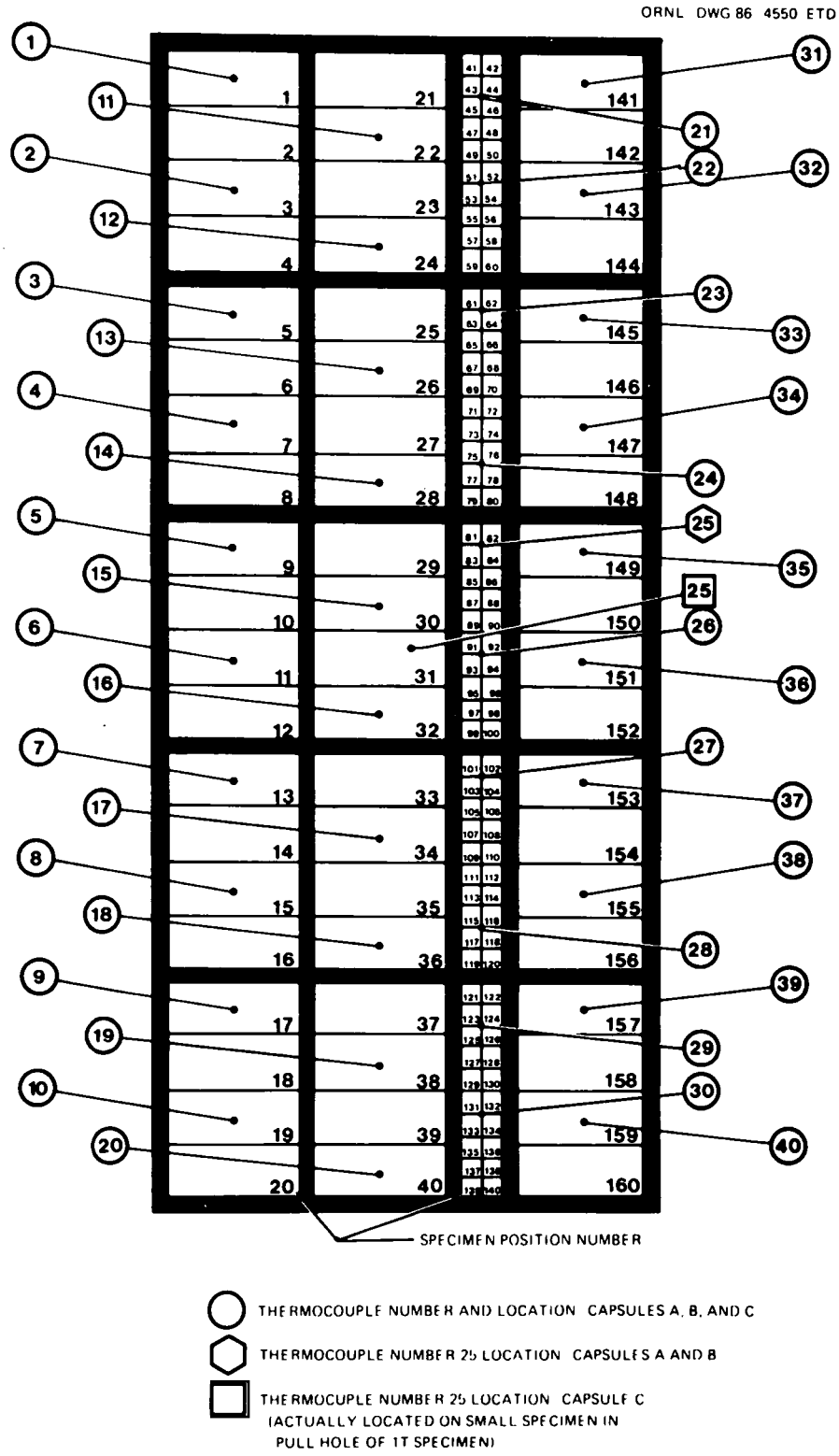

Fig. A1. Location of thermocouples and specimen positions for the Fourth Series.

Table A1. Location of 1T specimens in capsule A

Position number	Specimen number	Position number	Specimen number	Position number	Specimen number
1	2G-280	21	2G-344	141	2G-373
2	2G-281	22	2G-345	142	2G-375
3	2G-282	23	2G-346	134	2G-401
4	2G-285	24	2G-348	144	2G-402
5	2G-287	25	2G-349	145	2G-403
6	2G-288	26	2G-351	146	2G-404
7	2G-298	27	2G-353	147	2G-406
8	2G-316	28	2G-354	148	2G-407
9	2G-318	29	2G-356	149	2G-409
10	2G-328	30	2G-358	150	2G-411
11	2G-329	31	2G-360	151	2G-412
12	2G-331	32	2G-362	152	2G-413
13	2G-332	33	2G-363	153	2G-414
14	2G-334	34	2G-365	154	2G-416
15	2G-335	35	2G-366	155	2G-418
16	2G-337	36	2G-368	156	2G-419
17	2G-338	37	2G-369	157	2G-421
18	2G-339	38	2G-370	158	2G-420
19	2G-340	39	2G-371	159	2G-422
20	2G-342	40	2G-372	160	2G-423

Table A2. Location of Charpy specimens in capsule A

Position number	Specimen number	Position number	Specimen number
41	2GA-700	42	2GA-701
43	2GA-702	44	2GA-703
45	2GA-704	46	2GA-705
47[a]	2GA-500	48[a]	2GA-501
49	2GA-706	50	2GA-707
51	2GA-708	52	2GA-709
53	2GA-710	54	2GA-711
55	2GA-712	56	2GA-713
57	2GA-714	58	2GA-715
59	2GA-716	60	2GA-717
61	2GA-718	62	2GA-719
63	2GA-720	64	2GA-721
65[a]	2GA-502	66[a]	2GA-503
67	2GA-722	68	2GA-723
69	2GA-724	70	2GA-725
71	2GA-726	72	2GA-727
73	2GA-728	74	2GA-729
75	2GA-730	76	2GA-731
77	2GA-732	78	2GA-733
79	2GA-734	80	2GA-735
81	2GA-736	82	2GA-737
83	2GA-738	84	2GA-739
85[a]	2GA-504	86[a]	2GA-505
87	2GA-740	88	2GA-741
89	2GA-600	90	2GA-601
91	2GA-742	92	2GA-743
93	2GA-602	94	2GA-603
95	2GA-744	96	2GA-745
97	2GA-604	98	2GA-605
99	2GA-746	100	2GA-747
101	2GA-606	102	2GA-607
103	2GA-748	104	2GA-749
105	2GA-608	106	2GA-609
107	2GA-750	108	2GA-751
109	2GA-752	110	2GA-753
111[a]	2GA-506	112[a]	2GA-507
113	2GA-754	114	2GA-755
115	2GA-756	116	2GA-757
117	2GA-610	188	2GA-611
119	2GA-758	120	2GA-759

Table A2. (Continued)

Position number	Specimen number	Position number	Specimen number
121	2GA-612	122	2GA-613
123	2GA-760	124	2GA-761
125	2GA-614	126	2GA-615
127	2GA-762	128	2GA-763
129	2GA-616	130	2GA-617
131	2GA-764	132	2GA-765
133	2GA-618	134	2GA-619
135[a]	2GA-508	136[a]	2GA-509
137	2GA-766	138	2GA-767
139	2GA-768	140	2GA-769

[a]Tensile specimen.

Table A3. Location of 1T specimens in capsule B

Position number	Specimen number	Position number	Specimen number	Position number	Specimen number
1	68W-AB	21	68W-KC	141	69W-102
2	68W-AD	22	69W-149	142	69W-105
3	68W-BA	23	68W-KE	143	69W-106
4	68W-BB	24	69W-153	144	69W-108
5	68W-BC	25	68W-LA	145	69W-112
6	68W-BD	26	69W-157	146	69W-113
7	68W-CC	27	68W-LB	147	69W-114
8	68W-CD	28	69W-159	148	69W-116
9	68W-CE	29	68W-LC	149	69W-118
10	68W-DA	30	69W-160	150	69W-119
11	68W-DB	31	68W-LD	151	69W-120
12	68W-DC	32	69W-165	152	69W-121
13	68W-DE	33	68W-MA	153	69W-122
14	68W-EA	34	69W-166	154	69W-126
15	68W-EC	35	68W-MB	155	69W-137
16	68W-ED	36	69W-167	156	69W-142
17	68W-EE	37	68W-MD	157	69W-143
18	68W-HC	38	69W-172	158	69W-144
19	68W-JB	39	68W-ME	159	69W-146
20	68W-KB	40	69W-173	160	69W-148

Table A4. Location of Charpy specimens in capsule B

Position number	Specimen number	Position number	Specimen number
41	68W-201	42	69W-201
43	68W-202	44	69W-202
45	68W-203	46	69W-203
47[a]	68W-02	48	69W-211
49	68W-206	50[a]	69W-06
51	69W-233	52	68W-207
53	69W-234	54	68W-208
55	69W-235	56[a]	68W-05
57[a]	69W-09	58	68W-209
59	69W-237	60	68W-210
61	69W-240	62	68W-211
63	69W-241	64	68W-212
65[a]	68W-06	66	69W-242
67	68W-213	68	69W-243
69	68W-214	70[a]	69W-12
71	69W-246	72	68W-215
73[a]	68W-07	74	69W-247
75	68W-216	76	69W-248
77	68W-217	78	69W-250
79	MO-88	80[a]	69W-13
81	MO-89	82	MO-90
83	68W-219	84	69W-254
85[a]	M-31	86	121
87	122	88[a]	M-32
89[a]	M-33	90	123
91	68W-220	92	69W-255
93	124	94	125
95[a]	68W-09	96	126
97	127	98	128
99	129	100[a]	69W-14
101	130	102	131
103	68W-221	104	69W-260
105[a]	68W-10	106	68W-222
107	69W-261	108	68W-223
109	69W-262	110[a]	69W-15
111	68W-224	112	69W-263
113	68W-225	114	69W-264
115	68W-226	116	69W-265
117	68W-227	118	69W-266
119[a]	68W-11	120	68W-228

Table A4. (Continued)

Position number	Specimen number	Position number	Specimen number
121	69W-267	122[a]	69W-17
123	68W-229	124	69W-268
125	68W-230	126	69W-269
127[a]	68W-15	128	68W-231
129	69W-270	130	68W-232
131	69W-283	132	69W-285
133	69W-286	134	69W-291
135	69W-294	136[a]	69W-18
137	69W-336	138	69W-338
139	69W-340	140	69W-204

[a]Tensile specimen.

Table A5. Location of 1T specimens in capsule C

Position number	Specimen number	Position number	Specimen number	Position number	Specimen number
1	70W-104	21	70W-106	141	70W-107
2	71W-101	22	71W-108	142	71W-110
3	70W-108	23	70W-110	143	70W-111
4	71W-111	24	71W-112	144	71W-115
5	70W-112	25	70W-113	145	70W-115
6	71W-116	26	71W-117	146	71W-119
7	70W-117	27	70W-118	147	70W-119
8	71W-120	28	71W-121	148	71W-122
9	70W-123	29	70W-124	149	70W-125
10	71W-123	30	71W-126	150	71W-128
11	70W-126	31	70W-128	151	70W-129
12	71W-131	32	71W-133	152	71W-134
13	70W-130	33	70W-131	153	70W-132
14	71W-138	34	71W-139	154	71W-140
15	70W-133	35	70W-136	155	70W-137
16	71W-141	36	71W-142	156	71W-143
17	70W-138	37	70W-139	157	70W-140
18	71W-144	38	71W-146	158	71W-147
19	70W-142	39	70W-145	159	70W-148
20	71W-149	40	71W-150	160	71W-151

Table A6. Location of Charpy specimens in capsule C

Position number	Specimen number	Position number	Specimen number
41	70W-203	42	71W-207
43	70W-204	44	71W-208
45	70W-205	46	71W-214
47[a]	70W-07	48[a]	71W-03
49	70W-208	50	71W-217
51	70W-209	52	71W-221
53	70W-210	54	71W-222
55	70W-211	56	71W-223
57	70W-212	58	71W-224
59	70W-213	60	71W-227
61	70W-215	62	71W-228
63	70W-216	64	71W-236
65[a]	70W-08	66[a]	71W-06
67	70W-218	68	71W-240
69	70W-219	70	71W-241
71	70W-225	72	71W-242
73	70W-226	74	71W-243
75	70W-229	76	71W-244
77	70W-231	78	71W-247
79[a]	70W-10	80[a]	71W-09
81	70W-232	82	71W-250
83	70W-233	84	71W-253
85	02G-770	86	02G-776
87	02G-771	88	02G-777
89	02G-772	90	02G-778
91	02G-773	92	02G-779
93	02G-774	94	02G-780
95	02G-775	96	02G-781
97	70W-234	98	71W-255
99	70W-235	100	71W-258
101	70W-238	102	71W-259
103	70W-239	104	71W-260
105[a]	70W-13	106[a]	71W-11
107	70W-240	108	71W-261
109	70W-245	110	71W-262
111	70W-246	112	71W-265
113	70W-248	114	71W-266
115	70W-251	116	71W-267
117	70W-252	118	71W-269
119[a]	70W-14	120[a]	71W-15

Table A6. (Continued)

Position number	Specimen number	Position number	Specimen number
121	70W-254	122	71W-270
123	70W-256	124	71W-271
125	70W-257	126	71W-272
127	70W-284	128	71W-273
129	70W-285	130	71W-274
131	70W-287	132	71W-275
133	70W-289	134	71W-276
135[a]	70W-16	136[a]	71W-17
137	70W-290	138	71W-277
139	70W-291	140	71W-278

[a]Tensile specimen.

ORNL-DWG 86-4551 ETD

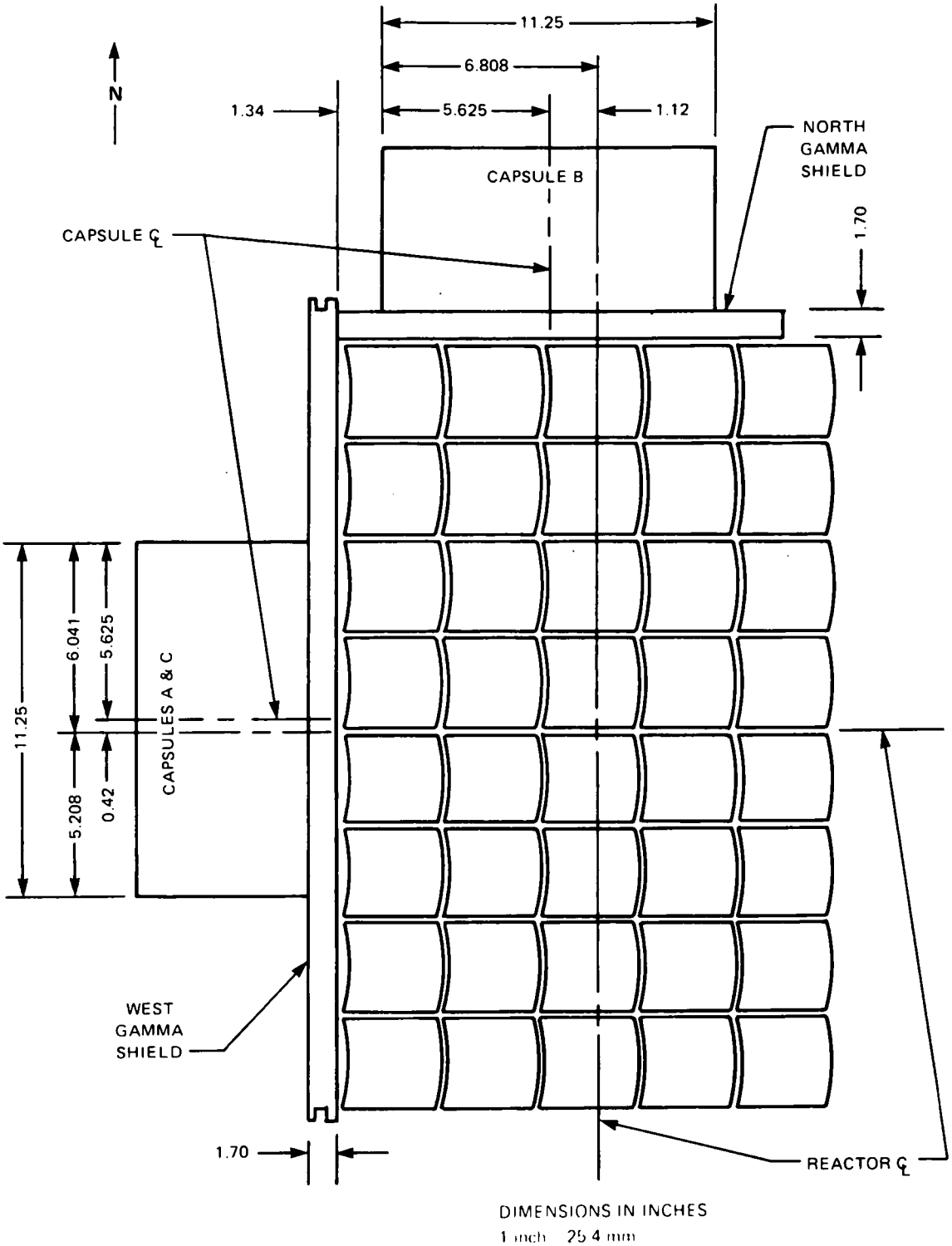

Fig. A2. Capsule irradiation positions at the BSR utilized for the Fourth Series.

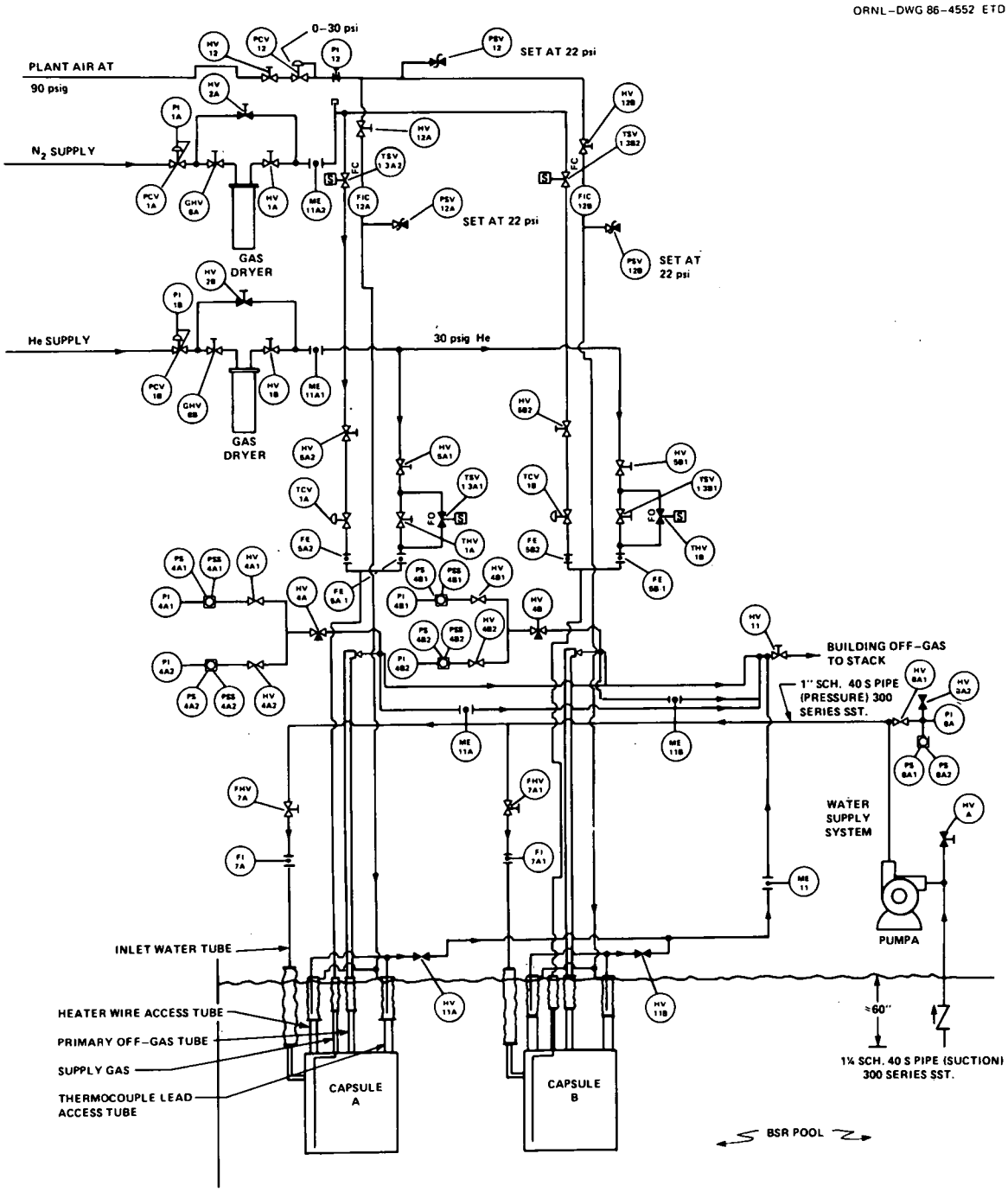

Fig. A3. Flow diagram of irradiation facility.

The first capsule (capsule A) was installed in the west face position at the BSR, and the reactor was started on October 11, 1979. However, when the reactor was brought to full power level, the specimen temperatures were too high. The reactor power level was reduced to 1 MW, and the specimen temperatures leveled out to about 270°C. This temperature level was reached with pure helium gas and without any electrical heating. A series of tests were then conducted at lower reactor power levels. These tests indicated that the values of gamma heating used in the capsule design were too low. Subsequent installation of a 42.5-mm gamma shield allowed careful control of temperatures at the target of 288°C. The irradiation of capsule A was begun again on December 18, 1979, and continued through October 17, 1980, having accumulated a total of 4630 h. The irradiation history summaries for each capsule are reported in Table A7.

Temperature control for all three capsules proved to be quite good. Typical ranges of temperatures are shown in Fig. A4, which presents a record of daily temperature ranges during the first 6 months of operation of capsule A. During the course of operation of the three capsules, a total of 22 magnetic tapes with temperature data were produced by the data acquisition system. From these tapes the maximum, mean, and median temperature, along with the standard deviation of each thermocouple, were calculated. These data are reported for each capsule in Tables A8 through A10. The standard deviation was calculated from the following equation:

$$\text{Standard deviation} = \sqrt{\frac{\Sigma(\text{temp} - \text{mean})^2}{\text{number of points}}} \; .$$

Additionally, tabular histograms of the operation of each thermocouple in each capsule are presented in Tables A11 through A13. The histograms show that for most of the irradiation time, nearly all thermocouples operated between 283 and 293°C. Those thermocouples that operated outside this range for any significant amount of time were located at the ends and/or corners of the capsule, where end losses caused somewhat lower operating temperatures.

Table A7. Chronological history of the irradiation of the three capsules of the Fourth Irradiation Series

Capsule designation	Irradiation position	Beginning of irradiation	End of irradiation	Total irradiation time (h)
A	West	12-18-79	10-17-80	4630
B	North	6-26-80	3-6-81	4329
C	West	4-1-81	1-17-82	4630

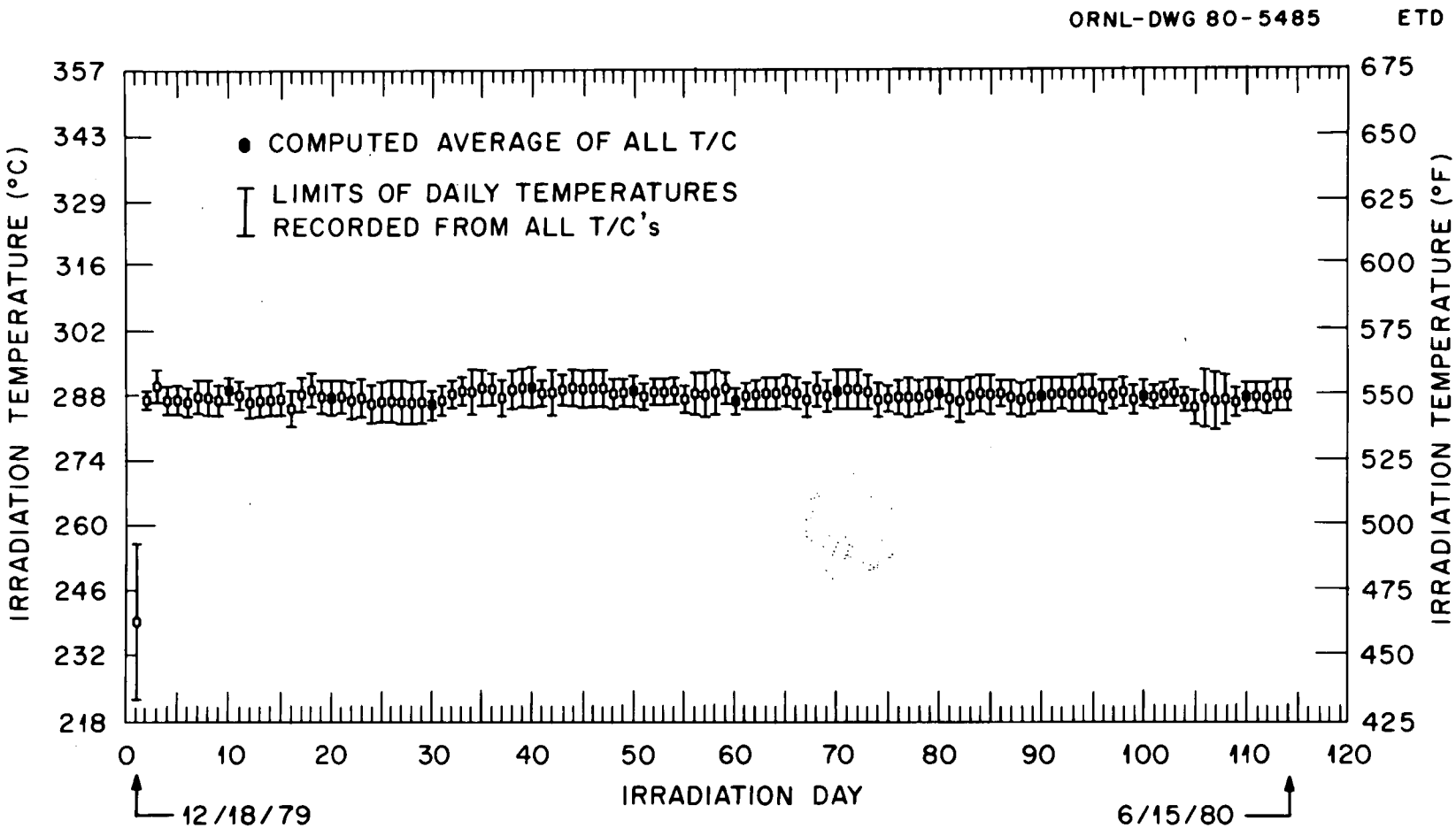

Fig. A4. Record of daily temperature range of 39 thermocouples during the first 6 months of operation of capsule A.

Table A8. Operating conditions of capsule A thermocouples through entire irradiation period

Thermocouple[a]	Temperature, °C			Standard deviation
	Maximum	Mean	Median	
1	292	286	287	9.1
2[b]				
3	296	290	291	9.1
4	293	288	290	8.9
5	294	289	290	8.8
7	290	286	287	8.7
8	290	285	286	8.7
9	290	284	285	8.6
10	290	283	285	8.6
11	294	288	289	9.2
12	294	288	290	9.3
13	293	288	289	9.0
14	293	288	289	9.1
15	292	287	289	8.8
17	292	286	288	9.0
18	290	285	287	8.7
19	294	288	289	8.9
20	290	284	285	8.7
21	292	286	287	9.2
22	295	289	291	9.3
23	293	288	289	9.1
24	293	288	289	8.9
25	292	287	288	8.9
26	291	286	288	8.8
27	289	285	286	8.7
28	289	284	285	8.6
29	290	284	286	8.7
30	290	284	285	8.7
31	291	285	286	9.2
32	295	289	290	9.3
33	293	287	288	9.0
34	293	286	288	9.0
35	293	288	289	8.9
37	289	284	285	8.6
38	292	286	288	8.8
39	294	286	287	8.8
40	292	284	285	8.8

[a]Thermocouples 6, 16, and 36 were connected to safety or control instrumentation and not to the data logger.

[b]Thermocouple 2 was inoperative.

Table A9. Operating conditions of capsule B thermocouples through entire irradiation period

Thermocouple[a]	Temperature, °C			Standard deviation
	Maximum	Mean	Median	
1	297	284	284	4.2
2	303	289	290	4.4
3	303	290	290	4.7
4	299	287	287	5.1
5	301	288	289	5.8
7	300	287	287	6.3
8	299	286	287	6.3
9	294	284	285	6.3
10	291	282	283	6.2
11	296	285	285	4.3
12	300	288	289	4.5
13	301	289	290	5.0
14	300	288	289	5.3
15	303	290	291	5.9
17	303	289	290	6.5
18	303	290	291	6.5
19	294	283	284	6.2
20	292	282	282	6.2
21	289	278	279	5.1
22[b]				
23	298	287	287	4.9
24	298	286	287	5.3
25	299	287	288	5.6
26	299	286	287	5.8
27	298	285	286	6.1
28	298	285	286	6.3
29	297	285	286	6.2
30	294	283	283	6.2
31	289	279	281	6.3
32	297	286	288	6.2
33	300	289	290	5.4
34	300	288	289	5.2
35	301	289	290	5.7
37	297	284	285	6.2
38	297	284	284	6.2
39	298	285	286	6.2
40	293	282	282	6.2

[a]Thermocouples 6, 16, and 36 were connected to safety or control instrumentation and not to the data logger.

[b]Thermocouple 22 was inoperative.

Table A10. Operating conditions of capsule C thermocouples through entire irradiation period

Thermocouple[a]	Temperature, °C			Standard deviation
	Maximum	Mean	Median	
1	294	286	287	8.3
2	298	289	290	8.4
3	295	287	288	8.3
4	294	286	287	8.3
5	295	287	288	8.4
7	296	288	289	8.7
8	296	287	288	8.7
9	295	286	287	8.9
10	293	284	285	8.9
11	298	290	291	8.4
12	296	288	289	8.3
13	294	287	288	8.3
14	294	287	288	8.3
15	295	288	289	8.5
17	297	288	289	8.7
18	298	288	289	8.9
19	296	287	288	8.9
20	294	285	286	8.9
21	296	288	289	8.4
22	297	289	291	8.4
23	293	287	288	8.2
24	292	286	287	8.3
25	296	290	291	8.6
26	293	287	288	8.4
27	294	287	288	8.6
28	298	289	290	8.8
29	297	288	289	8.9
30	296	287	288	9.0
31	292	285	287	8.2
32	295	288	290	8.3
33	292	287	288	8.2
34	290	286	287	8.2
35	291	286	287	8.3
37	292	285	285	8.5
38	295	286	287	8.7
39	295	287	288	8.9
40	293	285	286	8.9

[a]Thermocouples 6, 16, and 36 were connected to safety or control instrumentation and not to the data logger.

Table A11. History of operation of thermocouples in capsule A

Thermocouple[b]	Time in temperature[a] range, %					
	<282	282–285	285–288	288–291	291–293	>293
1	1	5	53	38	2	
2[c]						
3		1	3	39	55	2
4		1	5	74	18	
5		1	4	69	24	
7	1	7	71	20		
8	1	16	63	20		
9	6	53	38	2		
10	11[d]	49	38	1		
11		1	15	58	24	
12		1	14	56	26	
13		1	7	80	11	
14		1	8	81	9	
15		1	22	72	4	
17	1	22	16	56	4	
18	1	14	68	16		
19		1	26	51	21	
20	10[d]	44	42	3		
21	1	12	53	33		
22		1	3	46	47	3
23		1	8	81	9	
24		1	8	83	6	
25		2	43	54		
26		3	56	40		
27	1	20	73	5		
28	6	43	47	2		
29	4	34	56	5		
30	4	37	52	6		
31	2	32	48	16		
32		1	12	43	42	1
33	1	2	43	50	3	
34	1	3	51	43	2	
35		1	19	68	10	
37	5	46	47			
38		4	53	41	1	
39	1	19	51	26	2	
40	14[d]	36	41	7		

[a]Temperature ranges in °C.

[b]Thermocouples 6, 16, and 36 were connected to safety or control instrumentation and not to the data logger.

[c]Thermocouple 2 was inoperative.

[d]Values in the temperature range 279 to 282°C.

Table A12. History of operation of thermocouples in capsule B

Thermocouple[b]	Time in temperature[a] range, %						
	<279	279–282	282–285	285–288	288–291	291–293	>293
1	4	9	54	32	2		
2		2	1	5	54	35	2
3			2	3	54	40	1
4		1	5	63	31		
5			2	15	80	2	
7			2	68	27	2	
8			5	76	18		
9		2	43	50	3		
10	3	33	58	5			
11	3	3	35	54	5		
12	1	2	1	14	62	19	
13			2	7	69	21	
14			2	18	74	5	
15				1	24	75	
17			1	20	42	37	
18				8	34	57	1
19	1	12	71	14	2		
20	2	46	46	4	1		
21	51	40	10				
22[c]							
23	2	1	9	46	41	1	
24		1	6	59	33		
25			2	38	58		
26			4	68	27		
27		1	17	81	1		
28		1	22	68	9		
29		1	31	59	7	1	
30	1	22	63	11	2		
31	39	30	29	1			
32	3	3	16	26	36	15	
33	3	1	2	17	42	35	1
34		2	3	23	57	14	
35			2	9	55	34	
37	1	11	38	49	1		
38		2	62	32	4		
39	1	1	37	46	15		
40	5	45	44	6			

[a]Temperature ranges in °C.

[b]Thermocouples 6, 16, and 36 were connected to safety or control instrumentation and not to the data logger.

[c]Thermocouple 22 was inoperative.

Table A13. History of operation of thermocouples in capsule C

Thermocouple[b]	Time in temperature[a] range, %					
	<282	282–285	285–288	288–291	291–293	>293
1	1	5	59	34	1	
2			2	53	40	3
3		1	37	58	3	
4		2	78	19		
5		1	25	73	1	
7		2	26	64	7	
8		2	33	58	6	
9	1	9	54	35	1	
10	6	52	38	3		
11			3	45	48	3
12		1	14	75	9	
13		1	58	40	1	
14		1	31	67	1	
15			10	84	5	
17		1	25	59	14	
18		1	16	61	21	1
19		3	38	53	5	
20	2	32	53	12		
21		1	17	71	10	
22			5	44	48	2
23		1	50	48		
24		1	75	23		
25				46	52	
26			21	78		
27		2	53	42	2	
28			7	62	30	1
29		1	12	64	22	1
30		3	30	58	8	
31	1	14	69	15		
32			12	67	20	
33		1	52	46		
34		3	90	6		
35		4	87	9		
37	1	37	54	7		
38		6	63	28	2	
39		6	50	41	2	
40	3	23	65	8	1	

[a]Temperature ranges in °C.

[b]Thermocouples 6, 16, and 36 were connected to safety or control instrumentation and not to the data logger.

Appendix B

TENSILE AND CHARPY V-NOTCH IMPACT DATA

Table B1. Unirradiated tensile properties for Plate 02 and submerged-arc welds

Specimen number	Test temperature (°C)	Strength, MPa		Uniform strain (%)	Total elongation (%)	Reduction of area (%)
		Yield	Ultimate			
02G524	−140	684	836	12.9	23.4	58.3
02G525	−140	678	846	12.8	20.1	55.4
02G516	−90	559	746	11.8	20.7	62.6
02G517	−90	569	755	12.2	18.8	55.8
02G515	−40	505	683	11.1	19.9	68.1
02G514	−40	517	687	12.2	20.0	67.2
02G510	28	466	621	9.1	17.8	68.2
02G511	28	468	623	9.1	18.9	69.4
02G518	122	448	569	7.5	15.2	68.1
02G519	122	441	584	7.3	15.2	65.7
02G521	203	423	582	7.7	15.3	65.5
02G520	203	426	586	7.9	15.5	66.9
02G532	289	432	621	9.0	16.5	59.5
02G523	289	433	622	9.6	18.0	56.8
68W01	−140	772	821	9.3	18.9	69.0
68W04	−140	816	847	11.6	20.3	67.0
68W08	−40	588	693	9.7	20.5	72.7
68W12	124	519	599	5.5	13.6	72.1
68W14	287	493	618	6.9	15.2	72.8
68W13	287	497	624	7.4	15.9	73.1
69W10	−140	849	920	9.8	18.3	67.2
69W01	−140	873	927	12.4	21.5	65.8
69W02	−90	737	838	10.1	20.8	66.2
69W11	−40	679	779	8.4	16.8	67.9
69W03	−40	678	780	9.2	17.3	69.9
69W16	27	635	721	6.8	15.4	71.1
69W04	27	642	723	7.6	16.2	68.3
69W19	122	601	681	5.9	13.6	70.5
69W05	122	600	688	6.5	13.9	68.0
69W07	204	571	696	7.3	14.8	67.4
69W20	287	582	708	6.8	13.4	60.5
69W08	287	572	714	9.1	16.3	59.2

Table B1. (Continued)

Specimen number	Test temperature (°C)	Strength, MPa		Uniform strain (%)	Total elongation (%)	Reduction of area (%)
		Yield	Ultimate			
70W11	−140	664	784	12.7	22.9	62.7
70W01	−140	686	809	18.4	26.0	57.1
70W02	−90	574	715	11.8	23.3	64.2
70W12	−40	525	655	12.0	21.2	67.2
70W03	−40	524	658	11.5	22.4	68.0
70W04	27	480	593	10.3	19.8	68.1
70W15	27	476	594	9.1	18.2	69.4
70W17	123	452	556	8.3	16.9	67.8
70W05	123	453	558	8.3	16.1	68.8
70W06	203	436	561	7.3	15.8	66.7
70W18	288	429	573	8.4	16.3	64.1
70W09	288	436	578	8.1	15.4	65.5
71W01	−140	669	795	13.7	21.9	60.8
71W12	−140	681	806	13.9	23.5	58.7
71W02	−91	566	718	13.4	22.2	62.1
71W13	−40	511	658	12.4	20.5	65.2
71W04	−40	506	659	12.5	20.9	64.2
71W14	27	469	598	10.0	19.4	68.3
71W05	27	469	600	9.3	18.2	67.3
71W07	122	447	557	8.7	16.0	66.1
71W16	122	442	558	8.7	16.0	64.9
71W08	203	429	557	8.3	15.9	64.2
71W18	289	428	568	8.7	15.1	60.9
71W10	289	430	581	8.2	14.6	59.6

Table B2. Irradiated tensile properties for Plate 02 and submerged-arc welds

Specimen number	Fluence, 10^{23} n/m^2 (>1 MeV)	Test temperature (°C)	Strength, MPa		Uniform strain (%)	Total elongation (%)	Reduction of area (%)
			Yield	Ultimate			
02G503	1.76	33	609	749	10.4	18.1	61.1
02G506	2.14	33	617	753	9.4	16.8	52.9
02G508	1.39	121	566	699	9.5	16.1	62.5
02G505	2.20	121	581	712	8.2	14.4	54.4
02G509	1.36	288	519	696	9.3	15.3	61.3
02G504	2.25	288	533	706	8.5	14.7	50.3
68W02	0.77	36	555	634	6.1	15.0	72.5
68W07	1.45	36	573	656	6.9	16.0	69.6
68W06	1.30	121	537	612	5.7	14.0	77.0
68W15	1.22	288	521	633	6.8	15.3	70.2
68W09	1.66	288	575	641	6.3	16.1	76.9
69W06	0.81	35	704	776	8.4	17.4	65.0
69W17	1.32	35	717	792	7.1	15.3	65.7
69W12	1.35	121	674	747	7.0	14.4	66.8
69W15	1.54	121	675	749	6.5	14.1	68.9
69W14	1.62	288	652	755	7.4	14.2	59.2
69W18	0.99	288	653	756	6.8	14.0	59.5
70W08	1.71	28	534	649	10.3	19.0	64.6
70W16	1.33	121	495	597	10.1	18.0	68.7
70W10	2.02	121	499	607	9.1	17.1	60.8
70W07	1.04	288	467	615	9.1	16.9	62.0
70W13	2.09	288	472	615	9.2	15.7	48.8
71W15	1.82	29	539	649	10.3	18.8	62.2
71W17	1.30	121	487	592	9.2	17.0	63.8
71W09	1.98	121	498	604	10.1	18.0	60.3
71W03	1.02	288	461	592	7.9	14.5	60.1
71W11	2.06	288	470	608	8.3	13.6	48.5

Table B3. Curve fit coefficients for yield and ultimate strengths

Material	Yield strength[a]			Ultimate strength[a]		
	c_0	c_1	c_2	c_0	c_1	c_2
Unirradiated specimens						
Plate 02	492	−0.842	0.00234	646	−0.939	0.00300
Weld 68W	580	−1.075	0.00277	662	−0.864	0.00253
Weld 69W	660	−0.949	0.00239	746	−0.856	0.00262
Weld 70W	504	−0.816	0.00208	621	−0.868	0.00253
Weld 71W	493	−0.841	0.00226	624	−0.879	0.00250
Irradiated specimens						
Plate 02	630	−0.547	0.00064	775	−0.808	0.00191
Weld 68W	581	−0.525	0.00143	668	−0.714	0.00211
Weld 69W	730	−0.589	0.00112	806	−0.699	0.00182
Weld 70W	548	−0.529	0.00089	671	−0.837	0.00224
Weld 71W	558	−0.700	0.00131	673	−0.878	0.00217

[a]Coefficients of strength = $c_0 + c_1T + c_2T^2$, with strength in megapascals and T in degrees C.

Table B4. Unirradiated Charpy impact properties for Plate 02

Specimen number	Laboratory	Test temperature (°C)	Energy (J)	Lateral expansion (mm)	Fracture appearance (% shear)
02G782	ORNL	−46	10.2		
02G783	ORNL	−18	31.2		
02G851	MEA	−7	21.7	0.36	30
02G839	MEA	−7	24.4	0.43	20
02G840	ORNL	−7	27.1	0.33	20
02G900	MEA	−7	27.1	0.38	20
02G852	ORNL	−7	29.8	0.43	20
02G828	ORNL	−7	32.5	0.43	20
02G887	MEA	−7	33.9	0.58	30
02G899	ORNL	−7	35.3	0.46	20
02G827	MEA	−7	36.6	0.64	20
02G888	ORNL	−7	40.7	0.55	20
02G784	ORNL	10	52.9		20
02G841	MEA	21	52.9	0.79	40
02G829	MEA	21	55.6	0.86	40
02G842	ORNL	21	56.9	0.84	40
02G853	MEA	21	58.3	0.94	40
02G890	ORNL	21	58.3	0.77	35
02G910	ORNL	21	62.4	0.91	40
02G830	ORNL	21	67.8	0.88	30
02G889	MEA	21	69.2	1.07	40
02G909	MEA	21	70.5	1.12	40
02G854	ORNL	21	78.6	0.86	30
02G785	ORNL	38	80.7		35
02G831	MEA	66	107.1	1.60	80
02G880	MEA	66	108.5	1.40	85
02G879	ORNL	66	111.2	1.47	80
02G844	ORNL	66	112.5	1.60	90
02G832	ORNL	66	112.5	1.60	85
02G843	MEA	66	113.9	1.55	80
02G786	ORNL	66	122.0		85
02G891	MEA	66	127.4	1.75	100
02G902	MEA	66	127.4	1.60	100
02G901	ORNL	66	130.2	1.67	100
02G892	ORNL	66	130.2	1.70	90
02G787	ORNL	93	139.6	1.83	100
02G788	ORNL	121	141.0	1.96	100
02G882	MEA	149	130.2	2.11	100

Table B4. (Continued)

Specimen number	Laboratory	Test temperature (°C)	Energy (J)	Lateral expansion (mm)	Fracture appearance (% shear)
02G903	MEA	149	132.9	1.88	100
02G833	MEA	149	132.9	1.88	100
02G834	ORNL	149	135.6	1.81	100
02G881	ORNL	149	138.3	1.83	100
02G845	MEA	149	138.3	2.24	100
02G789	ORNL	149	139.6	1.83	100
02G893	MEA	149	143.7	1.83	100
02G904	ORNL	149	143.7	1.90	100
02G846	ORNL	149	149.1	1.93	100
02G894	ORNL	149	151.9	1.69	100
02G790	ORNL	177	145.1	2.10	100
02G884	MEA	204	127.4	2.06	100
02G835	MEA	204	130.2	1.78	100
02G883	ORNL	204	130.2	1.75	100
02G847	MEA	204	135.6	2.01	100
02G848	ORNL	204	136.3	1.81	100
02G836	ORNL	204	136.9	1.81	100
02G906	ORNL	204	138.3	1.47	100
02G905	MEA	204	141.0	2.01	100
02G791	ORNL	204	142.4	2.11	100
02G895	ORNL	204	146.4	1.93	100
02G896	MEA	204	157.3	1.75	100
02G792	ORNL	232	139.0	2.01	100
02G793	ORNL	260	140.3	2.06	100
02G838	ORNL	288	119.3	1.79	100
02G850	ORNL	288	132.9	1.78	100
02G885	ORNL	288	134.2	1.72	100
02G849	MEA	288	139.6		
02G908	ORNL	288	142.4	1.82	100
02G886	MEA	288	143.7	1.60	100
02G907	MEA	288	146.4	1.91	100
02G794	ORNL	288	146.4	2.01	100
02G898	MEA	288	149.1	2.11	100
02G837	MEA	288	150.5		
02G897	ORNL	288	151.9	1.77	100

Table B5. Unirradiated Charpy impact properties for weld 68W

Specimen number	Laboratory	Test temperature (°C)	Energy (J)	Lateral expansion (mm)	Fracture appearance (% shear)
68W241	ORNL	−62	31.2	0.39	30
68W238	ORNL	−62	35.3	0.48	30
68W237	ORNL	−62	42.0	0.59	20
68W242	ORNL	−46	54.2	0.68	35
68W234	ORNL	−46	86.8	1.06	60
68W235	ORNL	121	180.3	2.06	100
68W239	ORNL	121	192.5	2.00	100
68W243	ORNL	200	183.0		100
68W218	ORNL	200	185.7	2.26	100
68W233	ORNL	200	202.7		100
68W236	ORNL	288	183.0	1.89	100
68W240	ORNL	288	235.9	1.65	100

Table B6. Unirradiated Charpy impact properties for weld 69W

Specimen number	Laboratory	Test temperature (°C)	Energy (J)	Lateral expansion (mm)	Fracture appearance (% shear)
69W252	MEA	−46	16.3	0.28	30
69W204	ORNL	−46	18.3	0.26	20
69W298	MEA	−18	25.8	0.33	40
69W239	ORNL	−18	27.1		
69W205	ORNL	−18	31.9	0.37	30
69W297	ORNL	−18	32.5	0.08	30
69W218	MEA	−18	32.5	0.61	45
69W220	MEA	−18	44.7	0.76	45
69W333	ORNL	−18	47.5	0.30	35
69W219	ORNL	−18	48.8	0.29	50
69W244	MEA	−18	48.8	0.66	30
69W334	MEA	−18	51.6	0.81	40
69W278	MEA	−18	54.2	0.71	40
69W277	ORNL	−18	63.7	0.51	45
69W332	MEA	−12	73.2	1.12	50
69W322	MEA	−1	85.4	1.12	60
69W300	MEA	10	65.1	0.99	80
69W299	ORNL	10	70.5	0.64	60
69W330	MEA	10	89.5	1.19	100
69W245	MEA	10	96.3	1.30	80
69W206	ORNL	10	100.3	1.29	80
69W280	ORNL	10	105.8	1.06	85
69W223	ORNL	10	105.8	0.97	98
69W276	MEA	10	107.1	1.45	80
69W331	ORNL	10	111.2	1.09	80
69W281	MEA	10	112.5	1.47	90
69W222	MEA	11	119.3	1.52	80
69W207	ORNL	38	142.4	1.72	100
69W229	MEA	38	143.7	2.01	100
69W208	ORNL	66	141.0	1.70	100
69W209	ORNL	93	152.5	1.92	100
69W210	ORNL	121	135.6	1.75	100
69W339	ORNL	121	138.3	1.58	100
69W224	MEA	121	141.0	1.83	100
69W253	ORNL	121	146.4	1.58	100
69W282	MEA	121	146.4	1.78	100
69W287	ORNL	121	147.8	1.62	100
69W251	MEA	121	150.5	2.03	100

Table B6. (Continued)

Specimen number	Laboratory	Test temperature (°C)	Energy (J)	Lateral expansion (mm)	Fracture appearance (% shear)
69W337	MEA	121	151.9	1.88	100
69W323	ORNL	121	151.9	1.62	100
69W324	MEA	121	154.6	1.88	100
69W212	ORNL	149	135.6	1.80	100
69W289	MEA	149	146.4	1.98	100
69W213	ORNL	177	136.3	1.90	100
69W214	ORNL	204	134.9	1.70	100
69W228	ORNL	204	135.6	1.53	100
69W328	ORNL	204	146.4	1.69	100
69W288	ORNL	204	146.4	1.57	100
69W236	MEA	204	146.4	1.80	100
69W227	MEA	204	149.1	1.80	100
69W272	ORNL	204	151.9	1.71	100
69W259	MEA	204	151.9	1.98	100
69W327	MEA	204	157.3	2.13	100
69W215	ORNL	232	145.8	1.94	100
69W216	ORNL	260	142.4	1.93	100
69W258	ORNL	288	146.4	1.57	100
69W217	ORNL	288	146.4	1.84	100
69W274	ORNL	288	147.8	1.55	100
69W232	ORNL	288	147.8	1.55	100
69W293	ORNL	288	150.5	1.40	100
69W295	MEA	288	150.5		
69W273	MEA	288	157.3		100
69W257	MEA	288	160.0		
69W231	MEA	288	162.7		
69W326	MEA	288	176.3		

Table B7. Unirradiated Charpy impact properties for weld 70W

Specimen number	Laboratory	Test temperature (°C)	Energy (J)	Lateral expansion (mm)	Fracture appearance (% shear)
70W292	ORNL	−73	13.6	0.13	10
70W236	ORNL	−73	25.1	0.28	20
70W250	ORNL	−59	23.1	0.25	20
70W275	ORNL	−59	35.3	0.43	20
70W253	MEA	−54	17.6	0.36	20
70W261	ORNL	−54	21.7	0.02	20
70W260	ORNL	−54	29.8	0.09	25
70W282	MEA	−54	31.2	0.64	35
70W264	MEA	−54	24.4	0.33	40
70W230	ORNL	−46	54.9	0.76	40
70W241	ORNL	−18	51.5	0.39	40
70W237	MEA	−18	51.5	0.97	50
70W268	MEA	−18	75.9	1.30	50
70W277	ORNL	−18	75.9	0.67	50
70W206	ORNL	−18	92.9	1.23	70
70W278	MEA	−18	71.9	1.12	80
70W281	ORNL	18	105.8	1.25	98
70W255	ORNL	18	111.2	1.34	98
70W222	ORNL	−1	134.9	2.02	100
70W207	ORNL	10	119.3	1.73	100
70W214	ORNL	38	132.9	2.06	100
70W217	ORNL	66	122.0	1.74	100
70W220	ORNL	93	132.9	1.99	100
70W249	MEA	121	124.7	1.96	100
70W243	ORNL	121	126.1	1.87	100
70W242	MEA	121	127.5	1.96	100
70W221	ORNL	121	128.8	1.89	100
70W272	MEA	121	136.9	2.03	100
70W271	ORNL	121	141.0	1.92	100
70W223	ORNL	180	125.4	2.03	100
70W224	ORNL	204	122.0	1.91	100
70W258	MEA	204	130.2	2.08	100
70W279	ORNL	204	135.6	1.96	100
70W259	ORNL	204	138.3	1.91	100
70W280	MEA	204	141.0	2.03	100
70W276	MEA	204	149.1	2.34	100
70W227	ORNL	232	123.4	1.99	100
70W228	ORNL	288	128.8	1.92	100
70W283	ORNL	288	132.9	1.88	100
70W267	ORNL	288	141.0	2.11	100
70W286	MEA	288	141.0	2.16	100
70W244	MEA	288	146.4	2.24	100
70W266	MEA	288	162.7	1.96	100

Table B8. Unirradiated Charpy impact properties for weld 71W

Specimen number	Laboratory	Test temperature (°C)	Energy (J)	Lateral expansion (mm)	Fracture appearance (% shear)
71W220	ORNL	−46	9.5		10
71W204	ORNL	−18	31.9		40
71W268	MEA	−12	43.4	0.69	40
71W232	ORNL	−9	29.8	0.20	35
71W238	MEA	−9	35.3	0.69	40
71W231	MEA	−9	39.3	0.64	30
71W239	ORNL	−9	46.1	0.36	35
71W230	ORNL	10	44.7	0.38	35
71W229	MEA	10	51.5	0.94	30
71W254	MEA	10	65.1	1.12	70
71W252	ORNL	10	65.1	0.64	50
71W205	ORNL	10	71.9	1.15	80
71W206	ORNL	38	92.9	1.63	100
71W209	ORNL	66	101.7	1.52	100
71W210	ORNL	93	107.8	1.77	100
71W237	ORNL	121	92.2	1.31	100
71W235	MEA	121	92.2	1.52	100
71W226	ORNL	121	92.2	1.23	100
71W225	MEA	121	94.9	1.65	100
71W251	MEA	121	104.4	1.70	100
71W211	ORNL	121	113.9	1.79	100
71W212	ORNL	149	105.8	1.77	100
71W213	ORNL	177	101.7	1.62	100
71W215	ORNL	204	100.3	1.54	100
71W248	ORNL	204	103.0	1.42	100
71W263	ORNL	204	104.4	1.45	100
71W264	MEA	204	109.8	1.96	100
71W246	MEA	204	111.2	1.73	100
71W249	MEA	204	113.9	2.01	100
71W216	ORNL	232	98.3	1.64	100
71W218	ORNL	260	103.7	1.73	100
71W234	ORNL	288	92.2	1.33	100
71W219	ORNL	288	97.6	1.93	100
71W233	MEA	288	103.0	1.73	100
71W256	ORNL	288	109.8	1.48	100
71W245	MEA	288	119.3	1.78	100
71W257	MEA	288	123.4	1.78	100

Table B9. Irradiated Charpy impact properties for Plate 02

Specimen number	Fluence, 10^{23} n/m^2 (>1 MeV)	Laboratory	Test temperature (°C)	Energy (J)	Lateral expansion (mm)	Fracture appearance (% shear)
02G704	0.98	ORNL	38	32.5		20
02G747	2.24	MEA	66	21.7	0.05	40
02G759	1.92	MEA	66	24.4		
02G751	2.15	MEA	66	24.4	0.11	35
02G719	1.64	MEA	66	25.8	0.23	35
02G713	1.36	MEA	66	28.5		
02G707	1.13	MEA	66	32.5	0.17	40
02G738	2.22	ORNL	66	32.5		30
02G754	2.10	ORNL	66	33.9	0.08	30
02G748	2.25	ORNL	66	38.0	0.17	20
02G758	1.96	ORNL	66	40.7	0.19	30
02G718	1.67	ORNL	66	44.7	0.31	30
02G712	1.39	ORNL	66	46.1	0.31	40
02G706	1.15	ORNL	66	55.6	0.35	30
02G736	2.20	MEA	93	32.5	0.35	40
02G760	1.80	MEA	93	42.0	0.35	40
02G752	2.17	MEA	93	43.4	0.36	40
02G756	2.06	MEA	93	46.1	0.39	40
02G708	1.23	MEA	93	51.5	0.67	60
02G740	2.26	ORNL	93	54.2		50
02G715	1.44	MEA	93	59.7		
02G723	1.82	ORNL	93	59.7	0.63	40
02G727	1.92	ORNL	93	63.7	0.49	35
02G735	2.09	ORNL	93	78.6		40
02G731	2.02	ORNL	93	86.8	0.74	75
02G714	1.47	ORNL	93	94.9	1.02	60
02G703	0.87	ORNL	93	105.8	1.13	75
02G739	2.18	ORNL	121	94.9	1.07	75
02G741	2.22	ORNL	149	97.6	1.34	100
02G762	1.68	MEA	149	103.0	1.16	70
02G768	1.23	MEA	149	108.5	1.40	100
02G705	0.96	MEA	149	108.5	1.44	100
02G730	2.06	ORNL	149	109.8	1.27	100
02G767	1.28	MEA	149	109.8		
02G749	2.20	MEA	149	112.5	1.42	100
02G726	1.97	ORNL	149	113.9	1.23	100
02G722	1.86	ORNL	149	113.9	1.21	100
02G734	2.14	ORNL	149	122.0	1.16	100

Table B9. (Continued)

Specimen number	Fluence, 10^{23} n/m^2 (>1 MeV)	Laboratory	Test temperature (°C)	Energy (J)	Lateral expansion (mm)	Fracture appearance (% shear)
02G702	0.89	ORNL	149	124.7	1.50	100
02G716	1.54	MEA	149	130.2	1.39	80
02G744	2.30	ORNL	177	126.1	1.47	100
02G753	2.12	MEA	204	104.4	1.32	100
02G764	1.54	ORNL	204	105.8		100
02G765	1.51	MEA	204	109.8		
02G742	2.29	ORNL	204	111.2	1.49	100
02G761	1.77	MEA	204	113.9	1.20	100
02G757	2.01	MEA	204	119.3	1.29	100
02G737	2.15	MEA	204	122.0	1.41	100
02G729	1.97	ORNL	204	122.0	1.32	100
02G733	2.06	ORNL	204	124.7	1.44	100
02G701	0.78	ORNL	204	124.7	1.25	100
02G725	1.87	ORNL	204	124.7	1.31	100
02G721	1.70	ORNL	204	127.4	1.42	100
02G709	1.21	MEA	204	131.5	1.33	100
02G745	2.25	ORNL	232	113.9	1.64	100
02G743	2.24	ORNL	260	116.6	1.56	100
02G724	1.91	ORNL	288	115.2	1.49	100
02G720	1.74	ORNL	288	116.6	1.52	100
02G732	2.10	ORNL	288	119.3	1.40	100
02G728	2.01	ORNL	288	120.7	1.43	100
02G700	0.80	ORNL	288	122.0	1.33	100
02G746	2.29	ORNL	288	122.0	1.56	100
02G710	1.32	ORNL	288	123.4		100
02G763	1.64	MEA	288	123.4	1.46	100
02G717	1.51	MEA	288	124.7	1.29	100
02G711	1.29	MEA	288	124.7		
02G750	2.20	MEA	288	124.7	1.30	100
02G755	2.05	MEA	288	126.1	1.42	100
02G769	1.20	MEA	288	130.2	1.27	100

Table B10. Irradiated Charpy impact properties for weld 68W

Specimen number	Fluence, 10^{23} n/m^2 (>1 MeV)	Laboratory	Test temperature (°C)	Energy (J)	Lateral expansion (mm)	Fracture appearance (% shear)
68W221	1.63	ORNL	−51	23.1	0.02	20
68W222	1.58	ORNL	−51	38.0	0.05	30
68W226	1.49	MEA	−46	31.2		
68W209	1.04	ORNL	−46	35.3	0.16	30
68W231	1.19	MEA	−46	36.6	0.30	35
68W215	1.39	ORNL	−46	59.7	0.31	30
68W203	0.69	MEA	−46	97.6	0.64	40
68W219	1.61	ORNL	−40	54.2		40
68W216	1.49	MEA	−18	82.7	0.96	60
68W211	1.18	MEA	−18	113.9		80
68W220	1.65	ORNL	−18	116.6	0.90	100
68W207	0.87	ORNL	−18	124.7	1.10	80
68W224	1.55	ORNL	−18	151.9	1.48	100
68W213	1.34	ORNL	−18	154.6	1.68	90
68W223	1.56	ORNL	4	187.1	1.77	95
68W217	1.52	MEA	121	187.1	1.94	100
68W202	0.63	MEA	121	206.1	2.16	100
68W212	1.23	MEA	121	207.4	2.08	100
68W214	1.38	ORNL	121	208.8	1.53	100
68W204	0.88	ORNL	121	214.2	1.99	100
68W228	1.39	MEA	204	197.9	2.04	100
68W210	1.09	MEA	204	199.3	1.87	100
68W230	1.27	ORNL	204	208.8	1.61	100
68W225	1.52	ORNL	204	218.3	1.45	100
68W206	0.83	ORNL	204	252.2	1.30	100
68W227	1.46	MEA	288	197.9	1.66	100
68W229	1.31	ORNL	288	210.2	1.40	100
68W232	1.15	MEA	288	211.5	1.43	100
68W201	0.58	MEA	288	226.4	1.22	100
68W208	0.93	ORNL	288	238.6	1.16	100

Table B11. Irradiated Charpy impact properties for weld 69W

Specimen number	Fluence, 10^{23} n/m^2 (>1 MeV)	Laboratory	Test temperature (°C)	Energy (J)	Lateral expansion (mm)	Fracture appearance (% shear)
69W242	1.27	ORNL	10	32.5	0.08	35
69W202	0.63	MEA	10	35.3	0.22	45
69W264	1.49	MEA	10	39.3	0.29	40
69W211	0.75	ORNL	10	40.7		
69W246	1.42	MEA	10	42.0	0.29	40
69W235	1.00	ORNL	10	43.4	0.25	40
69W255	1.62	ORNL	10	48.8	0.20	45
69W254	1.57	ORNL	10	50.2	0.27	45
69W286	1.07	MEA	10	62.4	0.51	45
69W247	1.42	MEA	21	54.2	0.40	80
69W267	1.35	MEA	38	86.8	0.82	70
69W263	1.51	ORNL	49	75.9	0.65	70
69W261	1.59	MEA	49	82.7		
69W265	1.46	ORNL	49	88.1	0.74	90
69W269	1.24	MEA	49	92.2	0.98	70
69W338	0.94	MEA	49	96.3	1.03	100
69W203	0.69	ORNL	49	103.0	0.76	75
69W340	0.90	MEA	49	109.8		
69W283	1.12	ORNL	49	122.0	1.07	95
69W285	1.10	ORNL	49	123.4	1.03	98
69W248	1.46	MEA	66	105.8	1.12	100
69W262	1.57	MEA	121	116.6	1.26	100
69W233	0.89	MEA	121	128.8	1.41	100
69W240	1.21	MEA	121	132.9	1.43	100
69W268	1.28	MEA	121	132.9	1.57	98
69W266	1.43	ORNL	121	141.7	1.45	95
69W336	0.96	ORNL	121	143.0	1.37	100
69W243	1.31	ORNL	121	155.2	1.34	100
69W294	1.01	ORNL	121	160.0	1.46	100
69W241	1.25	MEA	288	134.2		
69W291	1.05	ORNL	288	144.4	1.27	100
69W260	1.59	ORNL	288	147.1	1.26	100
69W237	1.11	MEA	288	147.8	1.32	100
69W201	0.56	MEA	288	150.5		
69W250	1.48	MEA	288	154.6	1.21	100
69W270	1.17	ORNL	288	155.2	1.17	100
69W234	0.95	ORNL	288	160.0	1.17	100

Table B12. Irradiated Charpy impact properties for weld 70W

Specimen number	Fluence, 10^{23} n/m^2 (>1 MeV)	Laboratory	Test temperature (°C)	Energy (J)	Lateral expansion (mm)	Fracture appearance (% shear)
70W204	0.88	ORNL	−29	43.4	0.18	40
70W239	2.11	ORNL	−18	27.1	0.05	20
70W233	2.10	MEA	−18	32.5	0.28	40
70W252	1.90	ORNL	−18	32.5	0.21	40
70W257	1.65	MEA	−18	40.7	0.23	35
70W205	0.96	MEA	−18	40.7	0.27	60
70W289	1.40	ORNL	−18	44.7	0.28	45
70W209	1.20	ORNL	−18	54.2	0.71	40
70W212	1.41	ORNL	−18	56.9	0.39	30
70W234	2.16	ORNL	−7	48.8	0.18	40
70W245	2.04	ORNL	16	52.2	0.39	30
70W240	2.07	MEA	16	61.0	0.53	45
70W218	1.76	MEA	16	67.8	0.68	70
70W256	1.71	ORNL	16	80.0	0.53	60
70W251	1.94	ORNL	16	85.4	0.74	40
70W208	1.12	MEA	16	100.3	1.21	80
70W213	1.48	ORNL	16	103.0	0.97	85
70W211	1.34	ORNL	16	121.3	1.20	98
70W225	1.86	ORNL	27	81.4	0.69	70
70W216	1.65	ORNL	66	130.2	1.00	100
70W235	2.15	MEA	121	116.6	1.45	100
70W229	1.95	ORNL	121	118.0	1.41	100
70W291	1.18	MEA	121	126.1	1.80	100
70W254	1.76	MEA	121	127.4	1.65	100
70W285	1.53	ORNL	121	130.2	1.38	100
70W246	2.01	ORNL	121	130.2	1.45	100
70W238	2.13	MEA	204	127.4	1.38	100
70W231	1.98	ORNL	204	133.5	1.46	100
70W287	1.46	ORNL	204	135.6	1.61	100
70W248	1.98	ORNL	204	136.9	1.24	100
70W210	1.27	MEA	204	139.6	1.14	100
70W219	1.81	MEA	204	150.5	1.51	100
70W226	1.91	ORNL	288	127.4	1.12	100
70W232	2.07	MEA	288	128.8	1.13	100
70W215	1.59	ORNL	288	128.8	1.45	100
70W284	1.59	MEA	288	132.9	1.25	100
70W203	0.80	MEA	288	141.0	1.25	100
70W290	1.26	ORNL	288	143.7	1.30	100

Table B13. Irradiated Charpy impact properties for weld 71W

Specimen number	Fluence, 10^{23} n/m^2 (>1 MeV)	Laboratory	Test temperature (°C)	Energy (J)	Lateral expansion (mm)	Fracture appearance (% shear)
71W221	1.17	MEA	−12	25.8	0.06	30
71W242	1.83	MEA	10	28.5	0.12	35
71W236	1.62	MEA	21	35.3	0.38	40
71W228	1.57	ORNL	21	35.3	0.15	25
71W224	1.39	MEA	21	39.3	0.25	35
71W269	1.86	MEA	21	44.7	0.38	40
71W214	0.95	ORNL	21	46.1	0.23	40
71W253	2.06	ORNL	21	47.5	0.32	40
71W272	1.62	ORNL	21	56.9	0.30	40
71W266	1.94	MEA	38	61.0	0.62	50
71W227	1.45	MEA	49	52.9		40
71W271	1.68	MEA	49	71.9	1.23	80
71W240	1.73	ORNL	49	73.2	0.77	60
71W267	1.90	MEA	49	73.2		100
71W217	1.10	ORNL	49	75.9	0.66	80
71W261	2.03	ORNL	49	78.6	0.81	80
71W244	1.91	ORNL	49	82.7	0.89	100
71W276	1.37	MEA	66	89.5	1.22	100
71W265	1.97	MEA	121	94.9	1.26	100
71W208	0.87	ORNL	121	97.6		100
71W260	2.08	MEA	121	100.3	1.47	100
71W274	1.50	MEA	121	105.8	1.46	100
71W270	1.73	ORNL	121	105.8	1.08	100
71W278	1.16	ORNL	121	109.8	1.20	100
71W258	2.11	ORNL	121	113.9	1.02	100
71W223	1.32	MEA	204	94.9		
71W222	1.25	ORNL	204	104.4	0.86	100
71W241	1.78	ORNL	204	111.2	1.24	100
71W259	2.09	ORNL	204	118.0	1.39	100
71W247	1.95	MEA	204	119.3	1.31	100
71W275	1.44	MEA	204	119.3	1.21	100
71W255	2.12	ORNL	288	113.9	1.33	100
71W243	1.87	MEA	288	113.9	1.45	100
71W262	2.01	MEA	288	116.6		
71W250	2.03	ORNL	288	117.3	0.84	100
71W207	0.78	ORNL	288	124.7	1.23	100
71W277	1.23	MEA	288	126.1	1.26	100
71W273	1.56	ORNL	288	132.9	1.12	100

Table B14. Irradiated Charpy impact properties for Plate 02

Specimen number	Fluence, 10^{23} n/m^2 (>1 MeV)	Laboratory	Test temperature (°C)	Corrected test temperature[a] (°C)	Energy (J)
02G704	0.98	ORNL	38	53	32.5
02G747	2.24	MEA	66	54	21.7
02G759	1.92	MEA	66	60	24.4
02G751	2.15	MEA	66	56	24.4
02G719	1.64	MEA	66	66	25.8
02G713	1.36	MEA	66	73	28.5
02G707	1.13	MEA	66	80	32.5
02G738	2.22	ORNL	66	58	32.5
02G754	2.10	ORNL	66	60	33.9
02G748	2.25	ORNL	66	59	38.0
02G758	1.96	ORNL	66	63	40.7
02G718	1.67	ORNL	66	68	44.7
02G712	1.39	ORNL	66	74	46.1
02G706	1.15	ORNL	66	78	55.6
02G736	2.20	MEA	93	74	32.5
02G760	1.80	MEA	93	82	42.0
02G752	2.17	MEA	93	75	43.4
02G756	2.06	MEA	93	77	46.1
02G708	1.23	MEA	93	97	51.5
02G740	2.26	ORNL	93	84	54.2
02G715	1.44	MEA	93	90	59.7
02G723	1.82	ORNL	93	92	59.7
02G727	1.92	ORNL	93	90	63.7
02G735	2.09	ORNL	93	88	78.6
02G731	2.02	ORNL	93	89	86.8
02G714	1.47	ORNL	93	98	94.9
02G703	0.87	ORNL	93	110	105.8
02G739	2.18	ORNL	121	113	94.9
02G708	1.23	MEA	93	97	51.5
02G740	2.26	ORNL	93	84	54.2
02G715	1.44	MEA	93	90	59.7
02G723	1.82	ORNL	93	92	59.7
02G727	1.92	ORNL	93	90	63.7
02G735	2.09	ORNL	93	88	78.6
02G731	2.02	ORNL	93	89	86.8
02G714	1.47	ORNL	93	98	94.9
02G703	0.87	ORNL	93	110	105.8
02G739	2.18	ORNL	121	113	94.9

[a]Test temperature corrected for mean fluence, 1.77×10^{23} neutrons/m^2 (>1 MeV) and corrected for bath cooling effects.

NUREG/CR-4880
Vol. 1
ORNL-6484/V1
Dist. Category RF

INTERNAL DISTRIBUTION

1. D. J. Alexander
2. B. R. Bass
3. S. E. Bolt
4. R. H. Bryan
5. J. W. Bryson
6. R. D. Cheverton
7. J. M. Corum
8-12. W. R. Corwin
13. E. C. Fox
14. F. M. Haggag
15. S. K. Iskander
16. A. P. Malinauskas
17. J. G. Merkle
18-22. R. K. Nanstad
23. D. J. Naus
24. C. E. Pugh
25. G. C. Robinson
26. A. F. Rowcliffe
27. G. M. Slaughter
28. J. O. Stiegler
29-33. K. R. Thoms
34. P. T. Thornton
35. H. E. Trammell
36. ORNL Patent Office
37. Central Research Library
38. Document Reference Section
39. Laboratory Records Department
40. Laboratory Records (RC)

EXTERNAL DISTRIBUTION

41-42. MATERIALS ENGINEERING ASSOCIATES, 9700B George Palmer Highway, Lanham, MD 20706

F. J. Loss

43-45. NRC, Division of Engineering, Washington, DC 20555

M. E. Mayfield
C. Z. Serpan
M. Vagins

46. SOUTHWEST RESEARCH INSTITUTE, Engineering and Material Science Division, San Antonio, TX 78284

M. F. Kanninen

47. UNIVERSITY OF MARYLAND, Department of Mechanical Engineering, College Park, MD 20742

W. L. Fourney

48-50. VIRGINIA MILITARY INSTITUTE, Mechanical Engineering Department, Lexington, VA 24416

J. J. McGowan

51. E. T. Wessel, 3570 Meadowgate Drive, Murrysville, PA 15668

52. DOE, Oak Ridge Operations Office, Oak Ridge, TN 37831
    Assistant Manager, Energy Research and Development

53-54. DOE, OSTI, Oak Ridge, TN 37831

55-304. Given RF Category

☆U.S. GOVERNMENT PRINTING OFFICE: 1 9 8 8-5 4 8-1 1 8/8 0 0 6 1

NRC FORM 335 (2-84) NRCM 1102, 3201, 3202

U.S. NUCLEAR REGULATORY COMMISSION

BIBLIOGRAPHIC DATA SHEET

SEE INSTRUCTIONS ON THE REVERSE

1 REPORT NUMBER (Assigned by TIDC, add Vol. No., if any)

NUREG/CR-4880
ORNL-6484/V1

2 TITLE AND SUBTITLE

Characterization of Irradiated Current-Practice Welds and A533 Grade B Class 1 Plate for Nuclear Pressure Vessel Service

3 LEAVE BLANK

4 DATE REPORT COMPLETED

MONTH	YEAR
6	1988

5 AUTHOR(S)

J. J. McGowan, R. K. Nanstad, and K. R. Thoms

6 DATE REPORT ISSUED

MONTH	YEAR

7 PERFORMING ORGANIZATION NAME AND MAILING ADDRESS (Include Zip Code)

Oak Ridge National Laboratory
Oak Ridge, Tennessee 37831

8 PROJECT/TASK/WORK UNIT NUMBER

9 FIN OR GRANT NUMBER

B0119

10 SPONSORING ORGANIZATION NAME AND MAILING ADDRESS (Include Zip Code)

Division of Engineering Technology
Office of Nuclear Regulatory Research
U.S. Nuclear Regulatory Commission
Washington, DC 20555

11a TYPE OF REPORT

ORNL

b PERIOD COVERED (Inclusive dates)

12 SUPPLEMENTARY NOTES

13 ABSTRACT (200 words or less)

Studies of the effects of neutron irradiation on fracture toughness properties of steels have generally included a minimum number of tests for each material condition. The present study attempts to apply statistical analyses, with multiple testing at selected temperatures, to assess the accuracy and reliability of the results. Fracture toughness test specimens were irradiated in the Bulk Shielding Reactor at Oak Ridge National Laboratory at 288°C to target neutron fluences of 2×10^{23} neutrons/m^2 (>1 MeV). The materials were ASTM A533 grade B class 1 plate (HSST Plate 02) and four submerged-arc welds representing the current fabrication practice for nuclear pressure vessels. Both unirradiated and irradiated specimens were tested by two separate laboratories, and multiple tests were conducted at selected temperatures. Statistical analyses permitted the determination of material and test variability and an interlabo-ratory comparison. Behavior in both the transition and ductile-shelf regions was studied. The results demonstrated the relatively low radiation sensitivity of low copper/nickel welds and the qualitative agreement between Charpy impact and fracture toughness observations of toughness degradation.

14 DOCUMENT ANALYSIS - a KEYWORDS/DESCRIPTORS

b IDENTIFIERS/OPEN-ENDED TERMS

15 AVAILABILITY STATEMENT

Unlimited

16 SECURITY CLASSIFICATION

(This page)

Unclassified

(This report)

17 NUMBER OF PAGES

18 PRICE